MIL-R-978(SHIPS)

UNCLASSIFIED

FINAL REPORT - Part II
FOR
LAKE HEFNER MODEL STUDIES
OF WIND STRUCTURE AND
EVAPORATION

This report covers the period December 1953 to July 1954

COLORADO
AGRICULTURAL AND MECHANICAL COLLEGE

Department of Civil Engineering

Fort Collins, Colorado

NAVY DEPARTMENT BUREAU OF SHIPS ELECTRONICS DIVISIONS

Contract No. NObsr-57053
Index No. NE 120202
July 1954

UNCLASSIFIED

ACKNOWLEDGMENTS

The authors wish to acknowledge the efforts of Dr. M. L. Albertson, Head of Fluid Mechanics Research, under whose leadership this project was conceived and who was responsible for technical supervision of the work. Acknowledgment is also due Dr. C. S. Yih, who contributed much to the initial planning and development of the project.

Mr. W. B. Langbein and Mr. G. E. Harbeck of the U. S. Geological Survey, Mr. W. U. Garstka of the U. S. Bureau of Reclamation, Dr. R. D. Russell, Mr. E. R. Anderson, Mr. L. J. Anderson and Mr. J. J. Marciano of the Naval Electronics Laboratory, and Mr. B. K. Couper of the U. S. Navy Bureau of Ships deserve especial thanks for their interest and assistance during the experimentation and for the many suggestions regarding the preparation of the report.

Appreciation is also expressed to R. T. Shen, who prepared the drawings and edited the manuscript; and to Prof. T. H. Evans, Dean of Engineering, and Dr. Dean F. Peterson, Head of Civil Engineering for their helpfulness and assistance.

TABLE OF CONTENTS

LIST OF FIGURES

Fig. No. Page

Chapter I

INTRODUCTION

In October 1951, a model study of Lake Hefner was undertaken at Colorado A & M College under the sponsorship of the U. S. Bureau of Ships, Department of the Navy and in cooperation with the U. S. Geological Survey. The primary objectives of the model study were to determine the following:

1. Correlations of wind structure between model and prototype,
2. Correlations of evaporation between model and prototype.

Details concerning the prototype study are reported in Refs. 2 and 13.

The experimental work performed in an endeavor to obtain model data for correlation with the Lake Hefner Prototype Studies (13)[1] was accomplished during two separate periods of testing. The periods of testing were during the summers of 1952 and 1953 and have been called the 1952 Testing Program and the 1953 Testing Program respectively.

Results obtained from the 1952 Testing Program have been previously reported in Lake Hefner Model Studies of Wind Structure and Evaporation -- Final Report: Part I (3). The major results from the 1952 portion of the testing program on the 1:2000 scale model with wind from only a southerly direction were that the wind structure for model and prototype is similar above the laminar sub-layer which existed in the model and that the Reynolds analogy as modified by Kármán may be used to correlate evaporation rates from both the model and prototype when the shear velocity rather than the velocity is taken as one of the variables comprising the Reynolds number. The reader is referred to Part I (3) not only for a detailed account of these results but also for a description of the model, the techniques used, and the equipment which is not included herein.

1 The first number in parenthesis is the bibliographical entry number and the second number, which follows a colon if present, is the page number.

This report, Lake Hefner Model Studies of Wind Structure and Evaporation -- Final Report: Part II, describes the 1953 Testing Program and integrates the results with those of the 1952 Testing Program. The salient features which were investigated during the more recent testing program include the following:

1. Determination of the effect of wind direction by rotating the model 180°,
2. Determination of the effect of upstream barriers on the rate of evaporation from the model,
3. Determination of the similarity between the Reynolds analogy and data having Reynolds numbers intermediate to those for the Lake Hefner model and prototype,
4. Examination of the evaporation theories of other investigators to formulate a model-prototype relationship.

In addition, the steps are outlined and an example cited for the practical application of a modified form of the Kármán extension of the Reynolds analogy.

List of Symbols

The following symbols are used in this report. An effort was made to have these agree as closely as possible with those appearing in the Part I (3) and those in the Lake Hefner studies technical report (13). The English system of units -- pounds, feet, and seconds -- has been used wherever convenient. Any other system would be equally applicable provided proper cognizance is taken of the conversion factors.

Symbol	Definition	Units
e	water vapor pressure of the ambient air -- a subscript refers to the elevation at which it was measured	millibars
e_o	water vapor pressure of saturated air at the evaporation surface temperature	millibars
Δe	difference between the vapor pressure of the air in contact with the evaporation surface and the vapor pressure of the ambient air	millibars
g	acceleration due to gravity	feet/second^2
k_o	Kármán constant	dimensionless
ℓ	mixing length	feet
ln	denotes logarithms to base e	--
log	denotes logarithms to base 10	--
m	subscript referring to the model	--
n	exponent	--
p	subscript referring to the prototype	--
p_a	total atmospheric pressure	millibars
$\frac{1}{q}$	exponent	--
q_h	specific humidity	pound/pound
r	roughness ratio -- by definition $r = \frac{\epsilon_w}{\epsilon_\ell}$	dimensionless
r'	relative roughness -- by definition $r' = \frac{\sqrt{A}}{\epsilon_w}$	dimensionless
r_o	radius	feet
x	the distance in the model from the leading edge of the modeled terrain to the point at which the velocity profile is measured	feet

Symbol	Definition	Units
t	time coordinate	seconds
u'	the instantaneous velocity fluctuation from U	feet/second
$\overline{u'w'}$	temporal mean value of velocity fluctuation product	feet^2/second^2
w'	the instantaneous velocity fluctuation in the z direction	feet/second
z	vertical height above surface	feet
z_o	roughness parameter	feet
$z_{o\ell}$	roughness parameter of the land surface	feet
z_{ow}	roughness parameter of the water surface	feet
A	area of surface from which evaporation takes place	feet^2
$A(z)$	exchange coefficient	pound-second/feet^2
C_A	absolute humidity of the ambient air	pound/feet^3
C_o	absolute humidity of the air in contact with the surface from which evaporation takes place	pound/feet^3
C_z	absolute humidity of the air at height z	pound/feet^3
ΔC	difference between the absolute humidity of the air in contact with the evaporation surface and the absolute humidity of the ambient air	pound/feet^3
$\Delta C'$	difference between the mixing ratio of the air in contact with the evaporation surface and the mixing ratio of the ambient air	pound/pound
C_e	by definition $C_e = \frac{E}{\gamma \Delta C' U_o}$	dimensionless
C_f	drag coefficient	dimensionless
D	wind direction	dimensionless
D_X	total drag on a boundary of unit width over the length X	pound/feet
E	average rate of evaporation per unit area	pound/feet^2-second
E'	average rate of evaporation per unit area	inch/feet^2-day
E_t	total rate of evaporation	pound/second
L	length of evaporation surface	feet
N	form of Nusselt number -- by definition $N = \frac{E\sqrt{A}}{\Delta C\ \nu_e}$	dimensionless

Symbol	Definition	Units
R	Reynolds number -- by definition $R = \frac{U_o\sqrt{A}}{\nu}$	dimensionless
R_X	Reynolds number -- by definition $R_X = \frac{U_o X}{\nu}$	dimensionless
R_ξ	correlation coefficient	dimensionless
R_*	form of Reynolds number -- by definition $R_* = \frac{U_*\sqrt{A}}{\nu_e}$	dimensionless
S	shape factor of the surface from which evaporation takes place	dimensionless
T_{air}	temperature of the air	^oF
T_o	temperature of the evaporation surface	^oF
T_{AD}	temperature (model only) of the air as measured by the dry bulb of the forward tunnel psychrometer	^oF
T_{AW}	temperature (model only) as indicated by the wet bulb of the forward tunnel psychrometer	^oF
U	temporal mean wind velocity in horizontal plane -- a single subscript other than zero indicates the height above the surface in feet; a binary subsript indicates both the height above the surface in feet and the station at which the velocity was measured	feet/second
U_o	ambient wind velocity at height equal to or greater than δ	feet/second
U_{FT}	the mean wind velocity as measured at the forward tunnel location	feet/second
U_T	the mean wind velocity as measured by the traverse mechanism	feet/second
U_*	shear velocity -- by definition $U_* = \sqrt{\tau_o/\rho}$	feet/second
X	distance downstream from apparent leading edge of the test section	feet
γ	specific weight of dry air	pound/feet^3
δ	thickness of the boundary layer	feet
δ'	thickness of the laminar sub-layer	feet
δ_v	thickness of the vapor blanket	feet
ϵ	equivalent sand roughness	feet
ϵ_ℓ	equivalent sand roughness of the land surface	feet
ϵ_w	equivalent sand roughness of the water surface	feet
ν	kinematic viscosity of the air	feet^2/second

Symbol	Definition	Units
ν_e	coefficient of molecular diffusion for water vapor into air	feet^2/second
ξ	time	second
ρ	density of dry air -- subscript refers to elevation at which temperature was measured. Subscript zero denotes that the density is based on the temperature of the surface from which evaporation takes place	pound-second^2/feet^4
σ	Prandtl number -- by definition $\sigma = \frac{\nu}{\nu_e}$	dimensionless
τ_o	shear at surface	pound/feet^2
Γ	gamma function	--

Chapter II

THEORETICAL ANALYSIS

This Chapter is devoted to a review of the theoretical analysis and results which are presented in Part I of the Lake Hefner Final Report (3) along with the methods of adaptation of a work of O. G. Sutton (10) and a work of H. U. Sverdrup (11). The two objectives of interest in this project -- wind structure and evaporation -- will be treated separately.

Wind Structure

As indicated in Part I, the equation concerning wind structure resulting from the work of Prandtl and Kârmân was considered to be applicable to both the model and prototype wind profiles; that is

$$\frac{U_z}{U_*} = 5.75 \log \frac{z}{z_o} . \qquad (1)^1$$

As a result of the 1952 Testing Program, Figs. 1 and 2 were developed to demonstrate the correlations between the wind structures for the model and the prototype. A relationship between z_o and $U_{26.2\text{-Sta.}2}$ for the prototype, Fig. 3, was also evolved and was used in simplifying the expressions for the Kârmân extension of the Reynolds analogy which was employed in the evaporation phase of this study.

Evaporation

This section on evaporation will be devoted to a review of the Reynolds analogy which is presented in detail in Part I and to an exposition of the methods of adaptation to this study of a work of O. G. Sutton (10) and a work of H. U. Sverdrup (11).

---

1 Equations taken from Part I of the Lake Hefner Final Report (4) bear the same numbers that they had in Part I. All equations having a number which is less than 100 were taken from Part I. Equations originating in this report have been assigned numbers which are greater than 100. The reader is referred to Chapter I of this report for a delineation of symbols.

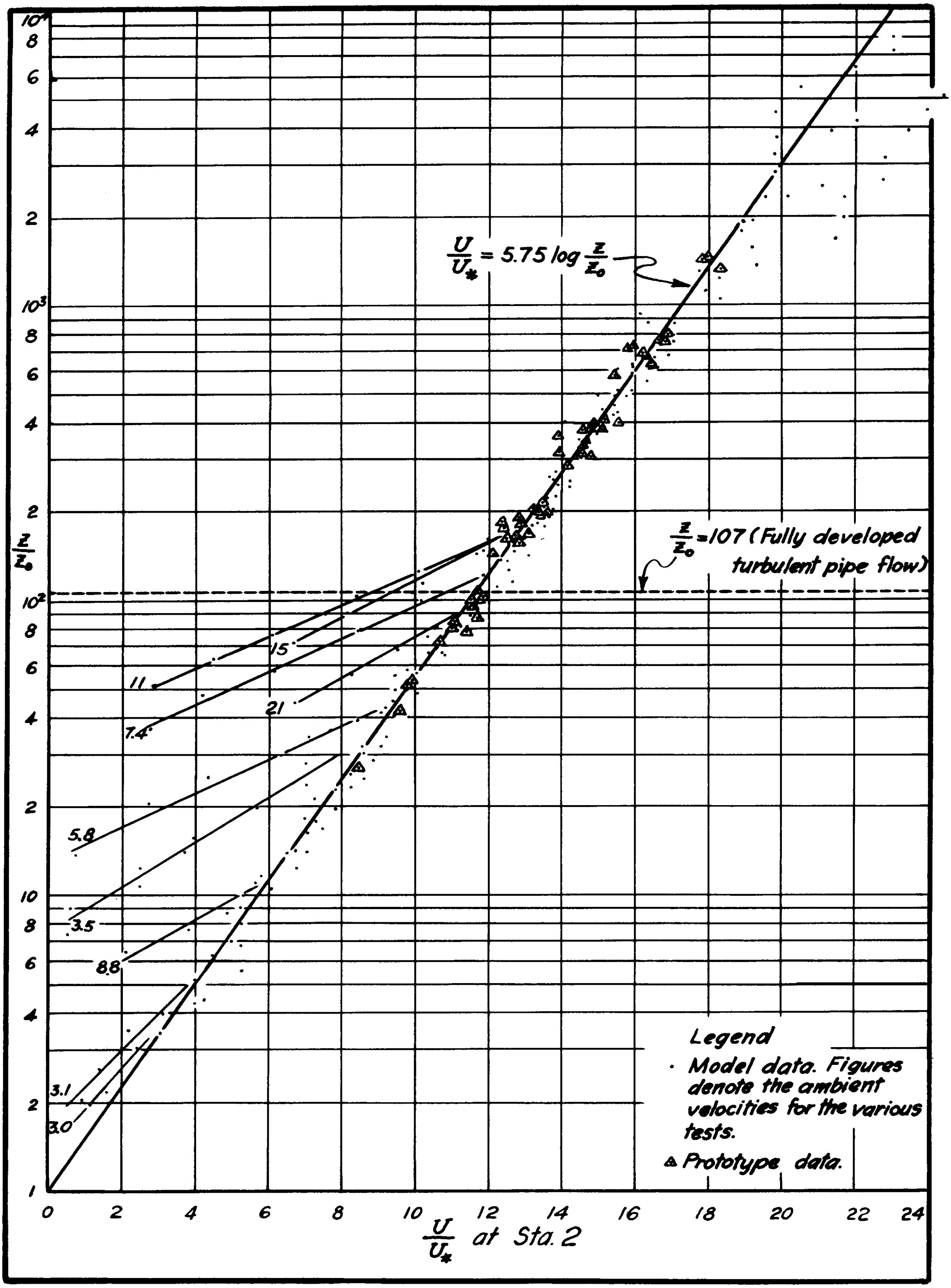

Fig. 1. Variation of z/z_o with U/U_* at Sta. 2.

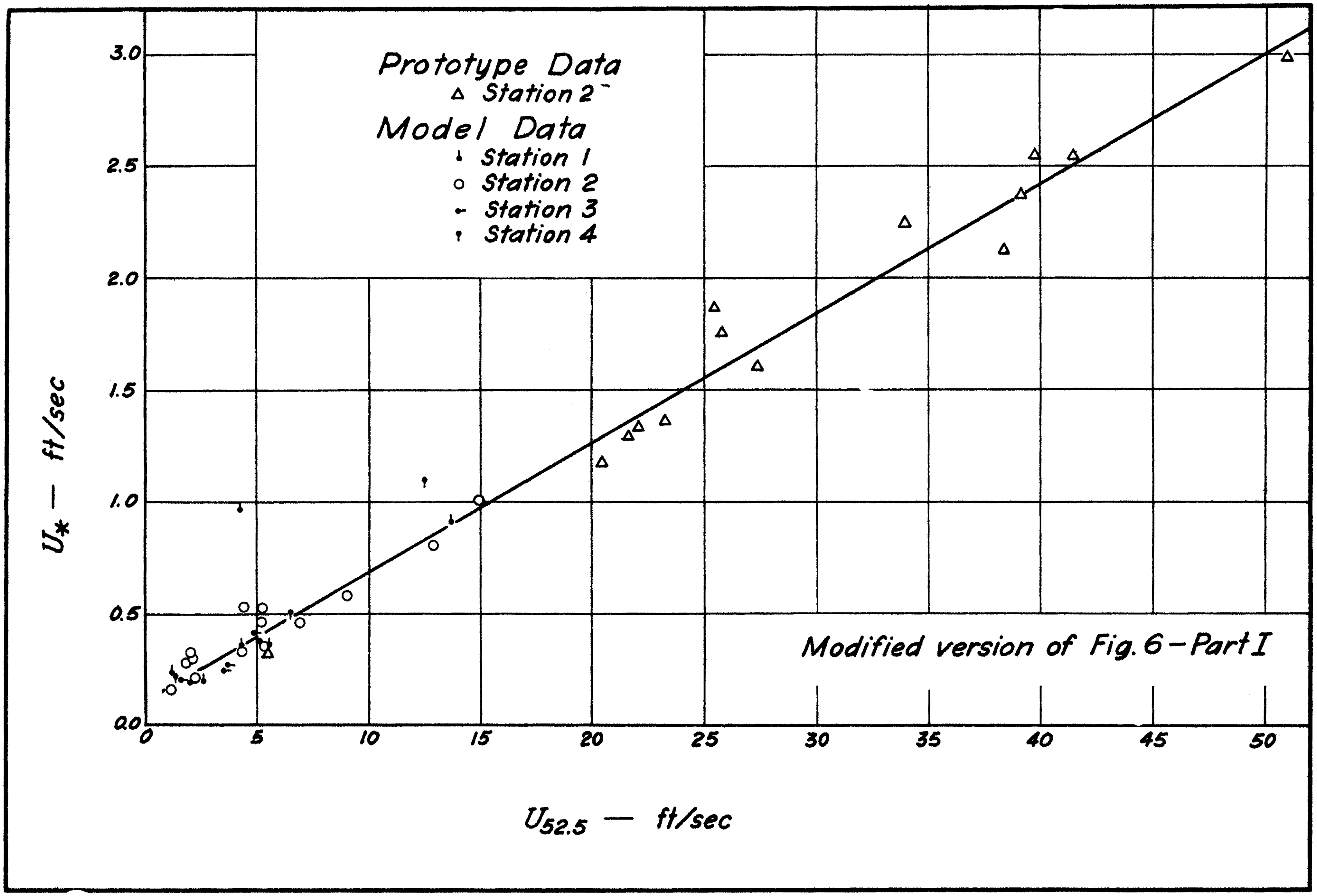

Fig. 2. Variation of U_* and $U_{52.5}$.

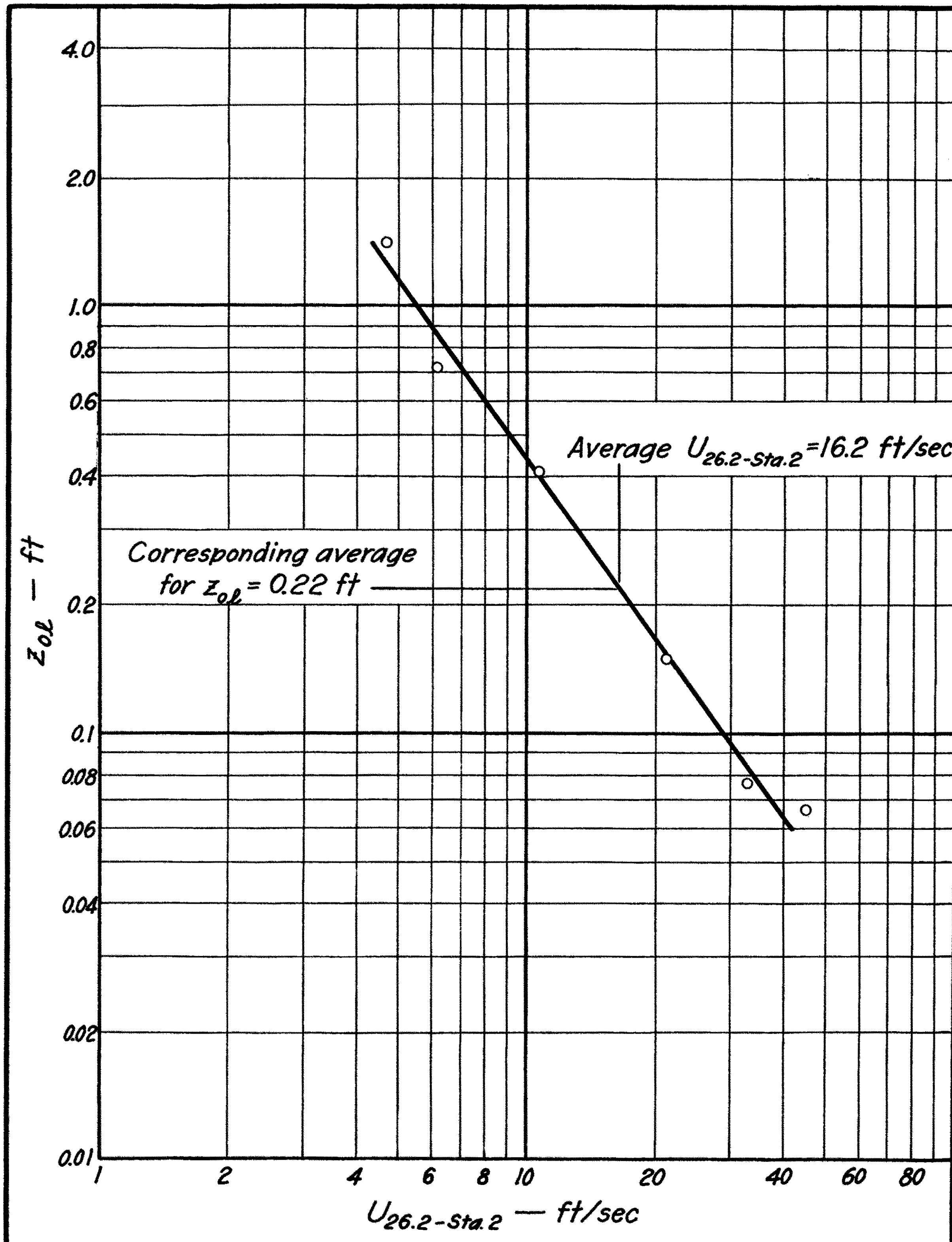

Fig. 3. Relation between $U_{26.2\text{-}Sta.2}$ and z_{ol} based on 1/2-hour prototype data.

Evaporation Correlation Derived on the Basis of the Reynolds Analogy.

The dimensional analysis in Part I indicated that the significant dimensionless parameters could be presented in the following simplified form:

$$N = \phi(R_*) \ . \tag{101}$$

With modeling techniques now known, $(R_*)_m$[1] and $(R_*)_p$ could not be made equal. In fact, the ratio of $(R_*)_m$ to $(R_*)_p$ is approximately equal to the scale ratio which in this study was 1:2000. The problem then existed of finding a sound basis for correlation of N and R_* for both model and prototype where the value of $(R_*)_m$ was approximately 1/2000 of $(R_*)_p$. Reynolds (7) postulated that an analogy exists between momentum transfer and mass transfer (evaporation in this case). With this in mind, recourse was made to the Kármán extension of the Reynolds analogy to arrive at a correlation between N and R_* over such a range as to include values of R_* for both model and prototype.

Briefly, this correlation was developed in the following manner. The relationship between N and a Reynolds number of the form of R rather than R_* is

$$N = \sigma C_e R \ . \tag{14}$$

In the case of zero longitudinal pressure gradient and turbulent flow with the presence of a laminar sub-layer, Kármán (4) expresses the Reynolds analogy between momentum transfer and mass transfer by

$$\frac{1}{C_e} = \frac{2}{C_f} + 5\left(\frac{2}{C_f}\right)^{\frac{1}{2}} \left\{ \sigma - 1 + 2.303 \log\left[1 + \frac{5}{6}(\sigma - 1)\right] \right\} . \tag{12}$$

In the case of zero longitudinal pressure gradient and completely turbulent flow with no laminar sub-layer, the analogy between momentum transfer and mass transfer may be expressed as

$$C_e = \frac{C_f}{2} \ . \tag{13}$$

The drag coefficient C_f has been evaluated in terms of R and other measurable variables for flow over solid boundaries. The application of appropriate

1 The subscript m and p refer to the model and prototype respectively.

velocity distribution laws permitted the expression of R in terms of R_* . An evaluation of several variables based on model and prototype conditions completed the work necessary to express N of Eq. 14 as a function of R_* for various ranges of R_* and for different surface roughnesses. The relationships between N and R_* evolved in this fashion are as follows:

Case I -- Smooth Boundary -- $10^3 \leq R_* \leq 10^5$

$$\frac{1}{N} = \frac{5.99}{(R_*)^{8/9}} - \frac{3.61}{R_*} \tag{22a}$$

Case II -- Smooth Boundary -- $R_* \geq 10^5$

$$\frac{1}{N} = \frac{0.0417}{R_*}\Big[4.68\,(1.194 + \log R_*)^{2.64} - 8.70\,(1.194 + \log R_*)^{1.32}\Big] \tag{24a}$$

Case III -- Rough Boundary -- $R_* \geq 10^5$

$$N = 0.0546\, R_* \,. \tag{26a}$$

The following data were available for testing the validity of the **Kármán** extension of Reynolds analogy:

1. Experimental data of Albertson (1),
2. Lake Hefner Model data collected in 1952 (3),
3. Approximation of the empirical Lake Hefner prototype equation (3) and (13)

$$N = 0.0203\, R_* \,, \tag{27}$$

4. Individual values of N versus R_* for the prototype data.

These data along with Eqs. 22a, 24a, 26a, and 27 are presented in Fig. 4.

This brief review of the 1952 analysis and results is presented in the way of background material for that which follows.

Evaporation Correlation Based on the Theory of O. G. Sutton (10).

Dimensional analysis, the Reynolds analogy, and experimental results have shown that an evaporation coefficient defined by N is dependent primarily upon the parameter R_* . As indicated in the preceding paragraphs, the Reynolds analogy furnishes a basis to correlate N and R_* for both the model

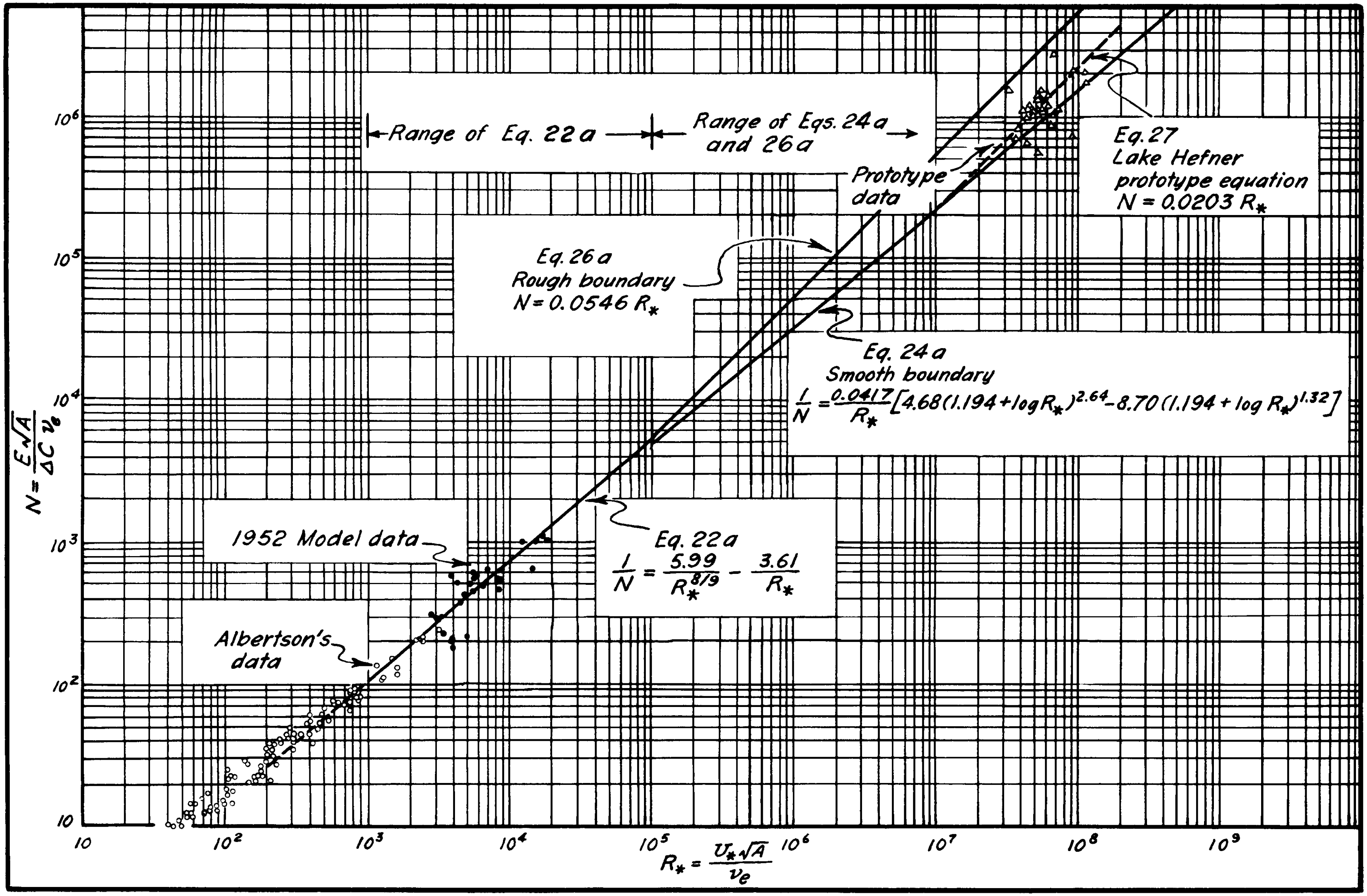

Fig. 4. Comparison of evaporation data with preliminary equations.

and prototype. Another approach to the comparison of N and R_* for the model and prototype is through the work of O. G. Sutton **(10)**.

In brief, the equations of evaporation from a smooth surface using the approach of Sutton are based upon the following reasoning:

1. The exchange coefficient A(z) is given by

$$\rho \overline{w'^2} \int_0^{t_o} R_\xi \, d\xi \tag{102}$$

where the correlation coefficient

$$R_\xi = \frac{\overline{w'(t)\ w'\ (t+\xi)}}{\overline{w'^2}} \,. \tag{103}$$

Bars indicate time averages.

2. The correlation coefficient is defined by Sutton to be of the form

$$R_\xi = \left(\frac{\nu}{\nu + \overline{w'^2}} \right)^n \tag{104}$$

where

$0 < n < 1.$

3. Using the mixing length theory

$$\overline{|w'|} = \ell \left| \frac{\partial U}{\partial z} \right| \tag{105}$$

and

$$\ell = k_o \frac{\left| \frac{\partial U}{\partial z} \right|}{\left| \frac{\partial^2 U}{\partial z^2} \right|} \,. \tag{106}$$

4. The distribution of eddy velocities is Maxwellian; therefore

$$\overline{w'^2} = \frac{1}{2} \pi \left(\overline{|w'|} \right)^2 \,. \tag{107}$$

From the foregoing relationships and taking $k_o = 0.4$, Sutton arrived at the result that

$$A(z) = \frac{(0.251)^{1-n}}{1-n} \rho \nu^n \left[\frac{\left(\left| \frac{\partial U}{\partial z} \right| \right)^3}{\left(\left| \frac{\partial^2 U}{\partial z^2} \right| \right)^2} \right]^{1-n} \tag{108}$$

since $A(z) = \rho \overline{w'\ell}$. Upon assuming that the variation of mean velocity with height follows a power law, that is

$$U(z) = U_1 \left(\frac{z}{z_1}\right)^{\frac{1}{q}} \tag{109}$$

and that

$$A(z) \frac{\partial U}{\partial z} = \text{constant}, \tag{110}$$

$\frac{1}{q}$ becomes $\frac{n}{2-n}$ and

$$A(z) = \left| \frac{(0.251)^{1-n} (2-n)^{1-n} n^{1-n}}{(1-n)(2n-2)^{2(1-n)}} \right| \rho \nu^n \frac{U_1^{1-n}}{z_1^{n-1}} \left(\frac{z}{z_1}\right)^{\frac{2(1-n)}{2-n}} \tag{111}$$

If the exchange coefficients for mass and momentum transfer are considered equal,

$$U(z) \frac{\partial C_A}{\partial x} = \frac{1}{\rho} \frac{\partial}{\partial z} \left[A(z) \frac{\partial C_A}{\partial z} \right] \tag{112}$$

can be solved when $U(z)$ and $A(z)$ are evaluated through Eqs. 109 and 111. The result is an expression for $C_A(x,z)$ which, when integrated over a circular area of radius r_o **(2:10)**, gives the total rate of evaporation as

$$E_t(r_o) = G' \, U_1^{\frac{2-n}{2+n}} \, r_o^{\frac{4+n}{2+n}} \tag{113}$$

where

$$G' = G \, \frac{2^{\frac{2}{2-n}} \sqrt{\pi} \, \Gamma\left(\frac{3+n}{2+n}\right)}{\Gamma\left(\frac{8+3n}{4+2n}\right)} , \tag{114}$$

$$G = \Delta C \left(\frac{2+n}{2-n}\right)^{\frac{2-n}{2+n}} \left(\frac{2+n}{2\pi}\right) \sin\left(\frac{2\pi}{2+n}\right) \Gamma\left(\frac{2}{2+n}\right) a^{\frac{2}{2+n}} z_1^{\frac{-n^2}{4-n^2}} , \tag{115}$$

$$a = \frac{\left(\frac{\pi}{2} k_o^2\right)^{1-n} (2-n)^{1-n} \, n^{1-n} \, \nu^n \, z_1^{\frac{n(n-1)}{2-n}}}{(1-n)(2-2n)^{1-n}} , \tag{116}$$

and

$$\Delta C = C_o - C_A .$$

Before $E_t(r_o)$ may be expressed in terms of R_* , the shear velocity must be introduced to replace U_1 . Since

$$\tau_o = A(z) \frac{\partial U}{\partial z} \tag{117}$$

and

$$U_*^2 = \frac{(0.251)^{1-n} \nu^n U_1^{2-n}}{(1-n)(2n-n)^{2-2n} (2-n)^n z_1^n}, \tag{118}$$

$$\frac{E_t}{\Delta C \ \nu \ r_o} = F(n,k_o) \left(\frac{U_* r_o}{\nu}\right)^{\frac{2}{2+n}} \tag{119}$$

where

$$F(n,k_o) = \frac{G' (1-n)^{\frac{1-n}{2+n}} \nu^{\frac{n}{2+n}} (2n-2)^{\frac{2-2n}{2+n}} (2-n)^{\frac{n}{2+n}}}{\Delta C \ z_1^{\frac{-n^2}{4-n^2}} \ \nu^{\frac{2n}{2+n}} \ z_1^{\frac{2n(n-1)}{(2+n)(2-n)}}} \tag{120}$$

If one assumes that $F(n,k_o)$ is the same for model and prototype, then

$$N_p = N_m \left[\frac{(R_*)_p}{(R_*)_m}\right]^{\frac{2}{2+n}} \tag{121}$$

The assumption that $F(n,k_o)$ is equal for model and prototype implies that the wind structure is similar in both cases and also that the prototype surface may be considered smooth.

Eq. 121 indicates that one model measurement carried out under conditions such that $q_m = q_p$ would be sufficient to evaluate N_p over the range of $(R_*)_p$ for which $q_m = q_p$ = constant.

The 1937 Evaporation Equation of H. U. Sverdrup (**11**).

In an attempt to obtain additional correlations between N and R_*, the evaporation equation proposed in 1937 by H. U. Sverdrup (**11**) which gave a good approximation to the Lake Hefner prototype data (**13:65**) was examined.

The equation by Sverdrup (**11:13**) may be written as follows in the notation consistent with that of this report:

$$E = \frac{0.623}{p_a} \frac{\gamma(e_o - e_z)}{\frac{1}{k_o U_*} \ln\left(\frac{z + z_o}{\delta' + z_o}\right) + \frac{\delta'}{\nu_a}} . \tag{122}$$

The salient elements of the hypothesis leading to Eq. 122 are as follows:

1. A laminar sub-layer exists for both rough and smooth surfaces,
2. The exchange coefficient $A(z)$ is a linear function of height above the surface, depends upon the roughness -- i.e., $A(z) = \rho k_o(z+z_o)U_*$, and is the same for the transport of mass and momentum,
3. The vapor pressure is a logarithmic function of the height z.

Application of Eq. 122 to a smooth surface. For a smooth surface Sverdrup (11:6 and 8) suggested the use of the following relationships:

$$\delta' = \frac{30\nu}{U_*} \tag{123}$$

and

$$z_o = \frac{\nu}{k_o U_*} - \delta' . \tag{124}$$

In the present report the authors reason as follows in evaluating z and introducing ΔC in Eq. 122. The value of z is considered to correspond to the average thickness of the vapor blanket over the evaporation surface. Assuming that the vapor boundary layer thickness δ_v is given by the same equation as that for the momentum boundary layer, one may write

$$\delta_v = \frac{0.377}{\left(\frac{U_o x}{\nu}\right)^{1/5}} . \tag{125}$$

Introducing the relationship that R is equal to $11.85\ R_*^{10/9}$ obtained by letting $\left(\frac{x}{\sqrt{A}}\right)^{1/9}$ equal one in Eq. 17 (3), integrating over the entire length, and taking a mean

$$(\delta_v)_{ave.} = 0.1275\ R_*^{2/9} \tag{126}$$

When $(\delta_v)_{ave.}$ as given by Eq. 126 is substituted for z in Eq. 122 and k_o is set equal to 0.4, the following relationship results:

$$N = \frac{R_*}{2.5 \ln (0.085\ R_*^{7/9} - 11) + 18} \tag{127}$$

Maintaining the approach of Sverdrup, but substituting for Eqs. 123 and 124 the following:

$$\delta' = \frac{11.5\nu}{U_*} \tag{128}$$

and

$$z_o = \frac{\delta'}{107} \text{ respectively,} \qquad (129)$$

Eq. 122 reduces to

$$N = \frac{R_*}{2.5 \ln(0.01832\, R_*^{7/9} + 0.00932) + 6.9} . \qquad (130)$$

Eqs. 128 and 129 are based upon the work of Nikuradse (6) and give the following apparent improvements:

1. z_o will be positive instead of negative,
2. The exchange coefficient $A(z)$ at $z = \delta'$ becomes $4.64\,\nu$ instead of ν.

Since the surface of the model may be considered to be hydrodynamically smooth, one might anticipate that Eqs. 127 and 130 are applicable to the model.

Application of Eq. 122 to a rough surface. When the surface is rough, Sverdrup suggested that z_o be considered equal to 0.6 cm and δ' be evaluated through Eq. 123. When z of Eq. 122 is considered to be equal to $(\delta_v)_{ave.}$ which is evaluated through Eq. 126, (the authors modification of the work of Sverdrup), Eq. 122 becomes

$$N = \frac{R_*}{2.5 \ln\left(\dfrac{\dfrac{0.1275}{R_*^{2/9}} + \dfrac{0.06}{\sqrt{A}}}{\dfrac{18}{R_*} + \dfrac{0.06}{\sqrt{A}}}\right) + 18} , \qquad (131)$$

where $\sqrt{A}$ is to be measured in meters.

If the prototype lake surface is considered rough (13:49), one might expect Eq. 131 to coincide with the prototype results.

Chapter III

EQUIPMENT AND PROCEDURES

This Chapter is devoted to a very brief description of the equipment used and the procedures followed in the 1953 Testing Program. The equipment and procedures are very similar to those used during the 1952 Testing Program. Only minor changes have been made and these appear in detail in Appendix A of this report. The reader is referred to Part I (3) for details not covered in this report.

Equipment

A model of Lake Hefner was built to a scale of 1:2000 in both the horizontal and vertical directions and was tested in a low-velocity wind tunnel. This wind tunnel is of the recirculating type but was used as a non-recirculating tunnel to avoid the effect of evaporation on vapor concentration under recirculating conditions. The test section was 9 ft square and 26 ft long. In order to prevent water losses due to waves and splashing, an evaporation surface made of plaster of Paris was used. This surface developed dry spots as did the surface used during 1952. Cognizance was taken of this fact in the determination of the area from which evaporation took place.

The hot wire anemometer circuits used for the 1952 Testing Program were revised to accommodate sensing elements made of platinum wire instead of the tungsten wire used in 1952. As in 1952, most of the thermometry was carried out with copper-constantan thermocouples. This also included the use of thermocouples for psychrometers. The automatic and manual water supply systems for the lake used in 1952 were used again in 1953.

The data comprising the 1952 Testing program were for a simulated south wind. The model was rotated 180° so that the air passing over the model simulated a north wind during the 1953 Testing Program. Two sheet metal barriers, one $1\frac{1}{2}$ in. high and the other 3 in. high, were placed in the tunnel at various positions upstream from the modeled lake so as to disturb the wind structure over the modeled lake.

Testing Procedures

The procedures followed in gathering data for the 1953 Testing Program were similar to those f lowed during the 1952 Testing Program. In brief these consisted of:

a. Taking temperature data at various times and places in and about the model,

b. Measuring temperature, humidity, and velocity profiles above various locations on the model,

c. Measuring the ambient air temperature, humidity, and velocity at various times, and

d. Measuring the amount of water evaporated from the model.

A summary of the model data collected during the 1953 Testing Program appears in Appendix B. The detailed data are presented in Appendix D.

Transformation of Data

As a result of the work grouped under what might be termed the 1953 Testing Program, additional correlations between N and R_* besides those stemming directly from the 1953 testing were derived on the basis of other evaporation investigations. The methods used in analyzing and interpreting these data were for the most part the same as those used for the 1952 data. These methods are explained in detail in Part I. This section will be devoted to a brief description of changes in the methods of analysis. These same changes are described in detail in Appendix C of this report.

Shear Velocity

During the course of the work under what is termed the 1952 Testing Program, the shear velocity U_* was obtained by the use of the Prandtl-Kármán relationship for wind structure; namely,

$$\frac{U}{U_*} = 5.75 \log \frac{z}{z_o} . \quad (1)$$

This same procedure of evaluating U_* was followed in working with the 1953 data to determine the effect of wind direction on evaporation when no barrier was placed upstream from the modeled lake. This method of computing U_* was found to be satisfactory when an upstream barrier was not placed in the tunnel; however, when an obstruction was placed in the tunnel, the velocity profile data downstream from the obstruction indicated that the wind structure was so modified that Eq. 1 was no longer valid, Fig. 5. Therefore, another method of determining U_* was resorted to so that U_* for obstructed flow would correspond to that for flow without a barrier present. The authors assumed that the shear, and therefore the shear velocity, would have a particular value for each ambient tunnel velocity, U_{FT} . A relationship between U_* at Sta. 6 and U_{FT} was developed for the condition when no barrier was present, Fig. 6. This relationship was based on an evaluation of the loss in the momentum of the air stream due to the boundary drag at the various velocities when a barrier was not placed in the wind tunnel. Details of this procedure are presented in Appendix C.

The object of referencing the barrier evaporation data to a U_* based on unobstructed air flow was to isolate the total effect upon evaporation rates which the barriers might cause -- the total effect being a result of a combination of changed shear velocity at the reference station and a changed shear velocity distribution over the lake for the same ambient velocity which existed with no barrier present. Comparison of evaporation data obtained with and without barriers should then reveal any significant effects. Since the relationship of Fig. 6 had to be developed for the barriers, it was found to be advantageous and convenient to determine U_* for all of the 1952 and 1953 data through the use of the correlation between U_* and U_{FT} depicted in Fig. 6.

<u>1953 Model Data</u>

The data collected during the 1953 Testing Program were in such a form that the parameters N and R_* were easily evaluated. The reader is referred

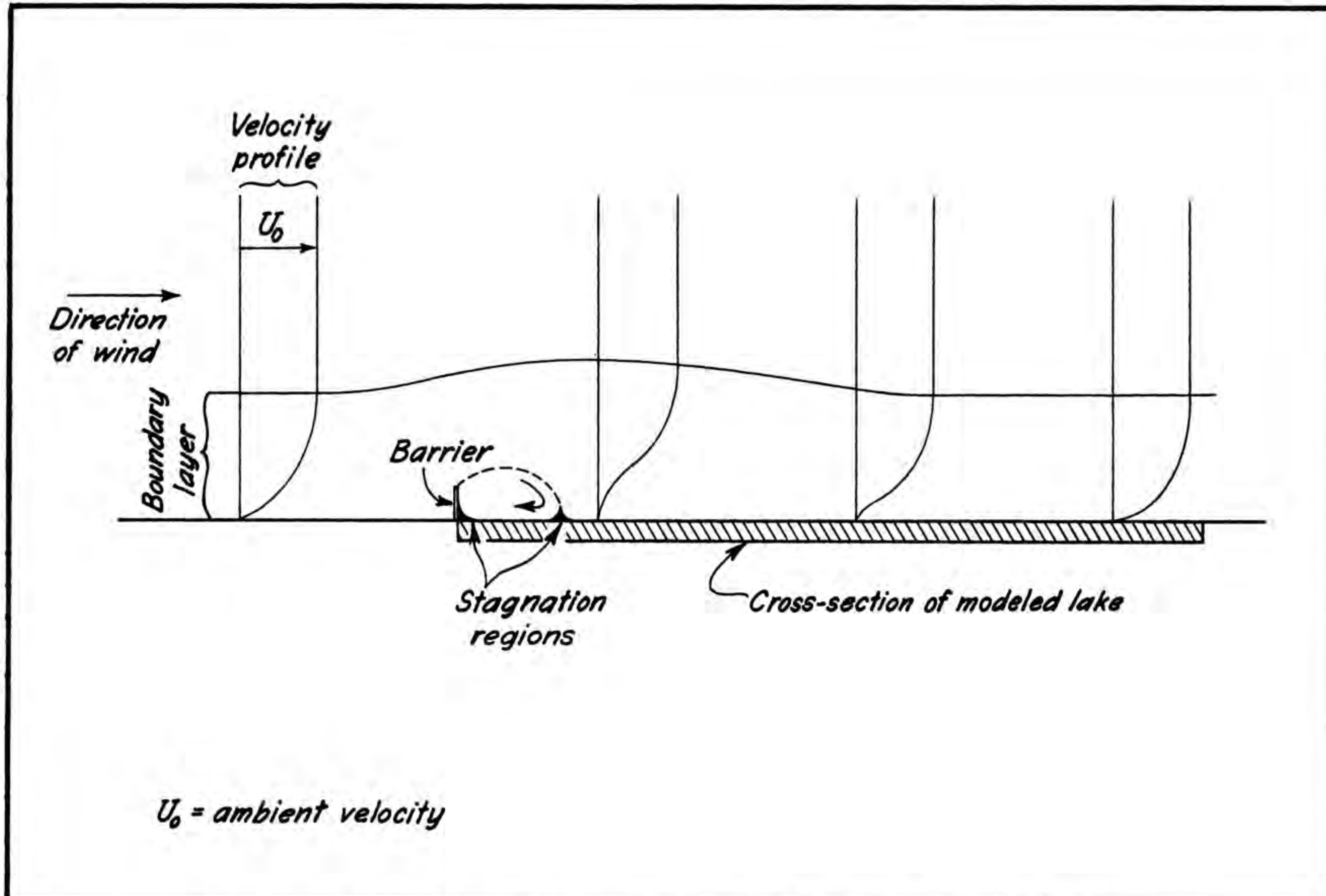

Fig. 5. Schematic diagram of air pattern over modeled lake under the influence of a barrier.

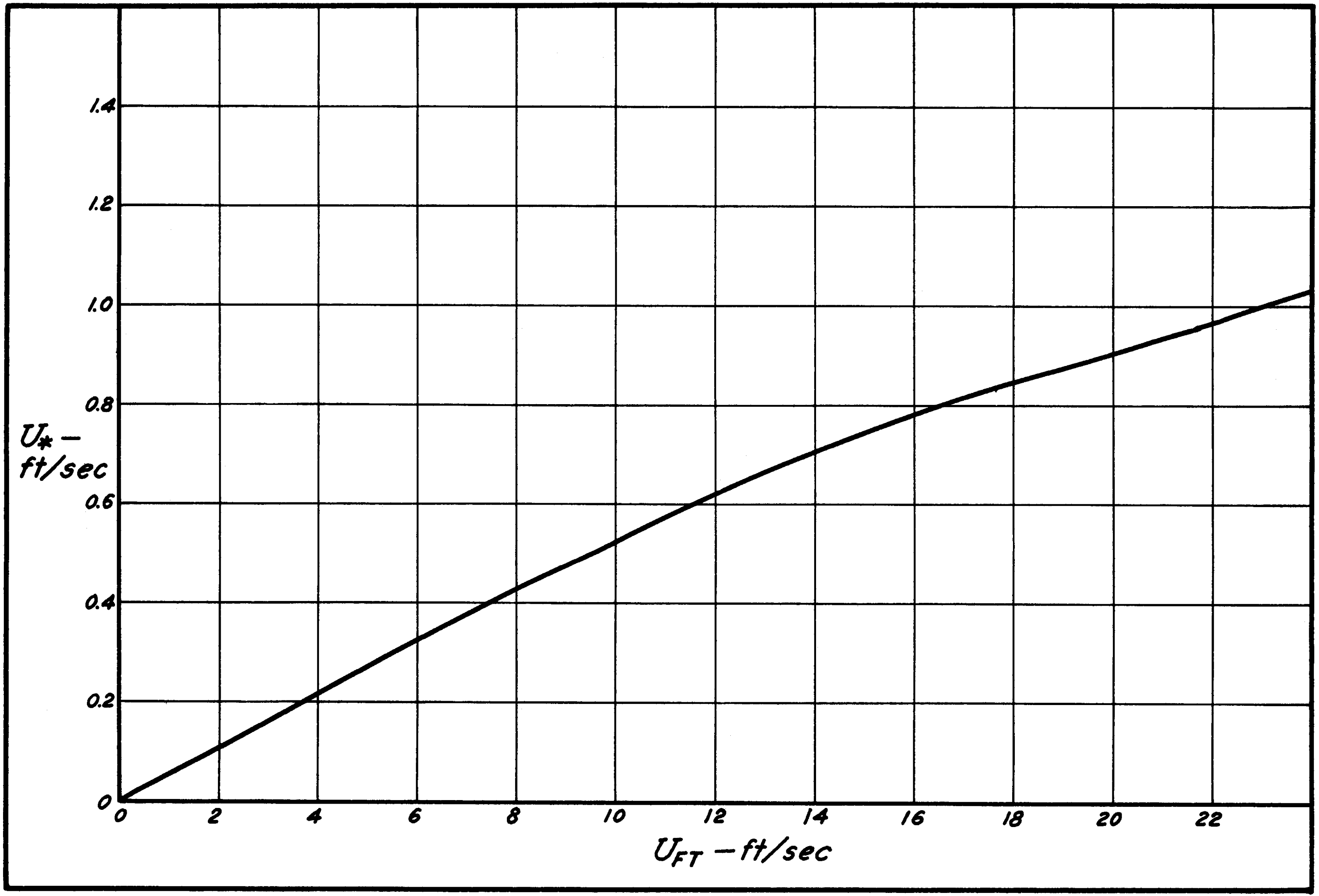

Fig. 6. Variation of U_* with U_{FT} based on momentum relation.

to Part I (3) for details of the methods. These data are summarized in Appendix B and presented in detail in Appendix D.

Data of Rohwer (8)

In order to check the Reynolds analogy approach for the range R_* between values covered by the Lake Hefner model data and prototype data, certain data were selected from those collected by Rohwer in 1926 and 1927. This check was made possible through the courtesy of Mr. Rohwer in making available the original data of his early work.

Rohwer's data were collected for a circular tank 84.8 ft in diameter and 6.66 ft in depth. All points obtained from the data were calculated with elements averaged over a 6-hr period. Periods representing all parts of the day were used with no systematic deviations appearing for any particular part of the day.

The variables comprising N and R_* were evaluated in the following manner:

E -- The amount of evaporation per unit area per unit time was obtained by first taking the difference in readings at the beginning and end of a period for each of four micrometer hook gages placed symmetrically about the periphery of the tank. The four differences for a given period were then averaged to obtain the water surface drop. This drop -- measured to the nearest 0.001 in. -- was then divided by the length of the period.

ΔC -- The value of C_o was obtained through a consideration of the water surface temperature measured by means of a mercurial thermometer held with the bulb $\frac{1}{2}$ in. under the surface and the entire thermometer shielded from direct sunlight. Air temperature and humidity were measured above the water surfaces of the 84.8 ft diameter tank and three evaporation pans of conventional size and shape. These latter measurements were accomplished by means of an aspirating psychrometer which drew air through a rubber tube having its open end about 1 in. from the water surface. The four sets of readings differed and that pair giving the greatest temperature difference was used in evaluating C_A. The thermometer pair yielding this condition was usually the upwind installation.

ν_e -- The value of ν_e was obtained from tables using the mean ambient air temperature of the period and a barometric pressure of 25.0 in. of mercury.

U_* -- The shear velocity was calculated from mean velocity readings at two elevations by assuming a logarithmic relationship and a **Kármán** constant of 0.4. The velocity for the higher elevation was taken from the data for an anemometer 2.5 ft above the ground (bridge anemometer) and mean values of the velocity were obtained from readings taken at the beginning and end of the period which gave the miles of wind passing during that period. Each mean velocity was corrected according to the correction table for 4-cup anemometers given in Ref. **12.** The lower velocity was taken as the ground velocity at a height of 0.25 ft and was considered to be that velocity determined through use of Fig. 9 in Ref. **8:49** and the higher level velocity.

$\sqrt{A}$ -- Since the evaporation took place from a circular area having a constant diameter of 84.8 ft, the variable $\sqrt{A}$ likewise had a constant value of 75.3 ft.

These data are presented in Appendix B.

<u>Sutton's Evaporation Equation</u> (**10**)

A correlation between N and R_* in the model data range of R_* was obtained by the use of Eq. 119 of Sutton's work. However, before an attempt was made to apply this equation, it was necessary to select a representative value of n for the model. After plotting vertical velocity profiles using log-log coordinates for the range of ambient velocities encountered in the model, the conclusion was reached that the exponent q of Eq. 109 varied from 3 at the lowest velocities to about 6.5 at the highest velocities. The median value of q for the model tests corresponded to about a value of 6 which made $n = \frac{2}{7}$.

When the foregoing value for n was adopted and k_o was set equal to 0.4, Eq. 119 as herein applied to the model reduced to

$$N = 0.220\, R_*^{\frac{7}{8}} \qquad (132)$$

where $\nu = 0.6\ \nu_e$ and $r_o = \frac{\sqrt{A}}{\sqrt{\pi}}$ was introduced.

In order to check the indicated correlation between model and prototype data given by Eq. 121, a value of n common to a model test and the prototype conditions was determined. From the measurements at Lake Hefner (13:60), the range of q for the prototype was from 5.72 to 6.66. A value of q = 6 seemed to be representative. When a value of q equal to 6 was considered representative of both model and prototype conditions and substituted into Eq. 121, there resulted the expression

$$N_p = N_m \left[\frac{(R_*)_p}{(R_*)_m}\right]^{\frac{7}{8}}. \qquad (133)$$

Eq. 133 may be reduced to computational form by selecting a set of coordinates (R_{*m} , N_m) for which q is approximately 6. Analysis of the data indicated that the value of q for the middle of the range of R_* for the model is approximately 6. When the model coordinates, $R_* = 7x10^3$ and $N = 5.6x10^2$ based on Fig. 4, were selected, Eq. 133 became

$$N_p = 0.243\, R_{*p}^{\frac{7}{8}}. \qquad (134)$$

<u>Sverdrup's Work of 1937</u> (**<u>11</u>**)

In Chapter II the steps necessary to put the work of Sverdrup into the dimensionless parameters, N and R_* , were indicated. The results of those transformations, Eqs. 127 and 130 for a smooth boundary (model) and Eq. 131 for a rough boundary (prototype), are in suitable form for comparison purposes.

Chapter IV

PRESENTATION AND DISCUSSION OF RESULTS OF THE 1953 TESTING PROGRAM

The object of the 1953 Testing Program was to supplement the data gathered during the 1952 Testing Program. This supplementary information pertains to the effect of upstream barriers on evaporation, the effect of the dam on evaporation from the model of Lake Hefner, and the work and data of other investigators which might indicate the applicability of the Kármán extension of the Reynolds analogy to evaporation as presented in Chapter II. This Chapter is devoted to a discussion of the results of the experiments conducted during the 1953 Testing Program.

Shear Velocity

As indicated in Chapter III the shear velocity was computed on the basis of both Eq. 1 and the loss of momentum. This was necessitated by the consideration of the barrier effects. The final results will all be presented in terms of U_* computed on the basis of the loss of momentum.

Upstream Barrier Effect on Evaporation

Mountains surround many lakes and reservoirs and the effect of these topographic features on evaporation rates is not fully understood. In a wind tunnel where conditions can be controlled, the effect of obstructions can be measured. Therefore, it was decided to place an obstruction upstream from the model and measure the effect of this structure on evaporation rates. If the barrier affected the evaporation rates in a systematic fashion for various sizes and positions of the barrier, then additional work regarding model and prototype correlations could be undertaken to determine in more detail the effects of these obstructions on evaporation rates. The object of these tests on the Lake Hefner model were strictly of an exploratory nature.

In order to investigate the effect of upstream barriers on the rates of evaporation from the model, two barriers were adopted: one was $1\frac{1}{2}$ in. high and the other was 3 in. high. These barriers corresponded to prototype heights of 250 ft and 500 ft respectively and were placed on the dam and at various distances upstream from the dam. It should be remembered that the shear velocities used for comparison purposes of the barrier data were based on the relationship depicted in Fig. 6, Chapter III.

The effect of the $1\frac{1}{2}$-in. barrier on evaporation is indicated in Fig. 7. The data group well about Eq. 22a, except in the vicinity of R_* equal to 3.2×10^3 where the data are slightly above the line. The effect of the 3-in. barrier on evaporation is indicated in Fig. 8 and the manner of grouping of these data is the same as that for the $1\frac{1}{2}$-in. barrier. The data for both the $1\frac{1}{2}$-in. and 3-in. barriers are plotted in Fig. 9.

The small difference between the barrier data and Eq. 22a, Fig. 9, in the vicinity of R_* equal to 3.2×10^3 might be explained by a consideration of the range of R_X under which the tests were conducted. As indicated in Fig. 22, Appendix C, the conditions under which some of the tests were conducted typified the transition zone between laminar flow and turbulent flow where it is possible to have laminar flow, turbulent flow, or a type of flow that can not be described as either. Within this region one might expect some of the results to differ from those for completely turbulent conditions.

Lake Hefner model data collected at the lower wind velocities are associated with the lower values of R_* and occupy the transition zone between laminar and turbulent flow. Therefore, the slight deviation from Eq. 22a of the data in Fig. 9 at the lower values of R_* may be expected and hence, dismissed because of non-conformity with the assumptions used in the derivation of Eq. 22a. Eq. 22a was derived on the basis of a fully-developed turbulent boundary layer above a smooth surface.

On the basis of Fig. 9, one can say that there does not appear to be any significant difference between either the data for the $1\frac{1}{2}$-in. barrier and those for the 3-in. barrier or between the barrier data and Eq. 22a. Therefore, Eq. 22a may be considered as representative of the model data when an upstream barrier is present. The reader is reminded that Eq. 22a was also found to be representative of the 1952 model data, Fig. 4.

The lack of barrier effect on evaporation rates might be explained in light of the effect of the barrier on the wind structure. Separation occurs at the top edge of the barriers and this induces increased turbulence in the downwind air stream. The work of Maisel and Sherwood (5) indicates that increased evaporation accompanies increased turbulence intensity. Therefore, one might expect increased rates of evaporation as a result of the introduction of the barrier upstream from the model.

Fig. 5 of Chapter III indicates that zones of stagnation and a region of reduced velocity can be found immediately downstream from the barrier. By this action, the effect of the barrier would be to reduce the amount of evaporation from certain areas. Therefore, as a result of the presence of a barrier, two opposing effects on the wind structure are occurring simultaneously; one tends to increase the evaporation, and the other tends to decrease the evaporation. Data gathered during the course of this investigation indicate that the two effects cancel each other.

Best-fit lines were determined by the method of least squares for all of the model data. The data for 1952 were considered to be representative of non-barrier conditions. The data for 1953 were obtained with the 3/4-in. model dam upwind from the lake which may be thought of as a barrier; amplification of the data for 1953 can be found in the following paragraphs. The $1\frac{1}{2}$-in. and 3-in. barriers were studied to determine the influence of higher barriers upwind from the evaporation surface. The best-fit lines for these data did not vary consistently with the height of the barrier. In fact, all differences were within the scatter of experimental error. Therefore, Eq. 22a was considered to be satisfactorily representative of all the data obtained with the barriers in place.

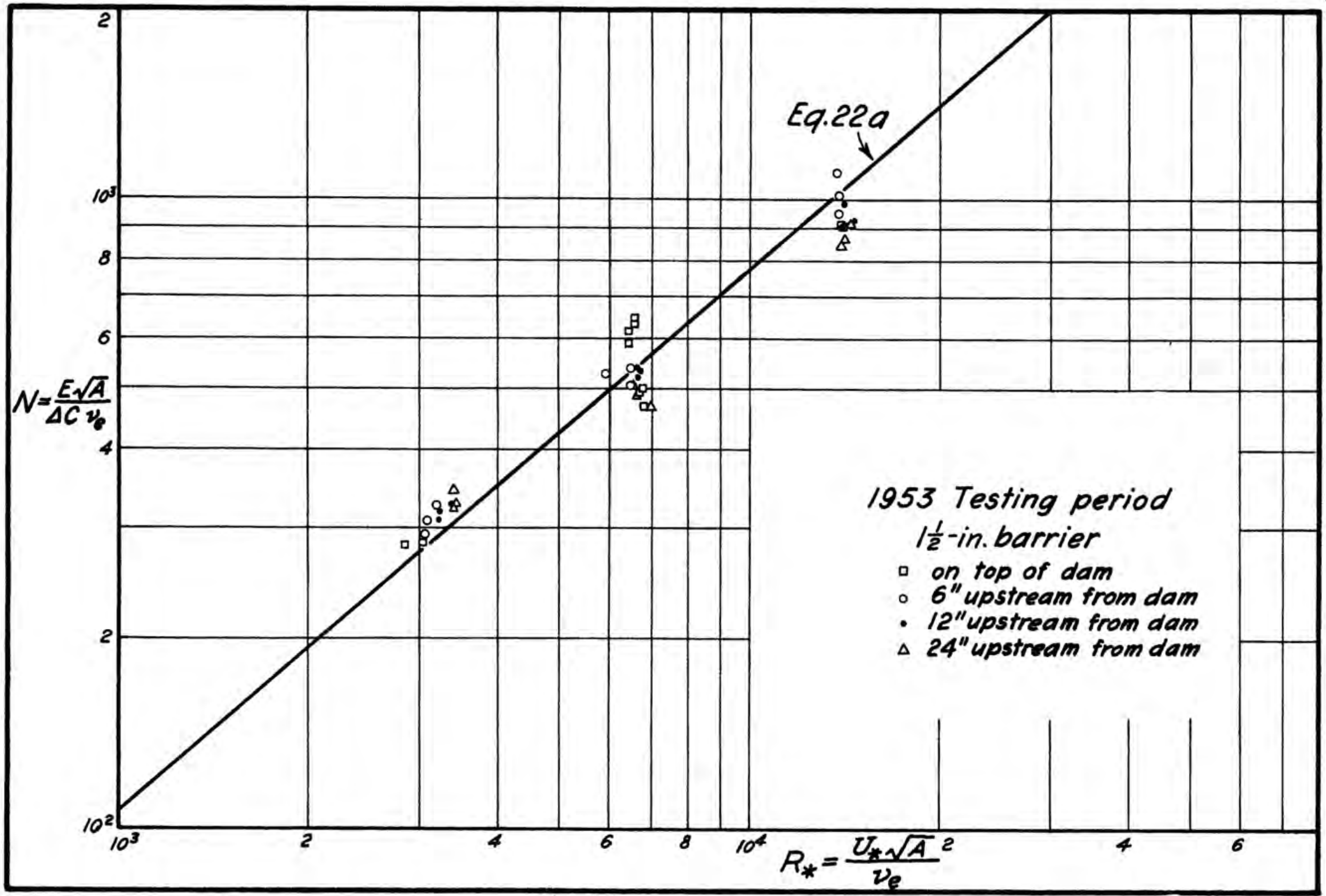

Fig. 7. Effect of 1½-in. barrier on evaporation.

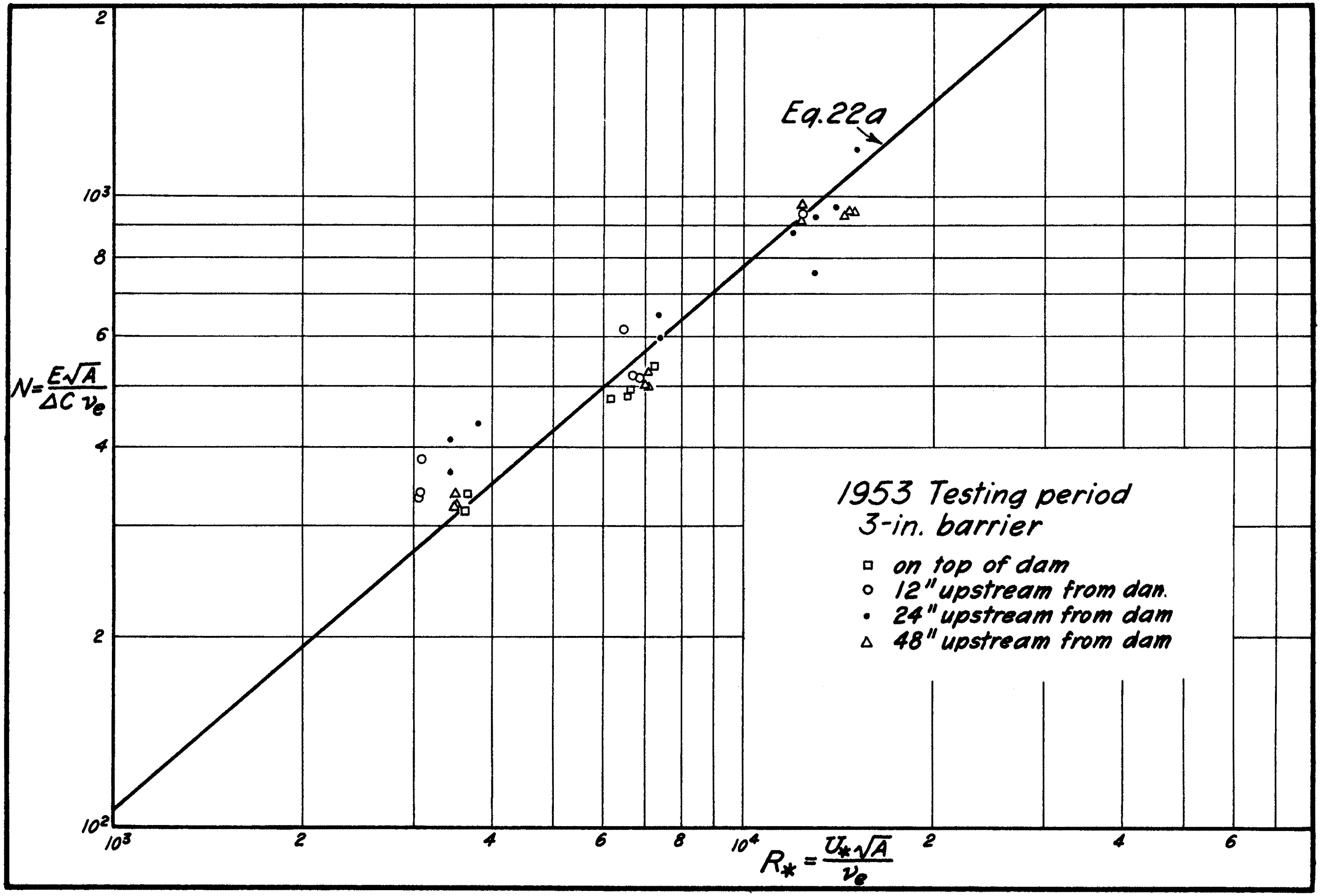

Fig. 8. Effect of 3-in. barrier on evaporation.

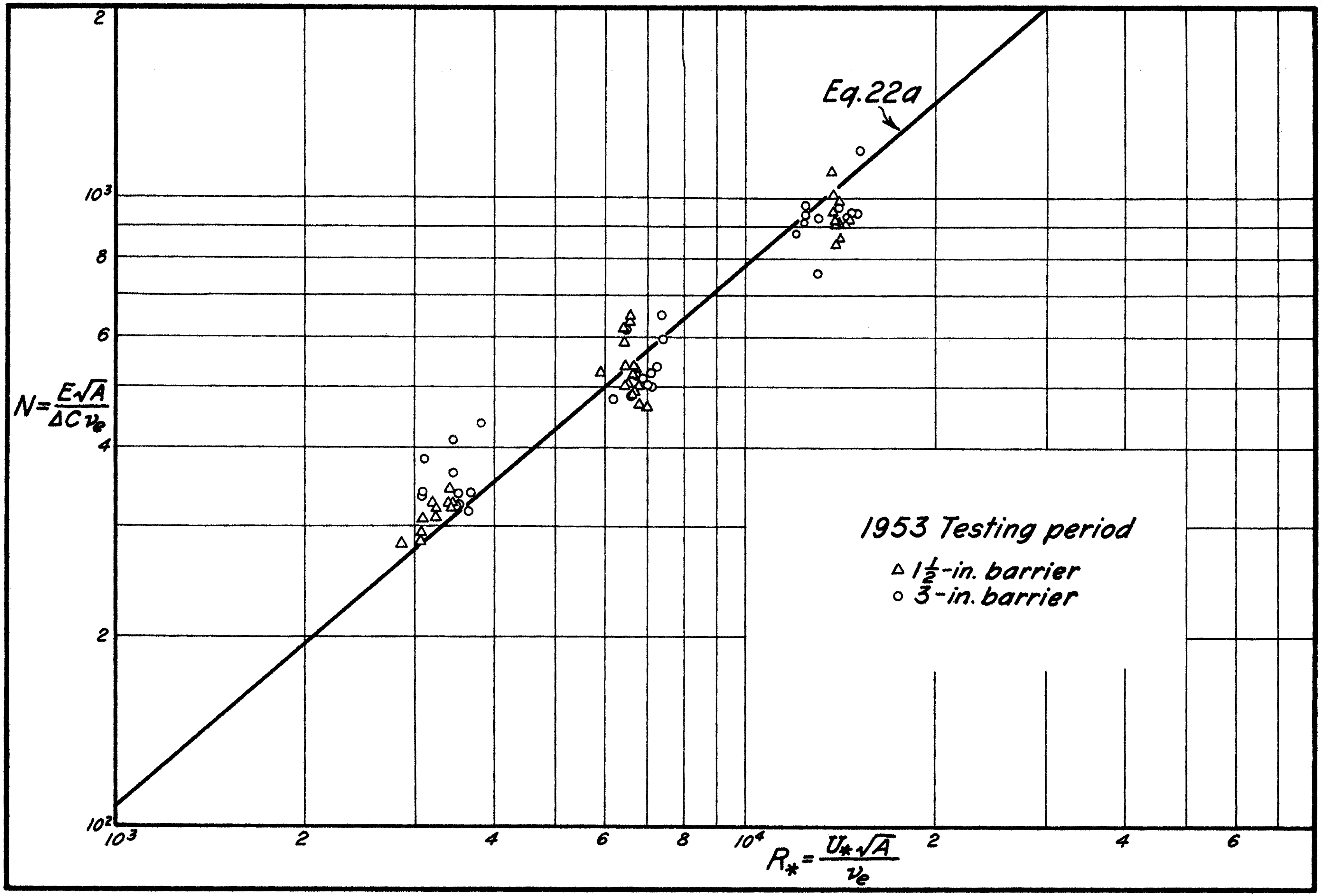

Fig.9. Comparison of barrier effects.

The barriers affected the results in such a fashion as to eliminate some of the scatter of the data. This is in all likelihood due to the more completely developed turbulent boundary layer caused by the barrier.

Effect of Wind Direction on Evaporation from the Model

The air blown over the model simulated a south wind during the 1952 Testing Program. One of the objectives of the 1953 Testing Program was to determine if the change in direction of the wind from the south to the north would have any effect on the correlations between N and R_* .

The correlation between N and R_* might be altered by a change in the wind direction because of two effects. First, the character of the approach terrain may differ for various wind directions in which case, the air pattern over the modeled lake might not be the same. Second, the maximum distance across the modeled lake normal to the direction of the wind might vary with different wind directions. With regard to approach terrain, the 180° change in wind direction is the severest that can be brought about with the Lake Hefner model because the terrain approaching the lake from the south is relatively flat with no abrupt changes in ground slope while the slope of the terrain approaching the lake from the north is suddenly broken by an earth dam, 70 ft high. This dam impounds the water of Lake Hefner. Therefore, if a change of wind direction were to have any effect on the evaporation, one might anticipate a systematic deviation between the results for a south wind and a north wind.

South Wind

The results of the 1952 Testing Program, during which the wind was from the south, are presented in Fig. 10. The shear velocity U_* for the data presented in Fig. 10 was computed on the basis of the Prandtl-Kármán equation, Eq. 1. These same data recomputed on the basis of change of momentum considerations are presented in Fig. 11. A review of both Figs. 10 and 11 indicates that the scatter of the data computed through loss of momentum considerations is less than that through Eq. 1. At the lower values of R_* , Fig. 11, the

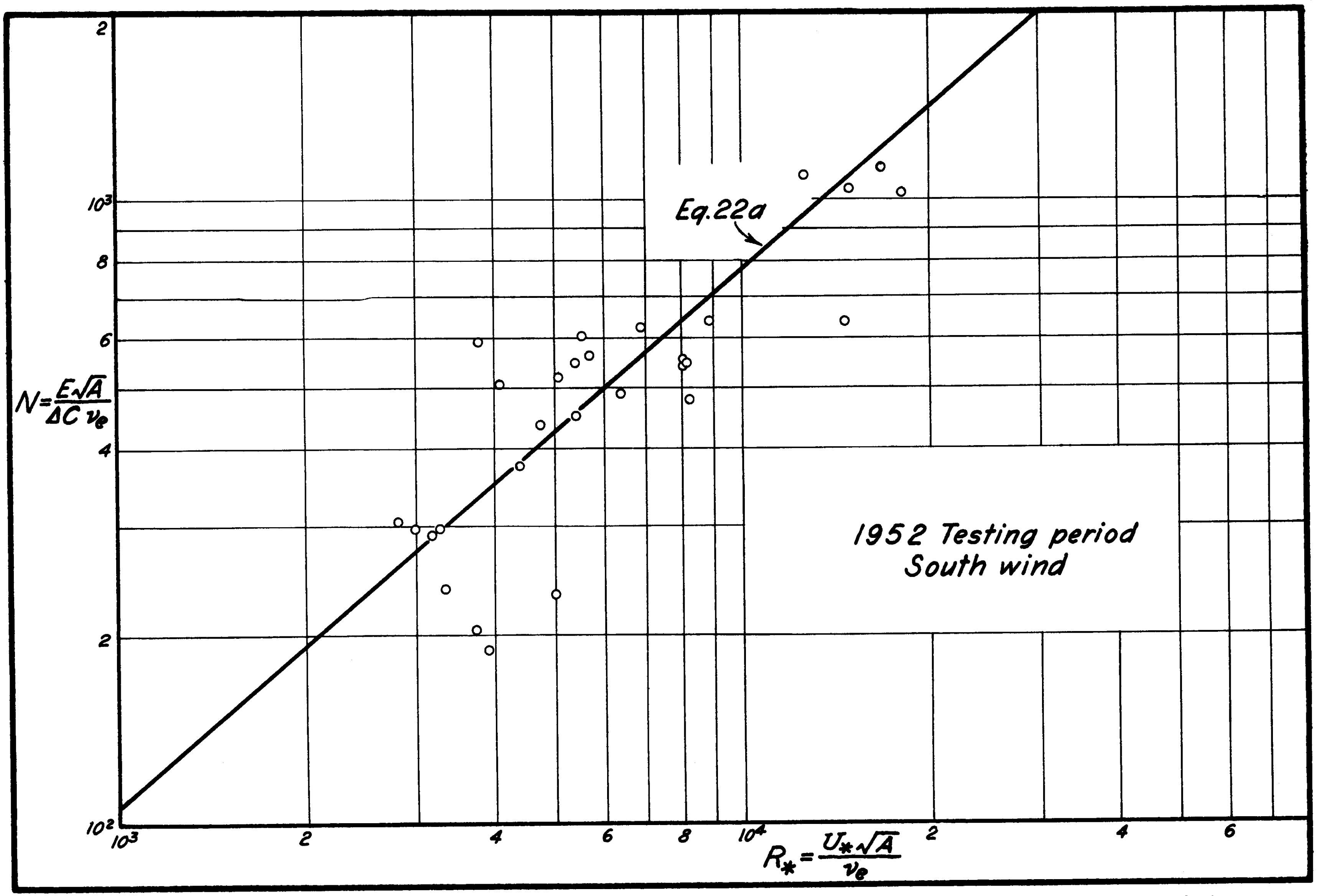

Fig. 10. Variation of N with R_* based on Prandtl-Kármán equation — 1952 data.

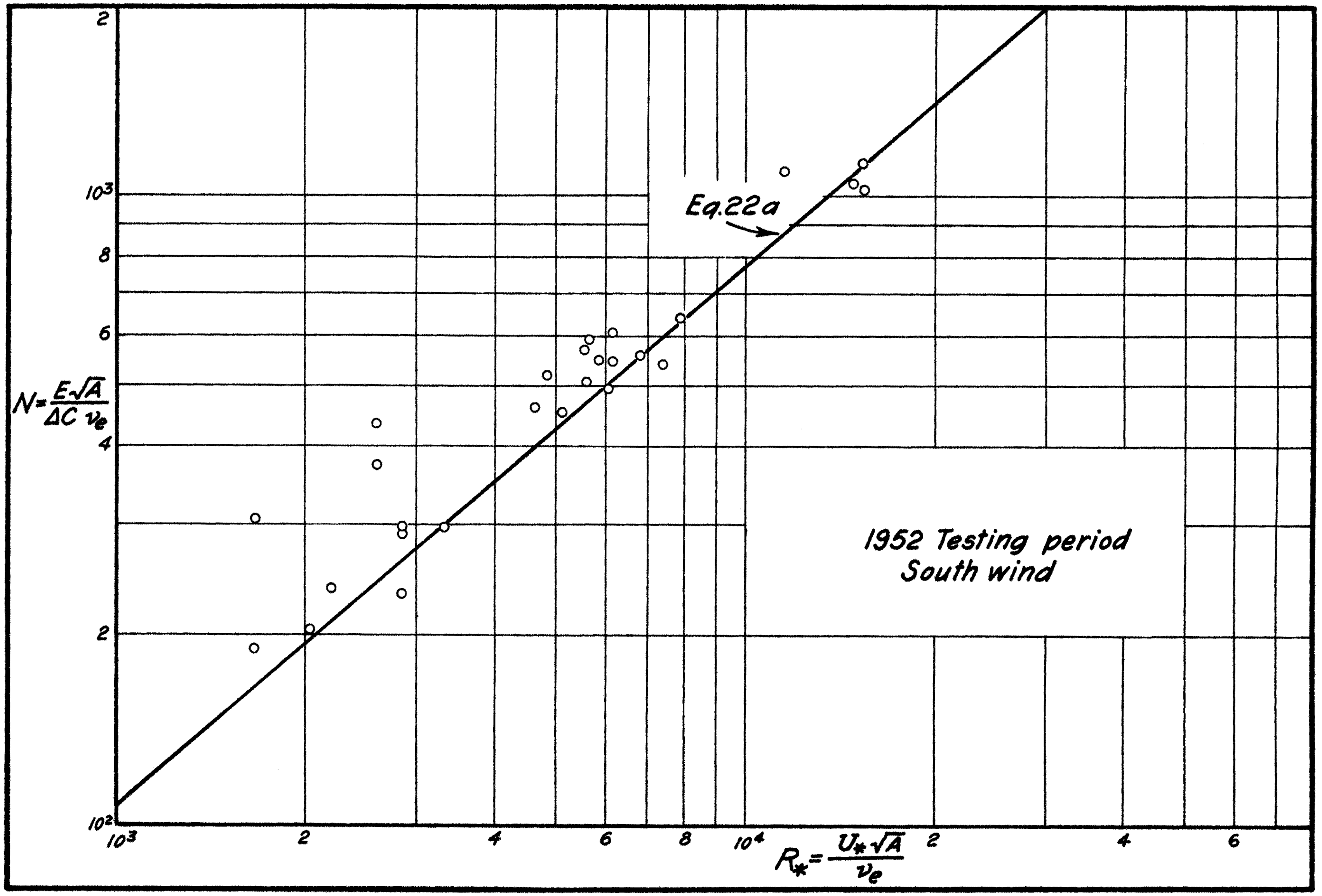

Fig. 11. Variation of N with R_* based on momentum relation —— 1952 data.

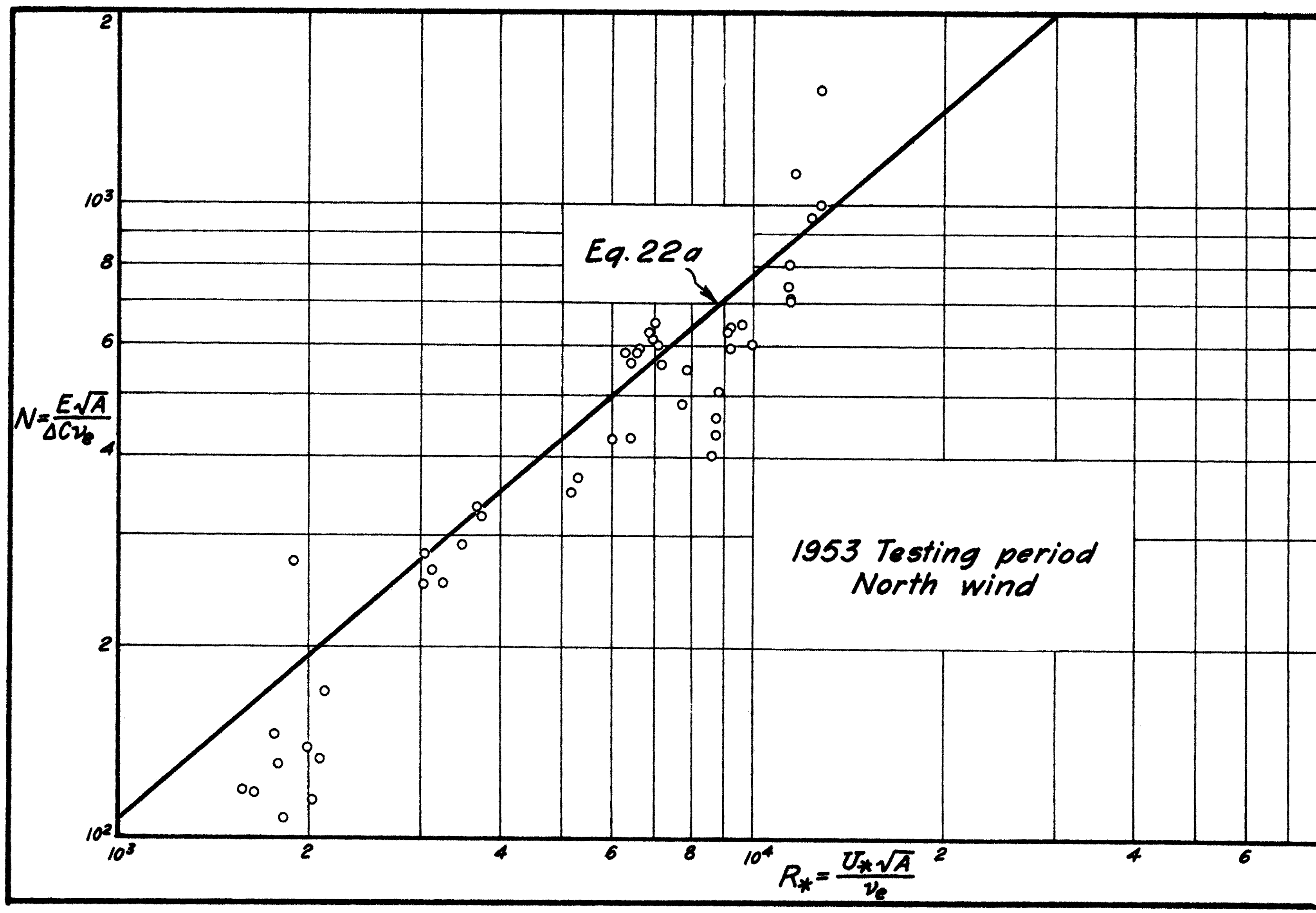

Fig. 12. Variation of N with R_* based on momentum relation —— 1953 data

data tend to deviate from Eq. 22a. Again, this drift from Eq. 22a might be a result of an incompletely developed turbulent boundary layer. The magnitude of R_* as computed through momentum considerations is usually less than that computed through Eq. 1. This decrease, however, lies within the experimental scatter of the data. Therefore, aside from the deviation at the lower values of R_*, Figs. 10 and 11 indicate that the data group about Eq. 22a. This implies that the relationship between N and R_* is essentially the same for either method of computing U_* and may be represented by Eq. 22a.

North Wind

The results of the 1953 Testing Program during which a north wind was simulated, are presented in Fig. 12. The shear velocities for the data presented in Fig. 12 were based on loss of momentum considerations.

Comparison of North and South Wind Data

Aside from considerations of the shape of the lake, the only difference between the physical conditions under which the north and south wind tests were conducted was the upstream terrain. In the case of the south wind, the approach terrain was rather flat whereas for the north wind it was interrupted by a dam, 70 ft high. The prototype dam was simulated in the model by a dam about 0.75 in. high which in essence acted as an upstream barrier. The data for both the north and south wind are compared in Fig. 13 which indicates that both sets of data group well about Eq. 22a. These results may be anticipated in light of the data for the $1\frac{1}{2}$-in. and 3-in. barriers which were already discussed.

As stated previously the shape of the surface from which evaporation takes place may affect the relationship between N and R_* when the direction of the wind changes. An inspection of Fig. 14 indicates that the shape of the modeled lake may be roughly approximated by a circle. If the lake is represented by a circle, then the maximum distance across the lake normal to the direction of the wind does not change with a change in wind direction. Therefore, so far as the model of Lake Hefner is concerned, one may conclude that

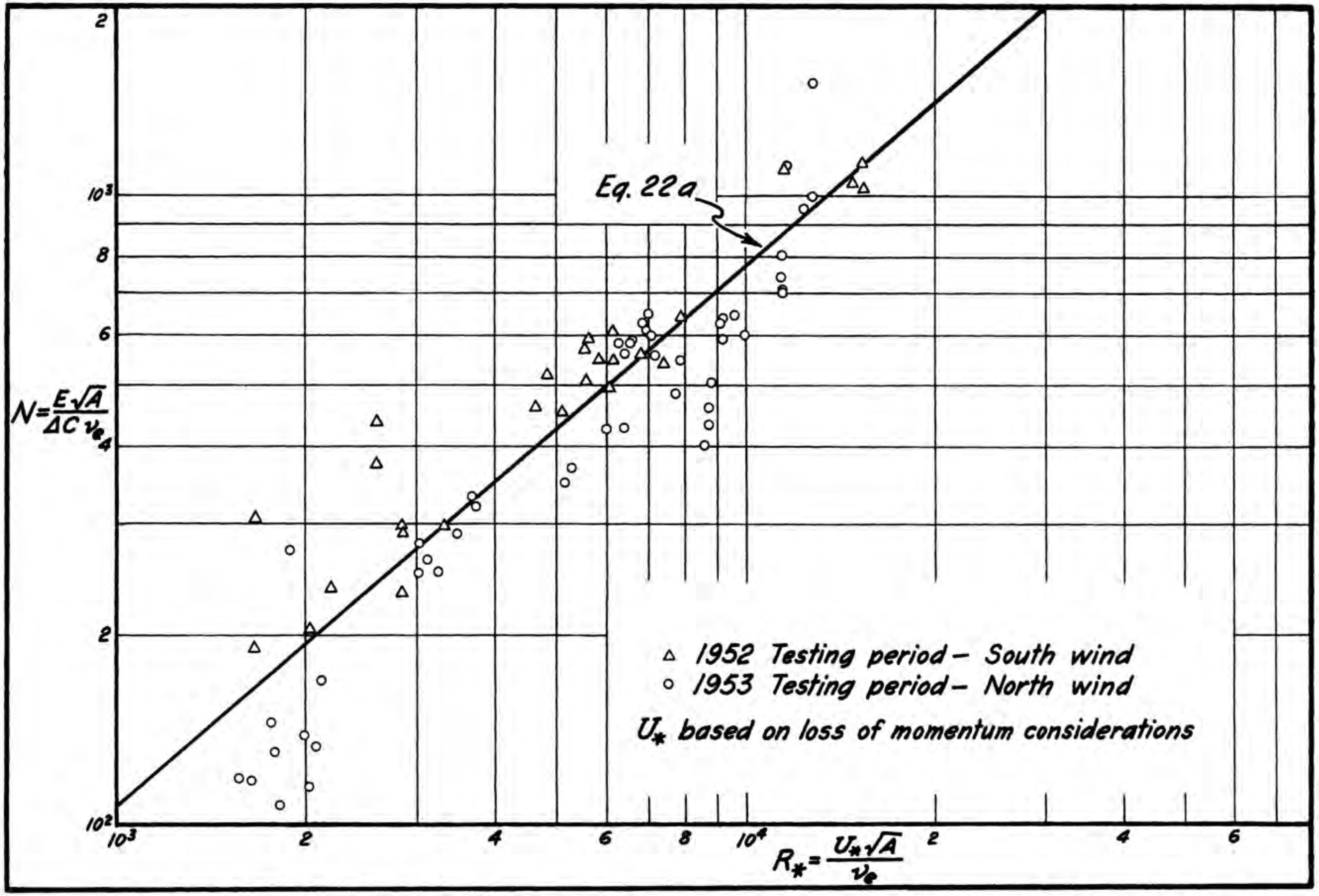

Fig. 13. Variation of N with R_* based on momentum relation——1952 and 1953 data.

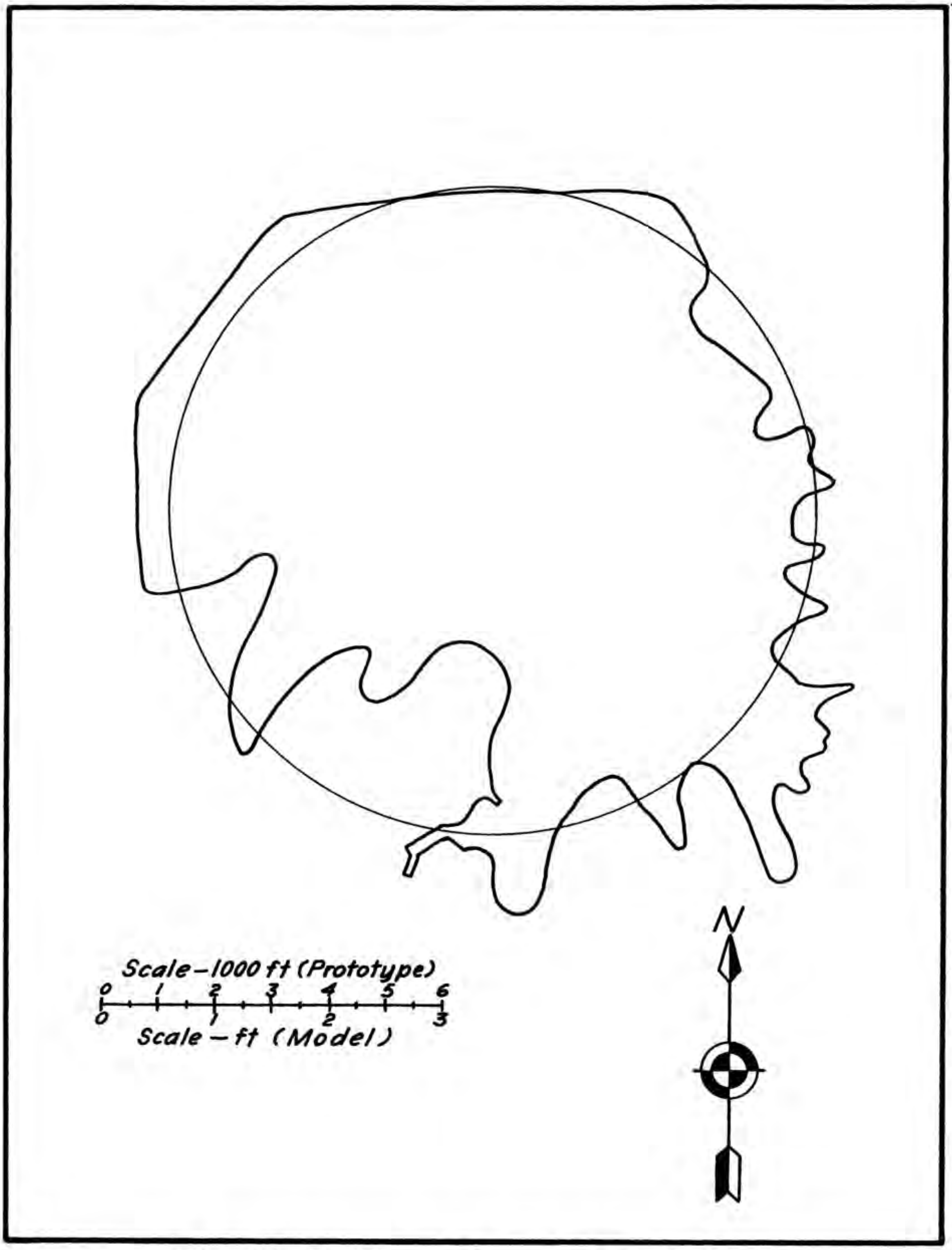

Fig. 14. Outline of modeled lake.

the shape of the modeled lake will not affect the rates of evaporation under different wind directions.

Since change of shape can be dismissed, so far as the model is concerned, as a factor influencing the rates of evaporation, the similarity of results for a north wind and for a south wind implies that either the dam in the model had little effect on the shear velocity or the shear velocity was increased in one region and decreased in another in a compensating fashion such that the combined effects cancelled each other.

As a result of this study, it may be concluded that the rates of evaporation from the model were the same for both north and south winds. Furthermore, since the ratio of the dam height to the distance across the lake is nearly 1/100, it is reasonable to assume that the effect of the prototype dam is also negligible.

Data and Equations Comparable with the Reynolds Analogy

In Fig. 4, Chapter II, no supporting experimental data are shown for the Kármán extension of the Reynolds analogy for the range of R_* from $2x10^4$ to $3x10^7$. Since it was impossible to secure data from the Lake Hefner model in this range of R_*, an effort was made to secure experimental data from other sources to check this range. A set of data useful for this purpose is that obtained by Rohwer (8).

The theoretical work of Sutton (10) and of Sverdrup (11) were also analyzed in an endeavor to obtain correlations between N and R_* based upon the respective theories. The works of Rohwer, Sutton, and Sverdrup are compared with the Lake Hefner Model Studies results through Figs. 15, 16, and 17. Fig. 15 includes only the model data range of R_*. Fig. 16 encompasses that range of R_* which is between that for the model and that for the prototype. Fig. 17 shows the variation of N for high values of R_* and includes prototype data.

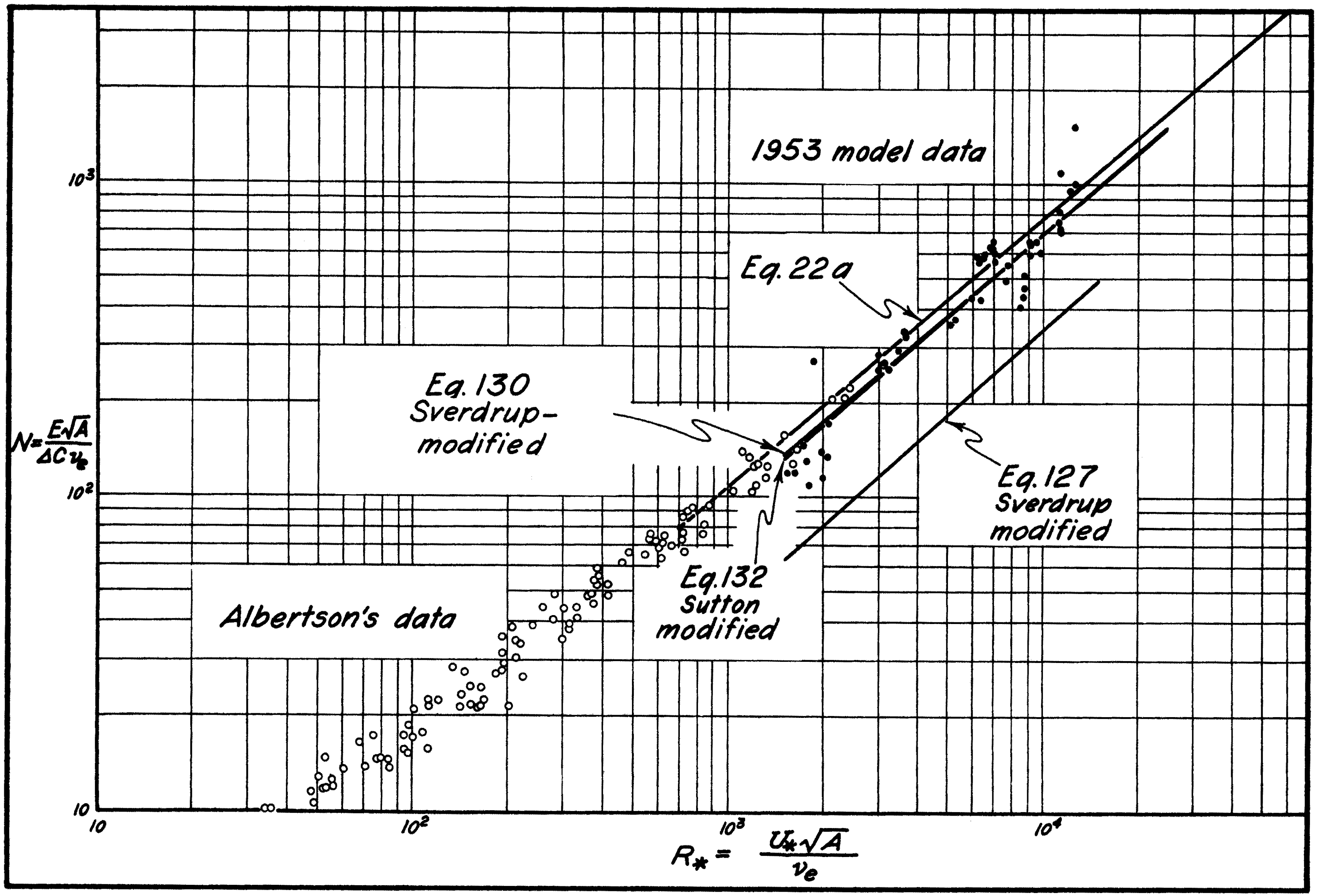

Fig. 15. Variation of N with R_* — model data.

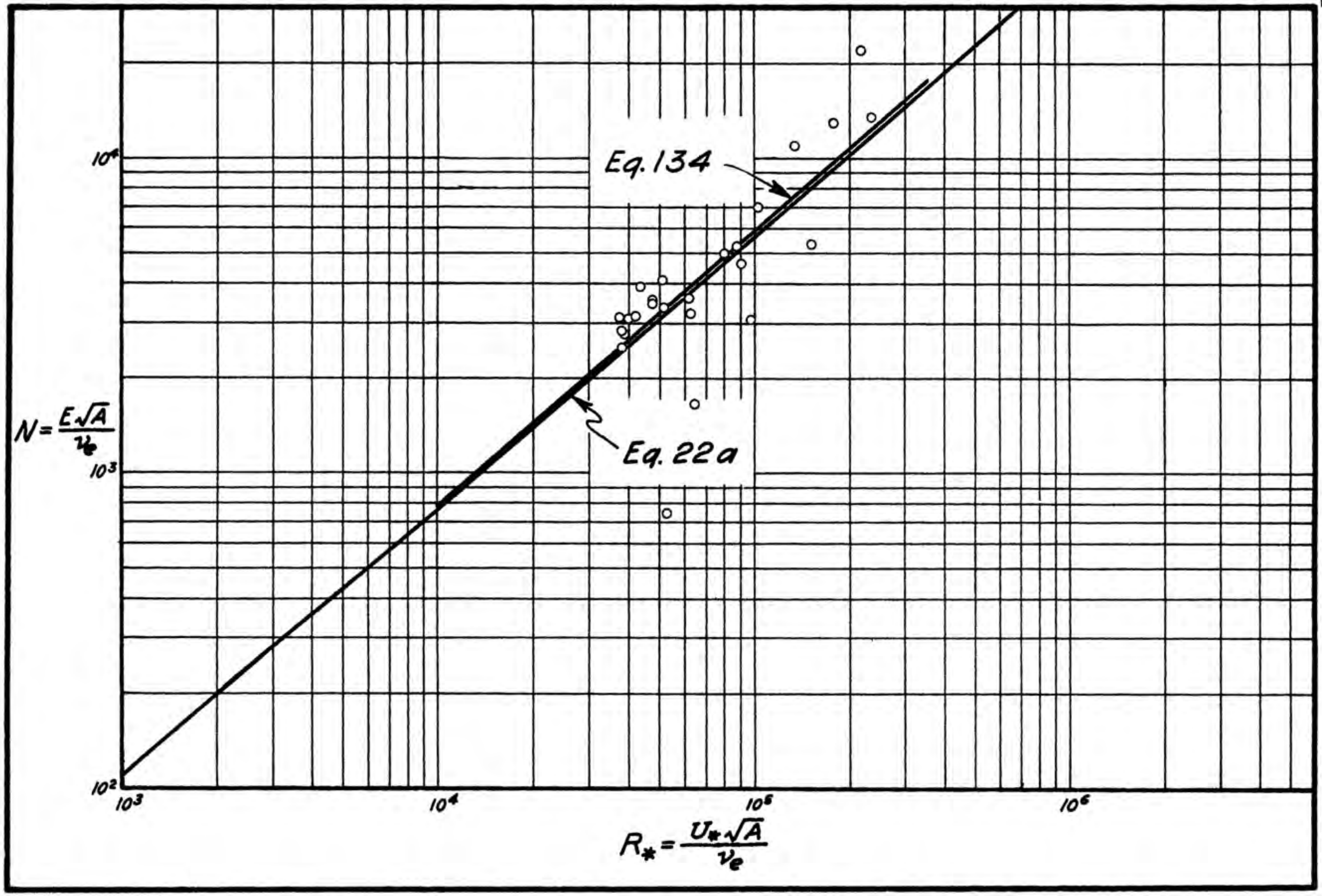

Fig. 16. Variation of N with R_* — Rohwer's data.

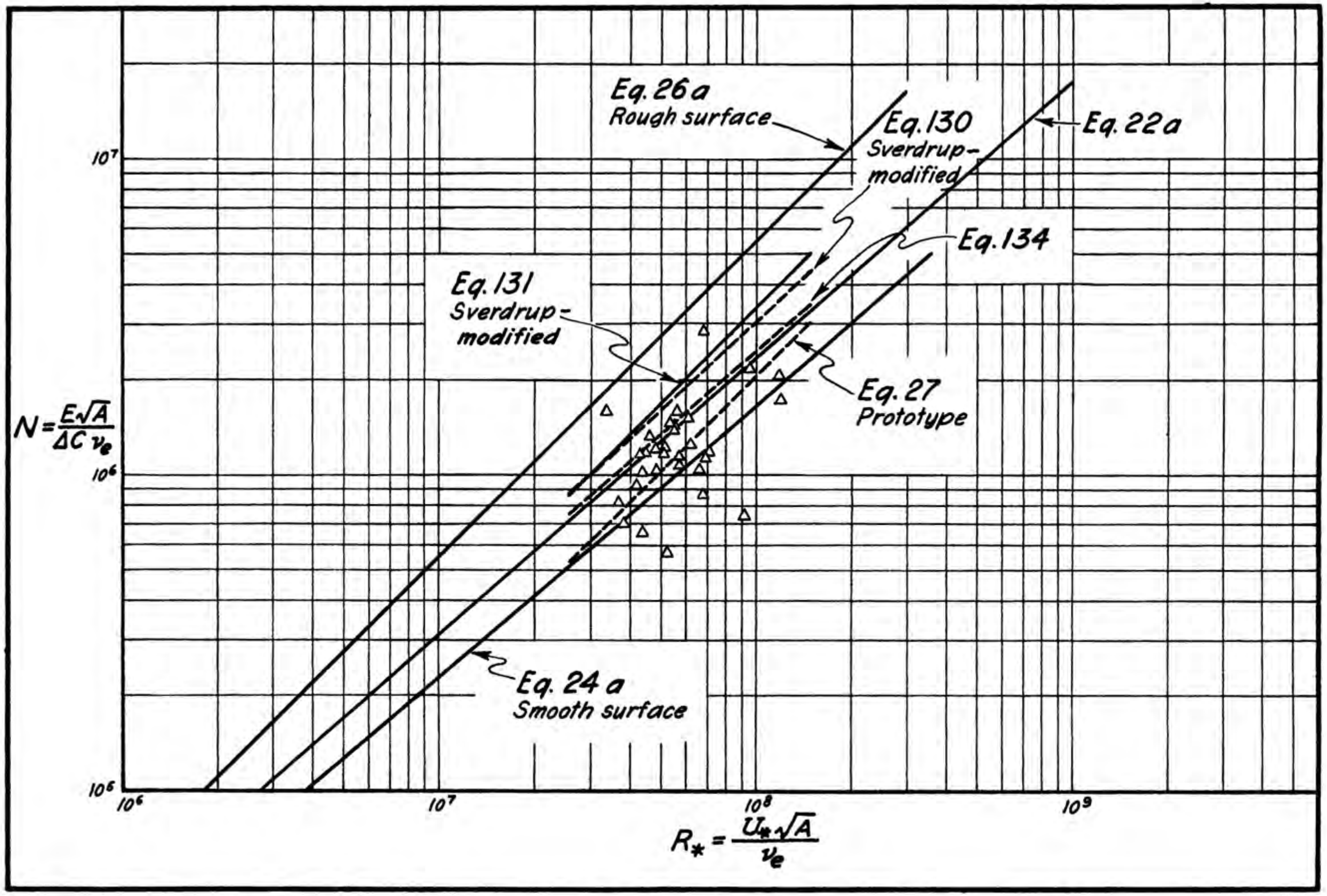

Fig. 17. Variation of N with R_* — Prototype data.

Data of Rohwer (8)

As explained in Chapter III certain data collected by Rohwer were used to obtain experimental results at values of R_* between those for the model and prototype, Fig. 16. The general trend of these data follow rather well the prediction of Eq. 22a although they fall slightly above it. The agreement seems significant, however, when the meagerness of the information used to obtain U_* is considered. In addition, the location at which the humidity was measured tends to give values of the ambient vapor concentration which are too large. This results in ΔC being too small which in turn causes N to be too large.

In the opinion of the authors, the data obtained from the studies of Rohwer confirm the applicability of Eq. 22a as a semi-empirical relationship for predicting evaporation rates when the meteorological elements and water surface temperature are known or estimated.

Sutton's Evaporation Equation (10)

Eq. 119 of Sutton was applied only to the conditions characteristic of the model in an endeavor to evolve a correlation between N and R_* which would be valid for the model range of R_*. The result was Eq. 132, Fig. 15. The slope given by Eq. 132 agrees very well with that of Eq. 22a but for a given value of R_*, the value of N is slightly small.

The work of Sutton was also used to develop a model-prototype relationship which is given by Eq. 133. By applying a set of characteristic values of N and R_* for the model to Eq. 133, Eq. 134 was developed which is intended to be representative of prototype conditions. An examination of Fig. 17 indicates that Eq. 134 represents the prototype data almost as well as Eq. 22a. As in the case of Eq. 22a, the deviation of Eq. 134 from Eq. 27 does not seem excessive when the scatter of daily prototype data is examined, Fig. 17. Eq. 134 is also shown in Fig. 16 with the data of Rohwer. As can be observed, Eq. 134 represents the data of Rohwer as well as Eq. 22a. In view of this agreement with the prototype data and Rohwer's data, Eq. 133 appears to give a practical model-prototype relationship. Further refinement does not seem possible until more information becomes available on the drag over large water surfaces and on the effect of vertical temperature gradients in the atmosphere upon drag.

The 1937 Equation of Sverdrup (11)

This work of Sverdrup is applicable to both smooth and rough surfaces. Each type of surface will be treated in turn.

Application to a Smooth Surface (Model). In Chapter II the steps necessary to transform Sverdrup's 1937 equation, Eq. 122, to a form containing N and R_* for a smooth surface were outlined. The result was Eq. 127 which may be considered applicable to the model of Lake Hefner. In Fig. 15, Eq. 127 is plotted along with Eq. 22a. The equation gives values of N which are much too small. One reason for this tendency appears to be the large value assumed for δ' as given by Eq. 123.

In an attempt to improve the results of Sverdrup's equation when applied to the model, δ' and z_0 were assumed to be represented by Eqs. 128 and 129 respectively. The result, Eq. 130, is also plotted on Fig. 15. The agreement with Eq. 22a -- a representation of the model data -- is much improved over that of Eq. 127.

Application to a Rough Surface (Prototype). The steps necessary to place Eq. 122 in a form consistent with this report and to make it applicable to a rough surface were outlined in Chapter II. The result was Eq. 131 which might be considered to be applicable to the prototype since this equation is for a rough surface. The graph of Eq. 131 is plotted in Fig. 17 and falls somewhat above but parallel to the curve given by Eq. 27 which indicates that the agreement between Sverdrup's modified equation, Eq. 131, and the prototype data is not very good. Although during the Lake Hefner prototype study (13), the agreement between this work of Sverdrup and the prototype data was found to be good. This difference in agreement as found during this study and during the actual Lake Hefner prototype study appears to be due to the determination of the height z at which C_z is measured.

An interesting result is obtained if Eq. 130 which was derived for a smooth surface and considered applicable only to the model range of R_* is extended to the prototype range of R_*. An examination of Fig. 17 discloses that Eq. 130 gives results which are similar to those given by Eq. 131 although the former was derived for a smooth surface only.

Application of Eq. 122. As interpreted herein, Sverdrup's equation, Eq. 122, in the modified form of Eqs. 127 and 131 does not yield results as closely in agreement with experimental data for both the model and the prototype as does the semi-empirical equation, Eq. 22a.

Chapter V

SUMMARY OF THE RESULTS AND APPLICATION OF THE LAKE HEFNER MODEL STUDY

The results of the Lake Hefner model study are presented in two reports -- Parts I and II of the Final Report. Part I of the Final Report covered only the results of the 1952 Testing Program. This report, Part II, covers the work performed under what is termed the 1953 Testing Program. Also, since nothing has been said as yet with regard to the significance and application of either the 1952 or 1953 results, this Chapter is devoted to a review of the results of the entire study and an attempt is made to indicate the importance of the findings and how they may be applied. The objectives of this study, wind structure and evaporation, will be treated in turn.

Wind Structure

The model and prototype wind structures will be compared on the basis of Figs. 1 and 2, Chapter II. These figures are based on only the 1952 data; however, the 1953 data confirm these results.

Fig. 1 -- Prototype Data

A review of Fig. 1 indicates that the prototype data for the 14 specially selected profiles are dispersed along the Prandtl-Kármán wind structure relationship, Eq. 1, in four groups. The data plot in four general groups because the velocity of the wind was measured at four different elevations and these elevations were the same for each velocity profile. Since the relationship between U_* , U_z , z , and z_o as expressed by Eq. 1 was used in ascertaining z_o and U_* , the data should fall near the line representing Eq. 1.

Fig. 1 -- Model Data.

Fig. 1 indicates that the model data may be grouped as follows:

First range - $1 \leq \frac{z}{z_o} \leq 10^2$,

Second range - $10^2 \leq \frac{z}{z_o} \leq 10^3$,

Third range - $10^3 \leq \frac{z}{z_o}$.

The data comprising the first range may be considered to be those for the lower portion of the boundary layer; that is, the portion usually below 0.1 in. In this region, the points from the various profiles have been joined by lines which become tangent to the line representing Eq. 1. For cases of relatively large ambient velocity, these lines become tangent to Eq. 1 at a value of z/z_o of approximately 107. This fact is significant because it agrees with the empirical relationship between z_o and δ' which has been derived by other investigators. In some cases, these lines become tangent to Eq. 1 at values of z/z_o which are less than 107. This deviation from the anticipated value may be due to inaccurate measurements or to the incomplete development of the boundary layer.

The data within the second range represent the turbulent portion of the boundary layer. The model data of Fig. 1 for the turbulent region group well around the line representing Eq. 1. There exists a certain amount of scatter but it is not excessive. Such a small degree of dispersion justifies representation of the data by an equation having the form of Eq. 1; however, the Kármán constant of 0.4 still remains open to question.

The data comprising the third range is scattered. This scatter may be due to the presence of a transition zone between the turbulent boundary layer and the ambient air of low turbulence intensity.

Fig. 1 -- Comparison of Model and Prototype Data.

The prototype data are in good agreement with the relationship expressed by Eq. 1. The model data for the turbulent zone of the boundary layer are also in accord with Eq. 1. The deviations of the model data in the lower range, $1 \leq z/z_o \leq 10^2$, are due in part if not altogether to the presence of the lower portion of the boundary layer where flow may be laminar or turbulent depending on the operation of the tunnel and air conditions outside of the tunnel. The deviations of the model data in the upper range, $z/z_o \geqq 10^3$, may be due to instrumentation or a transition zone between the turbulent boundary layer and the ambient air.

Fig 2 -- Prototype Data.

The values for the significant parameters of Fig. 2 were taken from the 14 profiles (see Part I) of the prototype data for Sta. 2. All but one of the profiles were for adiabatic conditions. The points representing the 14 profiles do not fall on one line as might be hoped for.

Fig. 2 -- Model Data.

The data of the 29 tests run during the 1952 Testing Program, irrespective of the station at which the velocity profile was measured, are represented in this figure. The data for each of the 4 stations have been given a separate symbol. A review of the data for each station indicates that there is no marked difference between the relationship of $U_{52.5}$ and U_* for each of the stations and therefore these model data may be treated as a group. When these data are treated as a group, a single line may be used to approximate the data.

Fig. 2 -- Comparison of Model and Prototype Data.

A straight line may be drawn through the points representing both model and prototype data. A curved line was drawn through these points in Part I. However, a least squares analysis of the data and consideration of the variability in model and prototype characteristics upwind of the lake indicate that a straight line is a better representation of the data. The indicated correlation between U_* and $U_{52.5}$ at homologous points in the model and prototype which differ in absolute elevation by the scale factor of 2000, shows that an approximate modeling of the prototype wind structure has been effected.

The feasibility of modeling wind structure may be brought out by the following analysis. When the Reynolds number is used as the criteria for wind structure similarity between model and prototype, the following relationships can be evolved:

$$R \approx \frac{\text{Inertia Forces}}{\text{Viscous Forces}},$$

$$R = \frac{\rho \frac{U^2}{L}}{\frac{\tau}{L}},$$

$$= \frac{U^2}{U_*^2}, \quad (28)$$

$$R_m = \left(\frac{U_m}{U_{*m}}\right)^2, \quad (29)$$

$$R_p = \left(\frac{U_p}{U_{*p}}\right)^2, \quad (30)$$

For dynamical similarity between model and prototype R_m should equal R_p; therefore, the following relationship should be satisfied --

$$\frac{U_m}{U_{*m}} = \frac{U_p}{U_{*p}}. \quad (31)$$

An examination of Fig. 2 shows that the model and prototype data indeed approximate the relationship

$$\frac{U_m}{U_{*m}} = \frac{U_p}{U_{*p}} = \text{constant}.$$

In accepting the results of Figs. 1 and 2, one should bear in mind the restricted nature of the date presented. The similarity of results for model and prototype is applicable in the model only in the turbulent portion of the boundary layer above the laminar sub-layer. Also, the prototype wind structure was modeled for the condition of a rather flat terrain and adiabatic lapse rates.

An unsuccessful attempt was made to corroborate the "apparent" agreement between actual data and Eq. 31 as depicted in Fig. 2. This endeavor was based on the application of boundary layer equations to the conditions existing at the model and prototype. Several sources of uncertainty were encountered which may account in part, if not entirely, for this lack of success. First, the relationship between ϵ_L and U for the prototype was uncertain. Second, the applicability of a constant relationship between z_o and ϵ over a wide range of velocities was doubtful.

Evaporation

The evaporation aspect of the Lake Hefner model study will be broken into three sections. The first will deal with various aspects of evaporation from the model of Lake Hefner. The second will be devoted to the Reynolds analogy and comparable data and equations. The third section suggests an application of the results of this study.

Evaporation from the Model of Lake Hefner.

The Lake Hefner model testing was divided into the 1952 Testing Program and 1953 Testing Program. During the 1952 Testing Program the air which was circulated over the model simulated a south wind. For the 1953 Testing Program, the model was rotated 180° from the position that it occupied for the 1952 period so that the air passing over the model simulated a north wind. It may be well to remark that the air approaching the prototype lake from the south is not disturbed by any abrupt change in terrain while that from the north is affected by the 70-ft dam which forms the north side of the lake. This dam was reproduced to scale (1:2000) in the model.

The object of subjecting the model to different wind directions was to evaluate if possible any effect wind direction might have on evaporation. A shift of wind direction may affect the overall rate of evaporation because of two possible physical changes. First, the shape of the surface from which evaporation takes place may have an effect in that the maximum distance across this surface normal to the direction of the wind may be changed. Second, the upwind topography may be altered which might affect the air pattern over the body in such a fashion as to affect the rate of evaporation. So far as the Lake Hefner model was concerned this 180° rotation was about the severest change to the upwind terrain that could be made.

The evaporation rates for the north and south winds are very similar and no systematic deviation of results can be attributed to the different wind directions.

With regard to the shape of the model, an inspection of the modeled lake outline indicates that the shape of Lake Hefner can be approximated by a circle. This being the case, the exposure of the evaporation surface to the approaching wind will be the same regardless of the wind direction. Since in the case of the Lake Hefner model, shape can be eliminated as a factor influencing the rate of evaporation from the model, the similar results for the north and south winds tend to indicate that the modeled dam had a negligible effect on the average rate of evaporation from the model. Because of the large Reynolds number difference for model and prototype, a direct evaluation of prototype dam effects from the model result does not appear justified. However, since the ratio of dam height to lake length is nearly 1/100, one is justified to infer that the prototype dam effects are negligible.

During the 1953 Testing Program two sizes of upstream barriers were placed in the tunnel in order to study the effect that they might have on the rate of evaporation. These barriers were made of sheet metal and extended the width of the tunnel. One barrier was $1\frac{1}{2}$ in. high and the other was 3 in. high. These barriers were placed at various positions upstream from the modeled lake. Neither barrier at any of the positions seems to have any effect on the overall rate of evaporation. The authors believe that the barriers probably reduced the evaporation over a portion of the evaporation surface and increased the evaporation from some other area with a negligible net effect. Since the scale used in modeling Lake Hefner was 1:2000, the $1\frac{1}{2}$-in. barrier represents an abrupt rise and fall in the terrain of 250 ft; the 3-in. barrier represents a 500 ft rise in terrain. This tends to imply that had the terrain around Lake Hefner been made up of mountains 250 and 500 ft high the evaporation results from a 1:2000 scaled model of this terrain would not have been significantly different from those for the same modeled lake having flat surrounding terrain.

The authors believe that the advisability of modeling the terrain depends on the magnitude of the changes of elevation of the terrain, the position of the changes of elevation with regard to the body of water, and the size and shåpe of the body of water. In the case of Lake Hefner, the authors believe that the vertical changes of elevation were not significant.

Reynolds Analogy and Comparable Data and Equations.

This section of Chapter V is devoted to a brief discussion of the Reynolds analogy and comparable data and equations. Each will be discussed in turn.

Reynolds Analogy. As indicated in the theoretical analysis, correlation of the evaporation between model and prototype is possible. But a direct comparison of evaporation from the model and the prototype on the basis of $(R_*)_m = (R_*)_p$ is not possible because of the difference in the values of R_* for the model and the prototype. This difference can be attributed for the most part to the scale used in this study.

A considerable amount of data concerning momentum transfer has been gathered for a wide range of Reynolds number. Based on the Reynolds analogy between mass and momentum transfer, it seemed reasonable therefore, that if the proper interpretation were given to these data, they could be extended to vapor transfer (evaporation). If this were possible, then the model data might be expected to follow this extension within their range of Reynolds number and the prototype data might also be expected to agree with this extension within their range of Reynolds number. If such agreement were verified, then the Reynolds analogy based on momentum transfer, could be used to predict evaporation rates. This is the approach which was adopted in the correlation of model and prototype evaporation.

As indicated in Chapter II the significant variables concerning evaporation can be grouped into the dimensionless parameters N and R_*. Through use of momentum transfer data and Kármán's extension of Reynolds analogy. and pertinent prototype and model data, Eqs. 22a, 24a, and 26a were obtained. These relationships between N and R_* are presented graphically in Figs. 15, 16, and 17.

Comparable Data. In order to ascertain the validity of this application of the Kármán extension of the Reynolds analogy to evaporation, the following sources of evaporation data were consulted:

1. Albertson's data (1).
   a. Individual values of N versus R_*.
2. Lake Hefner model data -- 1952 and 1953.
   a. Individual values of N versus R_*.
3. Rohwer's evaporation data (8).
   a. Individual values of N versus R_*.
4. Lake Hefner prototype data.
   a. Empirical evaporation equation based on Eq. 58 in Ref. 13:65

$$N = 0.0203 \, R_* , \tag{27}$$

   b. Individual values of N versus R_*.

These data are also presented in Figs. 15, 16, and 17.

The range of the Kármán extension of the Reynolds analogy presented in Fig. 15 commences at $R_* \geqq 10^3$. Some of Albertson's data are equal to and greater than this value of R_* in which region the agreement between the data and Kármán's extension of Reynolds analogy, Eq. 22a, is good. The Kármán extension of the Reynolds analogy extrapolated to $R_* = 6 \times 10^2$ is still in good agreement with Albertson's data. Therefore the data of Albertson tend to substantiate Karman's extension of Reynolds analogy for values of R_* equal to about 10^3.

The Lake Hefner model data for 1952 and 1953 are in the range of R_* greater than 1×10^3 and less than 2×10^4. Fig. 15 indicates that the agreement between these data and the Kármán extension of the Reynolds analogy represented by Eq. 22a is good.

Rohwer's data shown in Fig. 16 cover the range of R_* from 3×10^4 to 3×10^5 and tend to group slightly above the graph of Eq. 22a. Despite uncertainties in obtaining U_* and ΔC, the data of Rohwer are significantly near to the values predicted by the Kármán extension of Reynolds analogy as given by Eq. 22a.

The Lake Hefner prototype data may be represented by a modified version of the empirical equation, Eq. 58, found in Ref. 13:65; that is,

$$N = 0.0203\ R_* \ . \qquad (27)$$

Fig. 17 indicates that the line for Eq. 27 is above that for a smooth boundary, Eq. 24a, and below that for a rough boundary, Eq. 26a.

In the range of $R_* \geq 10^7$, Fig. 17 indicates that the extension of the Reynolds analogy for a smooth surface, Eq. 24a, gives results which are more nearly comparable to actual data than does the extension for a rough surface, Eq. 26a. An interesting fact is that Eq. 22a which was derived for a smooth surface, describes rather well the prototype data when extended to this range of R_*. The better correlation between N and R_* stemming from smooth surface considerations tends to imply that the water surface, although it may appear rough by the presence of waves, in reality behaves more nearly as though it were smooth. This statement is not meant to dismiss the water surface roughness in its entirety but rather is intended to imply that the water surface roughness is not as great as might be imagined from the appearance of the waves. This may be accounted for, at least in part, by the fact that not only do the waves travel in the direction of the wind but the water at the surface also moves in the direction of the wind. If a means were known by which water surface roughness could be more properly evaluated, then the extension of the Reynolds analogy might coincide more favorably with actual data. Additional research must be performed to correlate the relationships between wind, waves, and surface drag.

Comparable Equations. The results of the works of O. G. Sutton (10) and H. U. Sverdrup (11) were examined to determine if they would give satisfactory correlations between N and R_*.

An important result of the Lake Hefner model study is the deduction of a model-prototype relationship, Eq. 121, based on the work of O. G. Sutton (10). Applying certain model data to Eq. 121 resulted in a relationship for prototype behavior, Eq. 134, which gives very favorable results. In the prototype range of R_*, Eq. 134 gives results which are equally as good as those given by values of R_* greater than 10^3 is arbitrary since the near agreement with prototype data appears more or less coincidental.

Eq. 135, within the designated range of R_*, describes well the data of Albertson, the model data, the data of Rohwer, and the prototype data, Fig. 18. The authors believe that Eq. 135 will be refined as the understanding of the interrelationship between velocity distribution, drag, and spray over water surfaces improves. For the present, Eq. 135 appears to be a simple and yet adequate approximation of the relationship between N and R_* over the range of $10^3 \leq R_* \leq 10^9$.

One aspect which may limit the applicability of Eq. 135 is the shape of the surface from which evaporation takes place. Eq. 135 seems to be satisfactory for surfaces which may be approximated by a circle. The effect of other shapes on evaporation needs further investigation.

Suggested Application of Eq. 135.

The determination of evaporation through the use of Eq. 135 depends upon the evaluation of the variables U_*, $\sqrt{A}$, ν_e, and ΔC. In the sections that follow, consideration is given to the evaluation of these variables:

U_* -- If wind velocity data at an upwind station are available for two elevations, U_* can be determined through the application of Eq. 1. If the wind velocity is measured at only one height upwind, then the possibility exists of approximating the shear velocity U_* by means of the 1/7 - power relationship for velocity distribution.

$\sqrt{A}$ -- If the evaporation from a body of water is being considered, the area is probably known from which $\sqrt{A}$ can easily be computed.

ν_e -- As with the determination of the shear velocity, the kinematic viscosity ν can be evaluated from the ambient upwind air temperature and the barometric pressure. The use of the mean barometric pressure for the general locality has been found to be satisfactory. The variable ν_e can be determined from ν through use of the

Prandtl number $\sigma = \nu/\nu_e$. In this work, the Prandtl number was considered to be equal to 0.6.

ΔC -- The determination of ΔC is dependent upon the evaluation of C_o and C_A . In this study C_o was taken as the vapor concentration corresponding to the saturated state at the temperature of water surface. The water surface temperature measured at the center of the lake was considered to be representative of the average temperature. The ambient vapor concentration C_A may be evaluated easily with psychrometric readings at an upwind station.

As an illustration of how Eq. 135 may be applied to evaluate evaporation, the following example is cited:

U_* -- Wind velocity data are available at two elevations at the upwind predominant-wind location. The shear velocity as computed through Eq. 1 is found to be 0.85 ft/sec.

$\sqrt{A}$ -- The area of the body of water under investigation is known to be 8.1×10^7 sq ft. This results in $\sqrt{A}$ being 9×10^3 ft.

ΔC -- Psychrometric measurements are available from which C_A is found to be 7×10^{-4} lb/ft^3, based on an average water surface temperature of 20.3°C; C_o is 11×10^{-4} lb/ft^3. The difference between C_o and C_A, ΔC, is thereupon equal to 4×10^{-4} lb/ft^3.

ν_e -- For an average air temperature of 20°C and a barometric pressure of 25 in. of mercury, ν is found to be 1.94×10^{-4} ft^2/sec. For a Prandtl number of 0.6, ν_e is 3.24×10^{-4} ft^2/sec.

Based on these values for U_* , $\sqrt{A}$, and ν_e , R_* has a value of 2.36×10^7 . Then through use of Eq. 135, N is found to be 6.58×10^5 , and E , therefore, has a value of 9.49×10^{-6} lb/ft^2-sec. When converted to more familiar units, E is 4.62 in./mo or 715 acre-ft/mo (30 day month). This briefly outlines the method of using Eq. 135 to determine the amount of evaporation.

The authors believe that the evaporation from bodies of water surrounded by topography of low relief may be determined through Eq. 135. This equation may be applied to water surfaces varying in area from a few square feet to

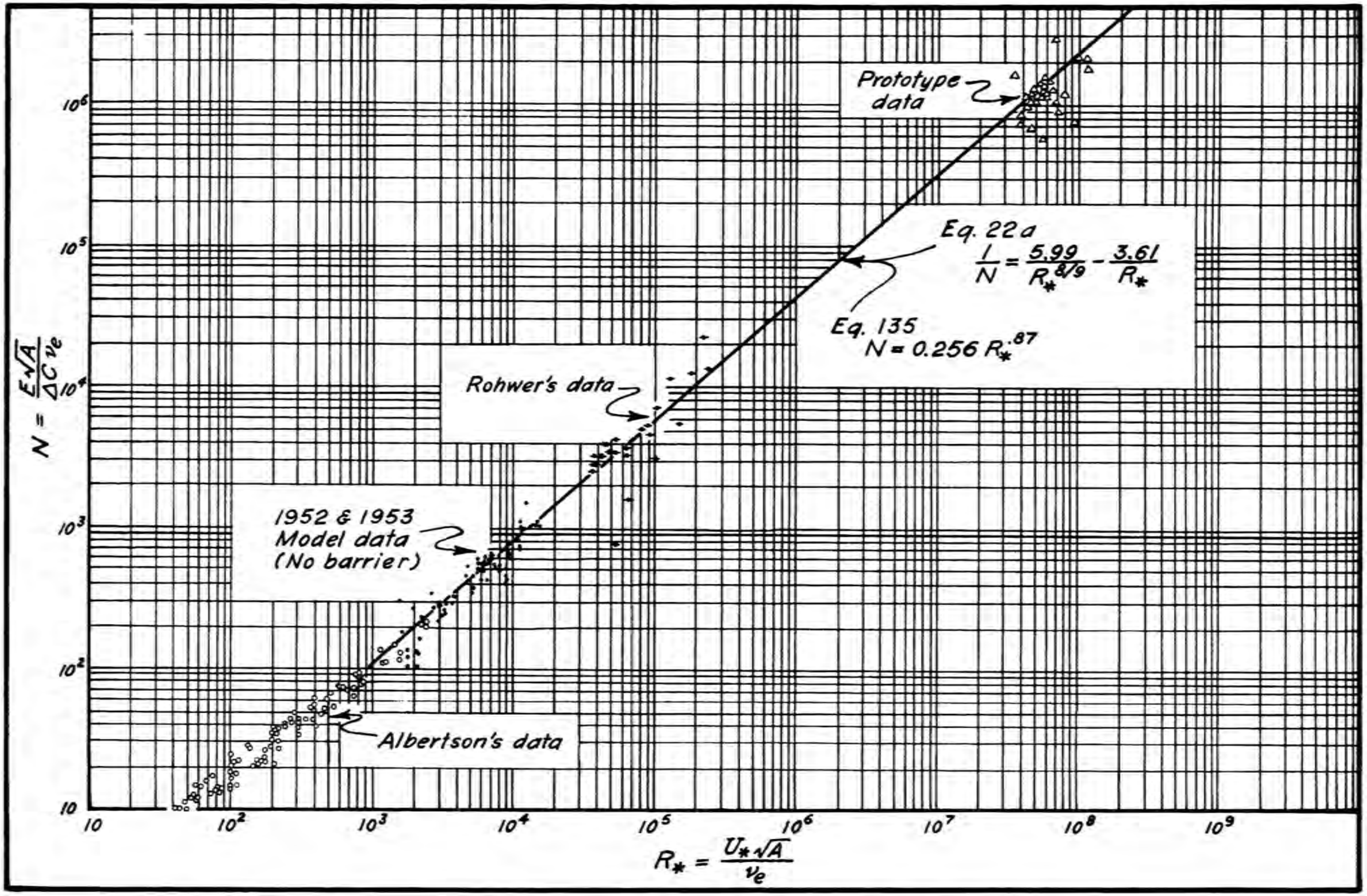

Fig. 18. Comparison of evaporation data with final equations.

several square miles. The Lake Hefner model and prototype were 25 sq ft and 3.6 sq mi in area respectively.

Investigation of evaporation from bodies of water surrounded by mountainous or hilly terrain needs further study. The irregular nature of mountainous and hilly terrain sets up complex wind patterns which may be difficult to evaluate for purposes of determining the evaporation through Eq. 135. Also, this type of terrain is conducive to air convection currents set up by uneven heating and cooling of the land surfaces which further complicate the problem.

Chapter VI

CONCLUSIONS

Objectives of the Lake Hefner model study were the following:

1. To determine the relationship between the model and prototype wind structure,
2. To determine what correlations might exist between model and prototype evaporation.

In the following paragraphs, conclusions drawn from the entire Lake Hefner model study with regard to the primary objectives of the study are listed and several recommendations for further study are given.

Wind Structure

The following conclusions which were given in Part I (3) have been further substantiated by measurements made in the 1953 Testing Program:

1. The boundary layer above the model was composed of two regions. The lower region was characterized by two different types of flow. In some instances the flow was laminar which is indicative of flow near a smooth boundary. In others, the flow was of a type which might be indicative of a boundary layer in a transitional state between that for a hydrodynamically smooth boundary and that for a hydrodynamically rough boundary. The upper portion of the boundary layer for both the model and prototype was turbulent and followed the Prandtl-Kârmân equation, Eq. 1. This similarity shows that the prototype wind structure was modeled (see Fig. 1) for the conditions of a flat terrain and an adiabatic lapse rate.
2. The data of Fig. 2 and Eq. 31 indicate that approximate dynamical similarity existed between the model and prototype.

Evaporation

Conclusions regarding evaporation correlations have been drawn after a study was made of all the Lake Hefner model data, the Lake Hefner prototype data, Rohwer's data, the work of Sutton, and the 1937 work of Sverdrup. These conclusions are as follows:

1. The evaporation coefficient N may be related to a form of Reynolds number R_* for both the model and the prototype.
2. The Kármán extension of Reynolds analogy yields Eq. 22a which represents the Lake Hefner model and prototype data and the data of Rohwer as well as any other single equation presented in this report. Eq. 22a has been simplified to Eq. 135, and for all practical purposes the relationship between N and R_* as given by Eq. 135 is the same as that given by Eq. 22a, Fig. 18. Therefore Eq. 135 may be used to relate N to R_* for the range -- $10^3 \leq R_* \leq 10^9$. Eq. 135 appears to describe rather well the relationship between N and R_* for areas which are approximately circular in shape. Whether this same relationship will hold for areas differing markedly from a circular shape is not known and this information will have to be determined through further investigations.
3. Eq. 121, derived from the work of O. G. Sutton (10), provided a model-prototype relationship between N and R_* which appears to be valid for the Lake Hefner model-prototype and Lake Hefner model - Rohwer systems.
4. Neither the Eqs. 127 and 130 resulting from Sverdrup's work (11) nor Eq. 132 from the work of Sutton (10) relate N to R_* for the Lake Hefner model data as well as does Eq. 22a.
5. The 180° rotation of the model has no discernible effect upon evaporation from the Lake Hefner model.
6. Upwind barriers having a height up to 1/20 the lake length have no effect upon the overall evaporation rate in the model.

Recommended Investigations

In the course of the Lake Hefner model studies several points arose which could not be adequately treated on the basis of information now available. Because they are important to a more precise treatment of evaporation from natural bodies of water, they are listed here as subjects for additional investigation.

1. In order to apply adequately the Reynolds analogy to natural bodies of water, reliable information on the relationships between wind, waves, and surface drag is needed. Indications resulting from this study and some field measurements reported in the literature (9) lead one to anticipate the possibility of drag over water surfaces being practically equivalent to drag over a smooth solid boundary.
2. Before an estimate of evaporation from a planned reservoir may be made, using Eq. 135 or the equations of Sverdrup and Sutton, a knowledge of the future average water surface temperatures of the planned reservoir is needed. To make such an estimate before the reservoir exists requires that more information be obtained on the effects of latitude, elevation, reservoir depth and climate upon the water surface temperature.
3. Additional information is needed to determine the effects of atmospheric stability or instability caused by vertical temperature gradients. This information is especially needed to accurately predict short-term evaporation rates.
4. Information concerning the distribution of water vapor and the effect of water vapor on turbulence and atmospheric stability is also needed. The possibility exists that some of this information could be obtained through controlled experiments as might be conducted in a wind tunnel.
5. Information about the effect of the shape of the surface from which evaporation takes place is needed. The work herein seems to apply satisfactorily to surfaces which are approximately circular in shape.

But nothing can be said with regard to the effect that shape may have on the relationship depicted by Eq. 135.

BIBLIOGRAPHY

1. Albertson, M. L. Evaporation from a plane boundary. Heat Transfer and Fluid Mechanics Institute (Preprints of papers) held at Stanford University, pp. 243-254, June 1951.

2. Anderson, E. R., Anderson, L. J., and Marciano, J. J. A review of evaporation theory and developement of instrumentation (Interim report: Lake Mead Water Loss Investigations). U. S. Navy Electronics Laboratory, San Diego, California, Report No. 159, February 1, 1950.

3. Cermak, J. E. and Koloseus, H. J. Lake Hefner Model Studies -- Final Report: Part I. Colorado A & M College, Department of Civil Engineering, Report No. 54JEC 20, November 1953.

4. Kármán, Th. The analogy between fluid friction and heat transfer. Trans. A.S.M.E., vol. 61, pp. 705-710, 1939.

5. Maisel, D. S. and Sherwood, T. K. Effect of air turbulence on rate of evaporation of water. Chemical Engineering Progress vol. 46, No. 4, April 1950. pp. 172-175.

6. Nikuradse, J. Strömung in glatten Rohren, VDI - Forschungsheft 356, 1932.

7. Reynolds, O. Proc. Lit. Phil. Soc. of Manchester, vol. 14, 1875.

8. Rohwer, Carl. Evaporation from free surfaces. Technical Bulletin No. 271, U. S. Dept. of Agric. in cooperation with Colorado Agricultural Experiment Station, December 1931.

9. Roll, Ulrich. Das Windfeld über den Meereswellen. Die Naturwissenschaften. Heft 8 pp. 230-234, 1948.

10. Sutton, O. G. Wind structure and evaporation in a turbulent atmosphere. Proceedings of the Royal Society of London, Series A, vol. 146, No. A 858, October 1, 1934, pp. 701-722.

11. Sverdrup, H. U. On the evaporation from oceans. Journal Marine Research, vol. 1, No. 1, pp. 3-14, 1937-38.

12. - - - - - - Instructions for airway meteorological service. U. S. Dept. of Agriculture, Weather Bureau. Circular N Aerological Division 4th Ed. 1939.

13. - - - - - - Water-loss investigations: U. S. Geological Survey. Volume 1 -- Lake Hefner studies technical report. Circular No. 229, 1952. (This report is also issued as N.E.L. Report 327, San Diego 52, California).

APPENDIX

Table of Contents

Appendix A

DETAILS OF EQUIPMENT AND PROCEDURES

This section of the report is devoted to a presentation of changes in equipment and procedures from those used and followed during the 1952 Testing Program. The reader is referred to Part I (3) for a description of the equipment and procedures which is applicable for the most part to the 1953 Testing Program.

Barriers

During the course of the 1953 Testing Program the effect of two upstream barriers on the rates of evaporation from the model was investigated. These barriers were placed on the modeled dam and at various distances upstream. One barrier was $1\frac{1}{2}$ in. high, corresponding to a prototype height of 250 ft and the other barrier was 3 in. high which corresponded to a prototype height of 500 ft. Both barriers were made from 16 gage sheet metal and extended the width of the tunnel. Both barriers had square cornered upper edges. This form of barrier was adopted so as to insure a knowledge of the point of separation as the air passed over the barrier. Such might not be the case if some streamlined barrier were used.

Anemometry

The hot wire anemometer circuits used during the 1953 Testing Program were the same in principle but physically different from the one used for the 1952 Testing Program. For the 1953 work, platinum wire 0.001 in. in diameter and approximately 0.39 in. long was used for the sensing element instead of tungsten wire. The platinum wire was found to be sturdier and more durable. Two anemometer circuits were used which eliminated the switching which was necessary with the single circuit used during the 1952 work. One circuit was used to measure the ambient air velocity at what is known as the forward tunnel position. The other circuit was attached to the sensing element on the traverse mechanism and was used in measuring the air velocity at various heights above the model. Details concerning the 1953 circuits are given in Fig. 19.

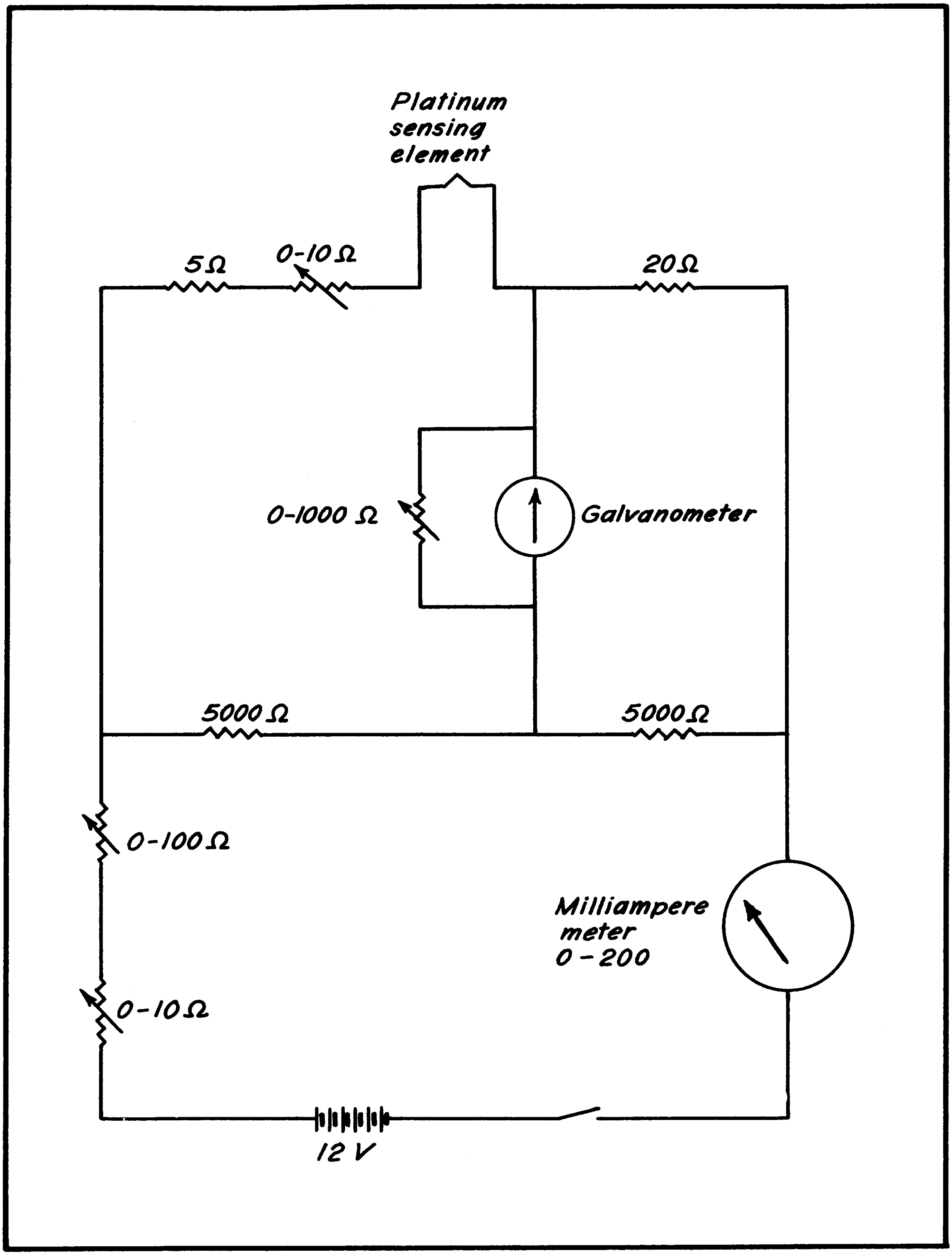

Fig. 19. Schematic diagram of the 1953 constant temperature hot wire anemometer circuit.

Appendix B

DATA SUMMARIES

This section of the appendix is devoted to tables which contain summaries of the model data and Rohwer's data.

Table I

Summary of 1952 Model Data - No Barrier

Test No.	Date	$\frac{\sqrt{A}}{\nu_e}$ $\frac{sec}{ft}$ $\times 10^4$	$N = \frac{E\sqrt{A}}{\Delta C \nu_e}$ $\times 10^2$	U_T $\frac{ft}{sec}$	U_{FT} $\frac{ft}{sec}$	U_* (Fig. 6) $\frac{ft}{sec}$	$R_* = \frac{U_* \sqrt{A}}{\nu_e}$ $\times 10^3$
1	9-27	1.516	6.42	12.0	10.0	0.523	7.93
2	10-8	1.525	2.34	3.9	3.5	0.188	2.86
3	10-20	1.613	3.76	3.2	3.0	0.161	2.60
4	10-20	1.613	4.38	3.7	3.1	0.162	2.61
5	10-21	1.539	5.21	6.0	5.8	0.316	4.86
6	10-22	1.541	4.61	6.2	5.6	0.301	4.64
7	10-22	1.542	4.53	7.2	6.1	0.332	5.12
8	10-22	1.549	4.93	8.0	7.2	0.390	6.04
9	10-23	1.520	2.98	3.6	3.5	0.188	2.86
10	10-23	1.522	2.90	3.6	3.5	0.188	2.86
11	10-23	1.535	2.98	3.1	4.0	0.217	3.33
12	10-25	1.515	6.29	11.0			
13	10-25	1.525	6.39	10.8			
14	10-28	1.552	5.50	9.4	7.4	0.398	6.18
15	10-28	1.552	10.10	20.8	15.0	0.743	11.52
16	10-29	1.576	5.41	8.0	8.8	0.470	7.41
17	10-29	1.587	5.58	10.0	8.0	0.430	6.82
18	11-3	1.649	11.33	22.2	21.0	0.933	15.39
19	11-3	1.643	10.49	20.0	20.0	0.905	14.88
20	11-3	1.648	10.27	21.2	21.1	0.938	15.48
21	11-4	1.550	6.05	7.6	7.4	0.398	6.17
22	11-4	1.540	5.49	7.6	7.0	0.379	5.84
23	11-4	1.542	5.66	7.6	6.6	0.360	5.55
24	11-4	1.552	5.09	5.5	6.6	0.360	5.59
25	11-4	1.571	5.92	5.2	6.6	0.360	5.66
26	11-6	1.667	3.03	2.3	1.9	0.100	1.67
27	11-6	1.661	1.90	2.5	1.9	0.100	1.66
28	11-6	1.679	2.05	2.3	2.3	0.121	2.03
29	11-6	1.667	2.38	2.5	2.5	0.132	2.20

Table II

Summary of 1953 Model Data - No Barrier

Test No.	Mo. & Day	Sta	Time of day	$\sqrt{A}$ ft	ν_e $\frac{ft^2}{sec}$ x10^{-4}	T_{AD} °F	T_{AW} °F	T_o °F	ΔC $\frac{lb}{ft^2}$ x10^{-4}	E $\frac{lb}{ft^2\text{-}sec}$ x10^{-6}	N x10^2	U_T $\frac{ft}{sec}$	U_{FT} $\frac{ft}{sec}$	U_* (Fig 6) $\frac{ft}{sec}$	R_* x10^3
1	8-10	1	14:19-15:34	5.00	3.42	84.3	63.7	65.8	3.91	15.60	5.85	9.60	7.98	0.429	6.28
2	8-10	6	15:55-16:33	5.00	3.44	86.1	64.3	66.6	4.19	16.18	5.62	9.22	8.20	0.440	6.40
3	8-12	1	9:54-10:37	5.00	3.31	74.6	59.2	59.9	2.62	10.88	6.30	9.40	8.52	0.453	6.85
4	8-12	2	10:55-11:31	5.00	3.35	78.7	58.5	60.3	3.64	14.26	5.84	9.40	8.15	0.439	6.55
5	8-13	1	9:07- 9:50	5.00	3.33	76.2	57.2	59.1	3.47	13.86	6.01	10.10	8.81	0.469	7.05
6	8-13	2	10:09-10:44	5.00	3.38	80.9	59.2	59.8	3.56	14.31	5.96	10.15	8.32	0.447	6.61
7	8-13	3	11:01-11:39	5.00	3.43	85.7	61.1	61.4	3.96	16.60	6.14	10.00	9.00	0.477	6.96
8	8-17	1	9:48-10:33	5.00	3.19	64.5	58.9	60.5	1.35	4.73	5.51	9.81	9.57	0.500	7.84
9	8-17	2	10:50-11:36	5.00	3.23	67.9	60.3	61.3	1.48	4.67	4.89	8.90	9.50	0.499	7.74
10	8-17	4	14:00-14:36	5.00	3.27	71.9	62.1	63.9	2.10	7.71	5.62	9.00	8.78	0.467	7.14
11	8-17	5	15:13-15:55	5.00	3.30	73.7	63.7	64.7	1.90	8.16	6.52	8.65	8.69	0.461	7.00
12	8-18	1	10:38-11:13	4.98	3.31	74.3	62.1	62.3	2.00	1.43	1.08	2.24	2.25	0.121	1.82
13	8-18	2	13:58-14:30	4.98	3.29	73.3	59.3	65.7	4.09	3.09	1.15	2.38	2.48	0.133	2.02
14	8-18	3	14:41-15:14	4.98	3.33	76.3	60.7	65.9	4.04	3.76	1.39	2.32	2.48	0.133	1.99
15	8-18	4	15:24-15:50	4.98	3.30	74.7	61.0	66.0	3.70	3.29	1.34	2.30	2.54	0.138	2.08
16	8-18	6	16:01-16:32	4.98	3.28	72.4	61.1	66.0	3.29	3.67	1.70	2.20	2.57	0.139	2.11
17	8-19	1	9:53-10:22	4.98	3.24	68.9	58.6	60.5	2.16	4.54	3.23	4.45	4.45	0.242	3.72
18	8-19	2	10:33-11:04	4.98	3.26	70.6	59.2	60.9	2.28	4.97	3.33	4.50	4.41	0.240	3.67
19	8-19	3	11:14-11:37	4.99	3.30	74.0	60.0	61.6	2.66	5.14	2.92	4.10	4.27	0.230	3.48
20	8-21	1	9:27-10:03	4.98	3.22	66.3	59.2	60.1	1.38	5.38	6.03	13.40	12.50	0.643	9.94
21	8-21	2	10:18-10:46	4.98	3.25	69.2	61.7	61.3	1.06	4.49	6.49	13.50	12.10	0.626	9.59
22	8-21	3	10:55-11:17	4.98	3.28	71.6	62.6	62.4	1.37	5.66	6.31	13.50	11.60	0.600	9.11
23	8-21	4	11:26-11:46	4.98	3.28	72.2	61.9	62.8	1.89	7.98	6.41	13.50	11.70	0.605	9.19
24	8-21	6	11:54-12:16	4.98	3.28	71.7	61.8	63.1	1.97	7.66	5.91	13.50	11.70	0.605	9.19
25	8-24	1	9:25- 9:52	4.93	3.31	73.5	61.1	59.5	1.53	15.65	15.20	18.00	18.40	0.859	12.79
26	8-24	2	10:07-10:31	4.93	3.32	76.0	62.1	61.2	1.92	13.00	10.00	19.00	18.40	0.859	12.76
27	8-24	3	10:43-11:07	4.93	3.36	79.0	64.3	63.3	2.01	13.07	9.55	19.00	17.70	0.838	12.30
28	8-24	4	11:20-11:45	4.93	3.40	82.9	67.0	65.1	1.91	14.65	11.19	18.00	16.50	0.800	11.60
29	8-27	1	14:07-14:32	4.71	3.40	82.0	65.2	71.5	4.88	4.79	1.32	2.76	2.36	0.129	1.79
30	8-31	6	15:32-16:26	5.00	3.50	91.7	70.7	72.5	4.02	7.64	2.73	2.40	2.44	0.132	1.89

Table II - Continued

Summary of 1953 Model Data - No Barrier

Test No.	Mo. & Day	Sta	Time of day	$\sqrt{A}$ ft	ν_e $\frac{ft^2}{sec}$ x10^{-4}	T_{AD} °F	T_{AW} °F	T_o °F	ΔC $\frac{lb}{ft^2}$ x10^{-4}	E $\frac{lb}{ft^2\text{-}sec}$ x10^{-6}	N x10^2	U_T $\frac{ft}{sec}$	U_{FT} $\frac{ft}{sec}$	U_* (Fig 6) $\frac{ft}{sec}$	R_* x10^3
31	9-21	6	14:15-14:58	4.97	3.22	66.5	51.0	55.5	3.45	9.58	4.29	8.00	7.73	0.415	6.40
32	9-22	6	12:14-12:46	4.80	3.42	85.0	58.0	61.7	5.21	1.60	4.29	8.10	7.95	0.427	5.99
33	9-22	1	13:23-13:58	4.80	3.44	86.6	58.1	64.6	6.26	16.65	3.71	7.75	7.00	0.379	5.29
34	9-22	2	14:15-14:39	4.80	3.46	88.3	58.9	65.5	6.56	16.65	3.52	7.69	6.80	0.370	5.13
35	9-23	6	11:22-11:54	4.83	3.36	79.5	49.8	60.2	6.90	24.30	5.07	14.50	11.80	0.610	8.78
36	9-23	1	12:23-12:56	4.83	3.38	80.6	50.6	61.4	7.12	23.10	4.63	14.50	11.80	0.610	8.72
37	9-23	2	13:20-13:50	4.83	3.38	81.1	50.7	62.4	7.48	22.80	4.35	15.90	11.80	0.610	8.72
38	9-23	6	14:12-14:38	4.83	3.38	81.3	51.0	63.1	7.58	21.40	4.03	14.00	11.60	0.600	8.58
39	9-24	6	13:20-13:47	4.95	3.34	78.6	52.4	57.1	5.11	27.80	8.05	16.50	15.70	0.770	11.40
40	9-24	1	14:07-14:31	4.95	3.36	78.9	51.3	57.4	5.59	28.20	7.46	16.70	15.70	0.770	11.32
41	9-24	2	14:48-15:12	4.95	3.35	79.0	51.5	57.9	5.64	26.80	7.03	16.40	15.70	0.770	11.38
42	9-24	6	15:30-15:50	4.95	3.34	78.3	52.0	58.4	5.53	26.50	7.11	17.10	15.70	0.770	11.40
43	9-25	6	11:45-12:18	4.99	3.20	65.5	51.4	53.5	2.70	4.62	2.66	4.20	3.75	0.201	3.13
44	9-25	1	12:38-13:11	4.99	3.26	70.9	53.8	55.0	2.99	4.97	2.54	4.25	3.94	0.212	3.24
45	9-25	2	13:34-14:06	4.99	3.32	75.2	54.7	57.2	3.81	7.10	2.81	4.10	3.75	0.201	3.02
46	9-25	6	14:24-14:54	4.99	3.33	78.0	57.0	58.7	3.73	6.27	2.52	3.60	3.75	0.201	3.01
47	9-30	6	11:52-12:26	4.97	3.28	73.1	55.7	57.8	3.30	3.16	1.45	2.36	2.14	0.116	1.76
48	9-30	1	12:51-13:19	4.97	3.33	77.1	57.6	59.4	3.54	2.80	1.18	2.32	2.07	0.110	1.64
49	9-30	2	13:36-14:12	4.97	3.38	81.6	58.5	61.1	4.36	3.52	1.19	2.20	1.98	0.107	1.57

Table III

Summary of 1953 Model Data - 1½" Barrier

Test No.	Mo. & Day	Time of day	Barrier Position	$\sqrt{A}$ ft	ν_e $\frac{ft^2}{sec}$ $x10^{-4}$	T_{AD} °F	T_{AW} °F	T_o °F	ΔC $\frac{lb}{ft^3}$ $x10^{-4}$	E $\frac{lb}{ft^2\text{-}sec}$ $x10^{-6}$	N $x10^2$	U_{FT} $\frac{ft}{sec}$	U_* $\frac{ft}{sec}$	R_* $x10^3$
1	9-1	14:16-14:47	D	4.95	3.42	85.7	69.0	71.8	3.71	16.70	6.48	8.51	0.455	6.59
2	9-1	14:56-15:22	D	4.95	3.46	87.3	69.1	71.8	3.87	16.02	5.93	8.40	0.450	6.44
3	9-1	15:39-16:11	D	4.95	3.46	87.4	67.7	71.6	4.49	19.42	6.19	8.40	0.450	6.44
4	9-1	16:21-16:44	D	4.95	3.41	84.2	66.7	71.2	4.35	18.89	6.30	8.47	0.452	6.56
5	10-5	13:49-14:28	D	5.00	3.22	67.0	46.4	51.9	4.30	13.90	5.01	8.10	0.436	6.76
6	10-5	14:55-15:33	D	4.95	3.22	67.0	46.7	52.6	4.37	14.00	4.93	8.10	0.436	6.70
7	10-5	16:08-16:36	D	4.99	3.20	64.9	46.0	53.2	4.41	13.17	4.66	8.10	0.436	6.80
8	10-7	12:32-13:08	6	5.00	3.34	77.9	49.3	54.3	5.45	19.56	5.38	8.08	0.433	6.49
9	10-7	13:35-14:17	6	5.00	3.36	79.2	49.9	55.3	5.66	20.05	5.27	7.45	0.400	5.95
10	10-7	14:51-15:31	6	5.00	3.36	79.5	50.3	57.1	6.01	20.53	5.08	8.10	0.436	6.49
11	10-8	10:45-11:13	6	5.00	3.22	66.5	46.7	50.8	3.90	8.19	3.26	3.84	0.207	3.21
12	10-8	11:30-11:53	6	5.00	3.24	69.2	48.6	52.2	3.97	7.90	3.07	3.75	0.201	3.10
13	10-8	12:10-12:35	6	5.00	3.27	71.3	49.4	53.8	4.36	8.35	2.93	3.76	0.201	3.07
14	10-8	14:25-15:00	D	5.00	3.32	75.6	51.4	57.2	5.05	9.49	2.82	3.53	0.190	2.86
15	10-8	15:14-15:47	D	5.00	3.31	74.8	51.4	57.8	5.14	9.68	2.84	3.76	0.201	3.04
16	10-9	19:31-19:56	D	5.00	3.20	65.5	45.7	54.4	4.88	28.47	9.12	19.70	0.895	13.97
17	10-9	20:09-20:31	D	5.00	3.18	63.2	44.7	52.9	4.53	26.15	9.08	19.86	0.900	14.13
18	10-12	19:41-20:06	6	5.00	3.07	53.2	45.3	51.3	2.43	16.43	11.01	17.92	0.844	13.75
19	10-12	20:18-20:43	6	5.00	3.05	51.7	43.9	49.5	2.28	14.17	10.20	17.97	0.846	13.87
20	10-12	20:56-21:27	6	5.00	3.06	52.6	44.0	48.4	2.18	12.69	9.52	17.98	0.846	13.83
21	10-14	11:34-12:06	12	4.99	3.22	67.2	52.2	56.6	3.39	7.18	3.28	4.05	0.218	3.38
22	10-14	12:26-13:05	12	4.99	3.24	68.3	53.1	57.2	3.39	7.03	3.19	3.93	0.210	3.23
23	10-14	13:25-14:10	12	4.99	3.25	69.6	54.0	58.1	3.46	6.97	3.10	3.93	0.210	3.22
24	10-15	11:54-12:34	12	5.00	3.20	64.9	51.3	53.3	2.61	8.92	5.34	7.98	0.427	6.66
25	10-15	12:55-13:26	12	5.00	3.22	67.2	52.0	54.3	2.91	9.81	5.24	7.98	0.427	6.63
26	10-15	13:44-14:21	12	5.00	3.24	68.6	52.1	55.1	3.28	11.43	5.37	7.98	0.427	6.58
27	10-16	19:28-19:52	12	5.00	3.02	48.3	41.2	48.7	2.47	13.70	9.22	19.40	0.885	14.66
28	10-16	20:02-20:23	12	5.00	2.99	46.3	39.9	46.6	2.14	12.60	9.85	17.90	0.843	14.09
29	10-16	20:39-21:02	12	4.99	3.02	49.2	41.4	45.6	1.94	10.62	9.04	18.00	0.847	13.99

Table III - Continued

Summary of 1953 Model Data - $1\frac{1}{2}$" Barrier

Test No.	Mo. & Day	Time of day	Barrier Position	$\sqrt{A}$ ft	ν_e $\frac{ft^2}{sec}$ $x10^{-4}$	T_{AD} °F	T_{AW} °F	T_o °F	ΔC $\frac{lb}{ft^3}$ $x10^{-4}$	E $\frac{lb}{ft^2\text{-}sec}$ $x10^{-6}$	N $x10^2$	U_{FT} $\frac{ft}{sec}$	U_* $\frac{ft}{sec}$	R_* $x10^3$
30	10-30	13:07-13:42	24	5.00	3.17	62.8	47.3	50.5	3.07	9.06	4.67	8.21	0.441	6.96
31	10-30	13:57-14:25	24	5.00	3.17	62.7	47.2	51.0	3.19	9.82	4.86	7.80	0.417	6.59
32	10-30	14:41-15:17	24	4.95	3.17	62.6	47.5	51.4	3.17	10.21	5.03	7.80	0.417	6.51
33	10-30	19:07-19:32	24	5.00	2.97	44.1	37.8	45.1	2.15	11.64	9.11	18.33	0.855	14.40
34	10-30	19:43-20:06	24	5.00	2.97	43.9	37.5	43.4	1.93	9.72	8.46	17.40	0.830	13.97
35	10-30	20:16-20:38	24	5.00	2.96	43.4	37.6	42.5	1.66	8.50	8.65	17.50	0.833	14.07
36	11-2	13:14-13:45	24	4.97	3.26	71.0	49.6	54.2	4.29	9.70	3.45	4.15	0.223	3.40
37	11-2	13:58-14:33	24	4.97	3.25	69.5	48.1	54.7	4.75	10.03	3.23	4.16	0.223	3.41
38	11-2	14:45-15:16	24	4.97	3.22	67.3	47.4	54.5	4.61	9.84	3.29	4.15	0.223	3.44

Legend

- D Barrier on dam
- 6 Barrier 6 in. upstream from dam
- 12 Barrier 12 in. upstream from dam
- 24 Barrier 24 in. upstream from dam

Table IV

Summary of 1953 Model Data - 3" Barrier

Test No.	Mo. & Day	Time of day	Barrier Position	$\sqrt{A}$ ft	ν_e $\frac{ft^2}{sec}$ $x10^{-4}$	T_{AD} ^oF	T_{AW} ^oF	T_o ^oF	ΔC $\frac{lb}{ft^3}$ $x10^{-4}$	E $\frac{lb}{ft^2\text{-}sec}$ $x10^{-6}$	N $x10^2$	U_{FT} $\frac{ft}{sec}$	U_* $\frac{ft}{sec}$	R_* $x10^3$
1	9-3	10:58-11:33	D	5.00	3.12	57.4	48.8	52.5	2.15	7.22	5.38	8.51	0.455	7.29
2	10-6	12:51-13:32	D	5.00	3.21	66.5	47.6	50.9	3.57	11.33	4.95	8.00	0.429	6.69
3	10-6	14:02-14:34	D	5.00	3.25	69.2	48.1	52.3	4.07	12.62	4.78	7.57	0.406	6.24
4	10-6	14:58-15:36	D	5.00	3.25	69.8	48.3	53.6	4.38	13.76	4.83	8.00	0.430	6.61
5	10-12	13:36-14:12	D	5.00	3.24	69.1	49.7	55.0	4.20	9.18	3.37	4.41	0.240	3.70
6	10-12	14:28-15:03	D	5.00	3.23	67.9	49.3	55.3	4.27	8.74	3.16	4.35	0.236	3.65
7	10-19	12:08-12:38	12	5.00	3.27	71.7	50.0	53.6	4.16	9.23	3.40	3.80	0.203	3.10
8	10-19	13:00-13:34	12	5.00	3.31	74.5	52.7	55.0	3.92	9.90	3.83	3.84	0.206	3.11
9	10-19	13:50-14:24	12	5.00	3.31	74.5	51.8	56.1	4.49	9.89	3.33	3.80	0.203	3.07
10	10-20	13:46-14:12	12	5.00	3.16	61.6	48.6	53.2	3.01	10.07	5.30	8.10	0.435	6.89
11	10-20	14:25-14:55	12	5.00	3.17	63.0	49.9	53.4	2.86	11.19	6.16	7.73	0.413	6.51
12	10-20	15:09-15:39	12	5.00	3.15	60.7	49.9	53.8	2.56	8.44	5.22	7.93	0.423	6.71
13	10-22	12:03-12:39	24	4.97	2.95	42.7	37.0	42.8	1.78	6.32	5.97	8.20	0.440	7.41
14	10-22	13:04-13:34	24	4.97	2.96	42.8	37.2	41.8	1.57	6.05	6.51	8.20	0.440	7.39
15	10-22	13:52-14:17	24	4.97	2.96	43.0	37.4	41.5	1.49	5.77	6.51	8.20	0.440	7.39
16	11-2	19:28-19:50	24	4.95	3.08	54.3	44.2	49.7	2.64	15.81	9.62	19.05	0.875	14.07
17	11-2	20:07-20:28	24	4.95	3.07	53.1	43.9	48.7	2.35	13.50	9.28	17.00	0.812	13.09
18	11-3	13:19-13:48	24	4.90	2.98	45.0	36.6	44.9	2.54	6.70	4.36	4.30	0.232	3.82
19	11-3	14:17-14:52	24	4.90	2.98	45.5	37.0	44.0	2.42	5.37	3.65	3.90	0.210	3.46
20	11-3	15:16-15:43	24	4.90	2.98	45.5	37.0	43.5	2.34	5.85	4.11	3.91	0.210	3.46
21	11-6	13:19-13:56	48	5.00	2.96	43.8	40.0	42.4	0.98	2.90	5.00	7.90	0.422	7.13
22	11-6	14:13-14:47	48	5.00	2.97	44.2	40.4	42.5	0.94	2.94	5.27	7.90	0.422	7.11
23	11-6	15:03-15:35	48	5.00	2.98	44.9	40.7	42.7	0.98	2.94	5.03	7.80	0.417	7.00
24	11-6	19:32-19:54	48	5.00	2.91	38.8	37.9	40.8	0.57	3.14	9.46	19.10	0.877	15.08
25	11-6	20:07-20:33	48	5.00	2.90	38.2	37.5	40.1	0.48	2.60	9.34	17.80	0.840	14.49

Table IV - Continued

Summary of 1953 Model Data - 3" Barrier

Test No.	Mo. & Day	Time of day	Barrier Position	$\sqrt{A}$ ft	ν_e $\frac{ft^2}{sec}$ $x10^{-4}$	T_{AD} ^oF	T_{AW} ^oF	T_o ^oF	ΔC $\frac{lb}{ft^3}$ $x10^{-4}$	E $\frac{lb}{ft^2\text{-}sec}$ $x10^{-6}$	N $x10^2$	U_{FT} $\frac{ft}{sec}$	U_* $\frac{ft}{sec}$	R_* $x10^3$
26	11-6	20:44-21:07	48	5.00	2.90	38.2	37.4	39.6	0.43	2.37	9.52	18.53	0.861	14.86
27	11-9	13:37-14:02	48	5.00	3.23	68.2	45.0	46.4	3.82	8.35	3.38	4.20	0.227	3.52
28	11-9	14:15-14:42	48	5.00	3.24	68.8	45.6	48.0	4.03	8.44	3.24	4.20	0.227	3.50
29	11-9	15:03-15:28	48	5.00	3.23	67.8	45.3	49.2	4.20	8.82	3.25	4.20	0.227	3.52
30	11-13	13:22-13:44	12	4.85	3.23	67.5	46.9	49.1	3.64	22.80	9.40	17.50	0.832	12.49
31	11-13	13:54-14:18	12	4.85	3.24	68.6	47.5	50.1	3.79	24.56	9.70	17.50	0.832	12.45
32	11-13	14:27-14:50	12	4.85	3.25	69.5	47.6	51.3	4.14	25.55	9.20	17.50	0.832	12.40
33	11-25	10:24-10:48	24	4.99	2.91	39.1	33.8	36.7	1.21	8.41	11.91	19.40	0.886	15.20
34	11-25	13:17-13:45	24	4.99	3.00	46.7	36.8	39.3	1.94	10.33	8.87	14.50	0.723	12.03
35	11-25	14:00-14:27	24	5.00	3.00	47.4	37.4	39.8	1.93	8.78	7.58	16.00	0.780	13.00

Legend

D	Barrier on top of dam
12	Barrier 12" upstream from dam
24	Barrier 24" upstream from dam
48	Barrier 48" upstream from dam

Table V

Summary of Rohwer's Data

Test No.	Date	Time[1]	Period[2] min.	T_{air} °F	T_o °F	ΔC grains/ft³	ΔC lb/ft³ x10⁻⁴	E lb/ft²-sec x10⁻⁵	ν_e ft²/sec x10⁻⁴	$U_{2.5}$ ft/sec	$U_{0.26}$ ft/sec	U_* ft/sec	$\sqrt{A}$ ft	N x10³	R_* x10⁴
1	10- 2-26	14:30	342	63.7	58.5	2.867	4.10	0.559	3.18	5.43	3.90	0.268	75.3	3.32	6.35
2	10- 7-26	14:30	347	70.9	58.4	3.530	5.05	1.151	3.26	8.18	5.95	0.382	75.3	5.27	8.81
3	10-13-26	14:30	343	64.4	58.3	3.506	5.01	0.987	3.19	7.89	5.70	0.384	75.3	4.65	9.06
4	10-25-26	14:30	352	62.3	51.9	2.472	3.53	1.932	3.17	14.79	10.50	0.753	75.3	13.00	17.90
5	11- 8-26	14:30	351	37.2	40.3	1.449	2.07	0.866	2.84	10.26	7.35	0.510	75.3	11.10	13.50
6	11-14-26	14:30	269	41.8	40.1	1.652	2.36	2.033	2.94	16.48	11.60	0.856	75.3	22.00	21.90
7	5-12-27	08:30	313	59.8	55.2	2.512	3.59	0.804	3.14	12.86	9.25	0.634	75.3	5.37	15.20
8	5-26-27	08:30	315	64.2	66.9	4.353	6.22	0.441	3.19	5.31	3.75	0.274	75.3	1.67	6.47
9	6- 6-27	02:30	418	50.4	63.3	2.286	3.27	0.374	3.04	2.98	2.10	0.154	75.3	2.83	3.82
10	6-17-27	02:30	426	55.0	64.5	2.344	3.35	0.570	3.09	3.95	2.75	0.210	75.3	4.15	5.12
11	7- 8-27	20:30	320	71.9	78.7	6.301	9.00	1.357	3.28	3.99	2.80	0.209	75.3	3.46	4.79
12	7-16-27	20:30	332	67.7	75.8	5.404	7.72	1.229	3.17	3.68	2.60	0.190	75.3	3.78	4.52
13	7-18-27	20:30	342	70.0	76.6	4.077	5.82	0.990	3.25	3.77	2.70	0.188	75.3	3.94	4.35
14	7-25-27	20:30	338	68.6	77.7	6.121	8.74	1.181	3.24	2.77	1.85	0.161	75.3	3.14	3.74
15	8-18-27	14:30	339	63.9	72.5	4.370	6.24	0.948	3.18	5.19	3.70	0.262	75.3	3.60	6.21
16	10- 5-27	20:30	369	48.4	54.8	2.299	3.28	0.329	3.01	2.82	1.95	0.153	75.3	2.51	3.83
17	10- 7-27	20:30	357	41.9	54.7	2.323	3.32	0.365	2.96	2.87	2.00	0.153	75.3	2.80	3.89
18	10-11-27	14:30	345	49.4	51.0	3.190	4.56	2.495	3.03	17.90	12.50	0.948	75.3	13.60	23.60
19	10-16-27	02:30	399	37.2	51.9	2.118	3.03	0.370	2.89	2.77	1.85	0.161	75.3	3.18	4.20
20	10-18-27	02:30	440	46.8	53.3	2.578	3.68	0.493	3.00	3.98	2.80	0.207	75.3	3.36	5.20
21	10-20-27	02:30	432	44.1	54.2	2.760	3.94	0.484	2.97	2.80	1.90	0.158	75.3	3.11	4.01
22	10-26-27	08:30	314	55.4	55.2	3.143	4.49	0.138	3.09	4.24	3.00	0.218	75.3	0.75	5.31
23	10-31-27	14:30	331	41.5	50.6	2.007	2.87	0.786	2.94	8.23	5.95	0.400	75.3	7.02	10.25
24	11- 1-27	08:30	318	38.5	49.2	1.932	2.76	0.328	2.91	7.86	5.70	0.379	75.3	3.08	9.80
25	11-28-27	08:30	319	42.0	49.2	1.463	2.09	0.408	2.95	6.38	4.60	0.312	75.3	4.98	7.96

1 MST at middle of test period.
2 Entries under period are the lengths of the test periods.

Appendix C

DATA TRANSFORMATION

This section is devoted to a description of the method used to calculate the shear velocity based on a consideration of the changes of momentum.

As indicated in Chapter III the Prandtl-Kármán relationship between velocity distribution and shear velocity was found satisfactory when the air pattern was not materially affected by surface objects. Such was not the case when the $1\frac{1}{2}$-in. and 3-in. barriers were placed in the tunnel for they altered the air pattern to such an extent that the Prandtl-Kármán relationship was no longer valid. Therefore, the shear velocity had to be determined by other means when the barriers were in the tunnel. The authors assumed that for a particular ambient air velocity when no upstream barrier was in position the shear velocity at a particular tunnel location always had the same value. Through a consideration of the interrelationship between shear and change of momentum, a correlation between U_* and U_{FT} was evolved, Fig. 6, Chapter III. By using this relationship it was possible to ascertain the shear velocity U_* from a knowledge of U_{FT}. The remainder of this section will be devoted to a description of procedures followed in arriving at the data for Fig. 6.

Through a consideration of the principle of momentum, the total drag for a unit width on a boundary over the length X may be written as

$$D_X = \rho \int_0^{\infty} U(U_o - U)\, dz \tag{136}$$

from which the momentum thickness θ can be obtained as

$$\theta = \frac{D_X}{\rho U_o^2} = \int_0^{\infty} \frac{U}{U_o}\left(1 - \frac{U}{U_o}\right) dz\ . \tag{137}$$

The total drag on a boundary D_X can also be written in terms of what is known as the mean drag coefficient C_f as follows

$$D_X = X\, C_f \frac{\rho U_o^2}{2} . \tag{138}$$

Through use of Eqs. 137 and 138 the momentum thickness can also be written in terms of the mean drag coefficient.

$$\theta = \frac{D_X}{\rho U_o^2} = X \frac{C_f}{2} \tag{139}$$

or

$$C_f = \frac{2\theta}{X} . \tag{139a}$$

A considerable amount of work has been performed on the relationship between C_f and R_X by other investigators. This work has led to the expressions of

$$C_f = \frac{1.328}{R_X^{\frac{1}{2}}} \tag{140}$$

for laminar flow and

$$C_f = \frac{0.074}{R_X^{1/5}} \tag{141}$$

for turbulent flow. In these equations, R_X is a form of Reynolds number and is equal to XU_o/ν . It seemed reasonable that the Lake Hefner model data should conform to the relationships between C_f and R_X evolved by other investigators. If such were the case, then these relationships could be used to help define a correlation between C_f and R_X .

In the course of gathering data during the 1953 Testing Program, velocity profiles without any upstream barrier present were measured at what are termed Stas. 1, 2, 3, 4, 5, and 6. Stas. 1, 2, 3, and 4 corresponded in location to the stations occupied in the prototype and Stas. 5 and 6 were upstream from the modeled lake, Fig. 20. By plotting $\frac{U}{U_o}\left(1 - \frac{U}{U_o}\right)$ against z , the momentum thickness θ can be obtained by planimetering the area under the curve, Fig. 21. This process is in effect the graphical integration indicated by Eq. 137. The mean drag coefficient C_f can then be found through use of Eq. 139a. The distance X in Eq. 139a is supposed to be the distance from the

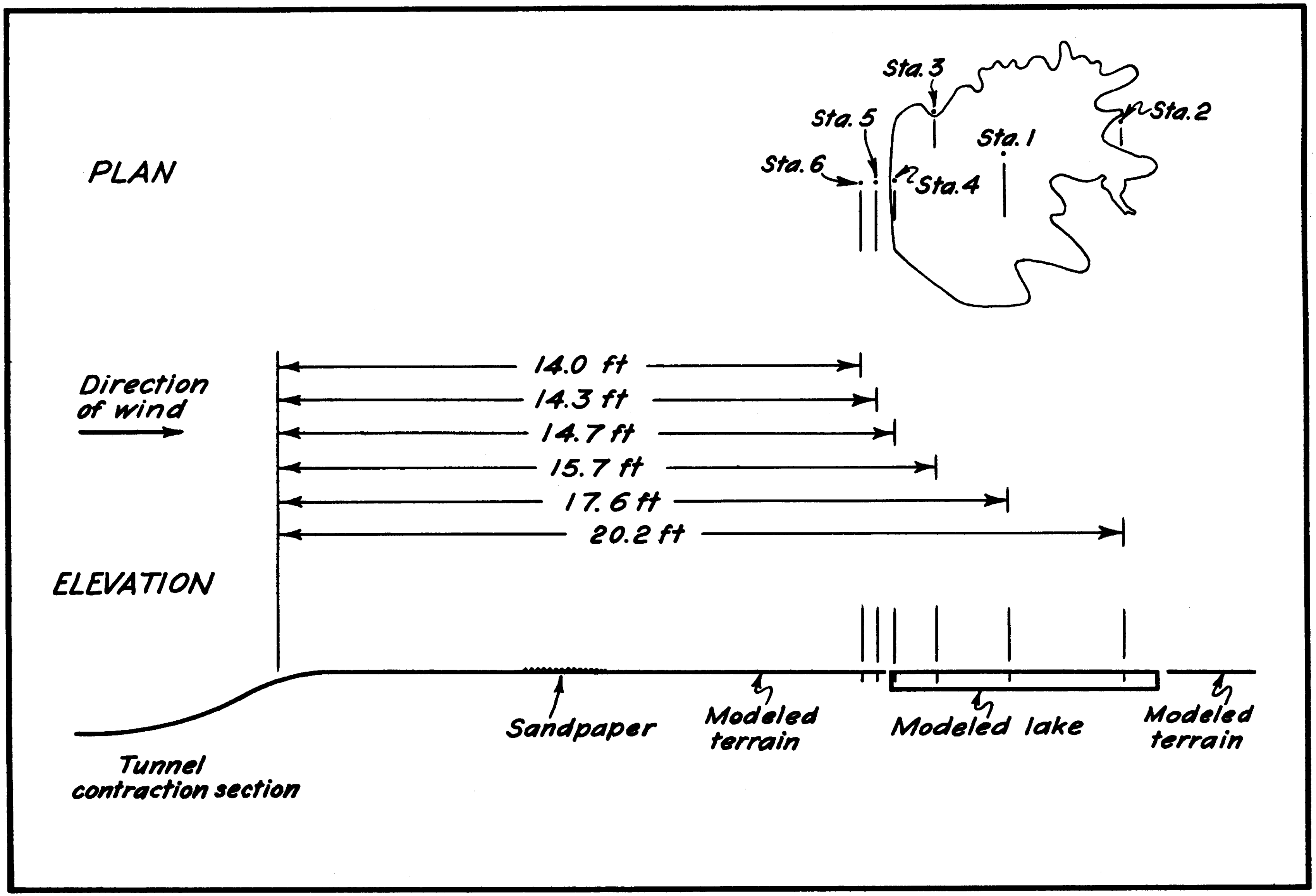

Fig. 20. Station locations for model.

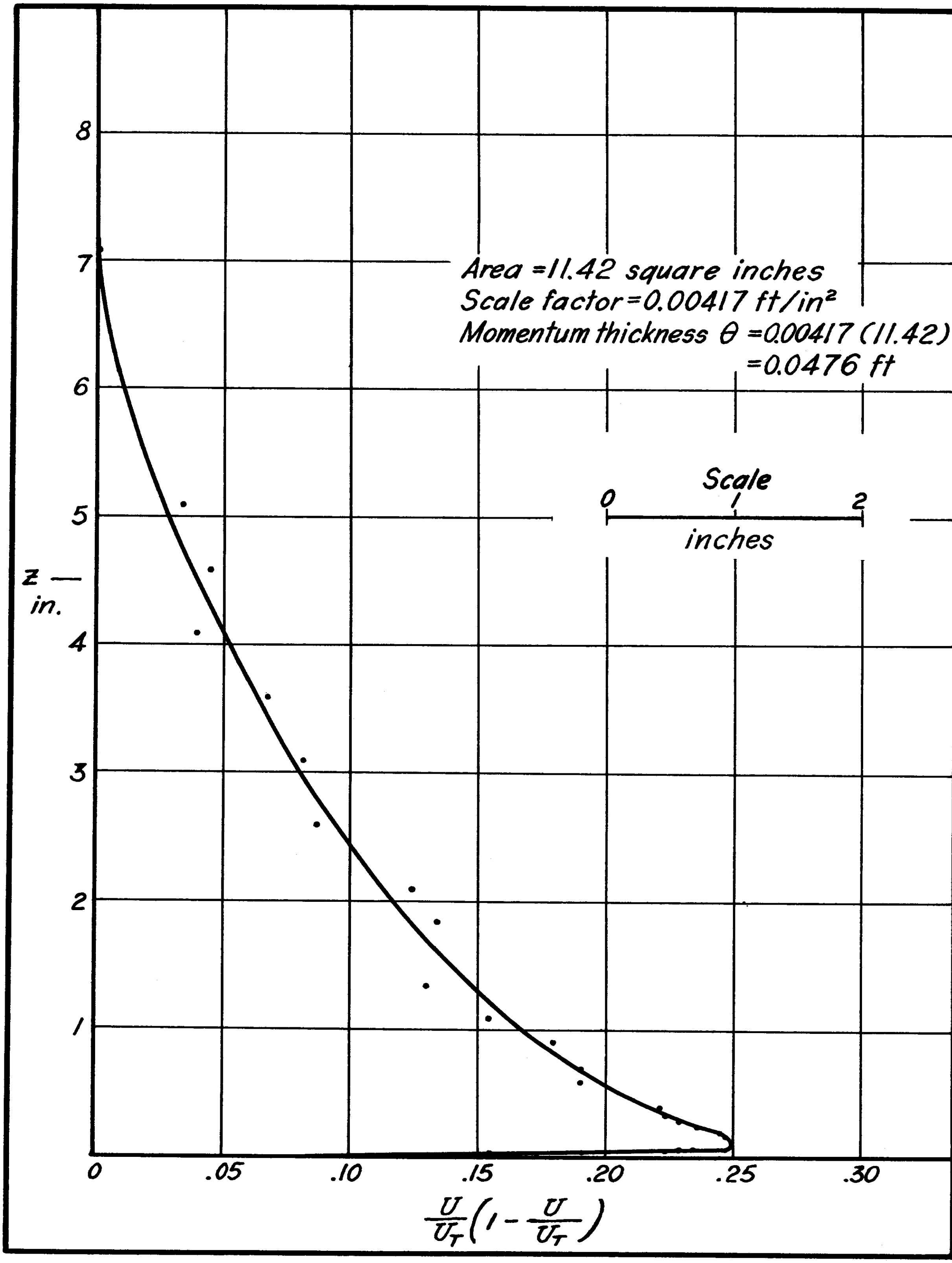

Fig. 21. Variation of $\frac{U}{U_T}\left(1-\frac{U}{U_T}\right)$ with z.

leading edge of the boundary to the point at which the velocity profile is measured. As indicated in Part I (3), the model of Lake Hefner was not constructed with a sharp leading edge. Instead, the transition between the tunnel and the model was effected in a gradual manner. Therefore the value of the distance X used in Eq. 139a cannot be measured exactly. After considering the position of the model in the tunnel, the tunnel shape, and the artificial roughness upstream from the model, the authors estimated that the effective length for X for the various stations was as follows; Fig. 20

Sta. 1 -- X = 17.6 ft,

Sta. 2 -- X = 20.2 ft,

Sta. 3 -- X = 15.7 ft,

Sta. 4 -- X = 14.7 ft,

Sta. 5 -- X = 14.3 ft,

Sta. 6 -- X = 14.0 ft.

The value of R_X corresponding to the various values of C_f were easily computed from a knowledge of U_o, X, and ν. The velocity U_o was considered to be equal to the velocity above the boundary layer as measured by the traverse mechanism. The value of X corresponded to the station distance as given in the above table. The kinematic viscosity ν was determined from air temperature and pressure considerations. During the course of the 1953 Testing Program, data for 49 velocity profiles without any upstream barrier were collected for which C_f and R_X could be computed. The points representative of these 49 profiles are presented in Fig. 22. Some of these data tend to group about Eq. 141 which is representative of turbulent flow while other data group about Eq. 140 which is indicative of laminar flow. Although, a great majority of the data fall in what might be considered the transitional region between laminar and turbulent flow in which scattered results might be anticipated. Following the data as well as possible, a smooth curve was drawn between the lines for Eqs. 140 and 141. This smooth curve and the lines for Eqs. 140 and

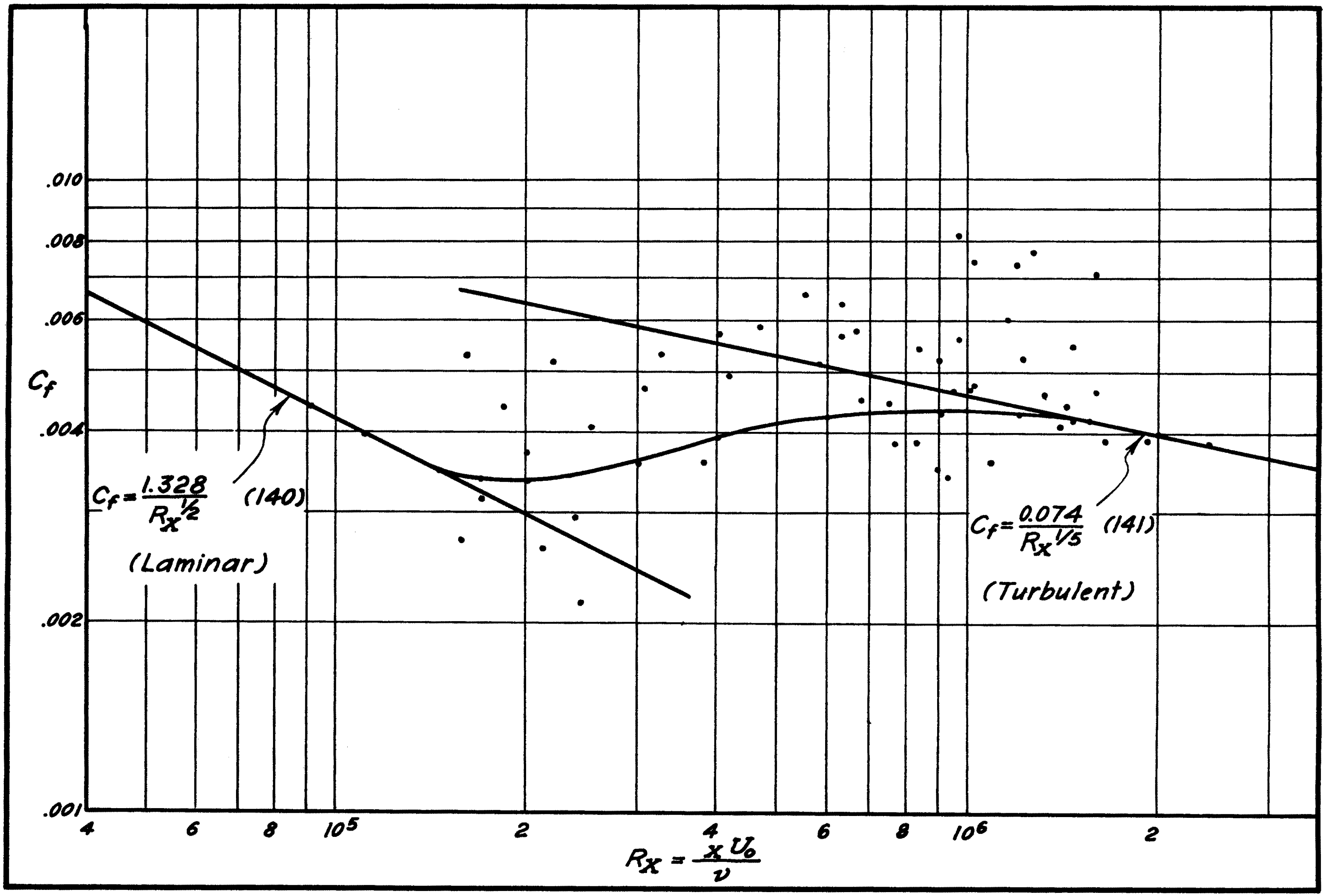

Fig. 22. Variation of C_f with R_x.

141 beyond the points of tangency were considered to be representative of the relationship between C_f and R_X for the model.

The shear at the surface, τ_o, may be expressed as follows:

$$\frac{d\ D_X}{d\ X} = \tau_o \tag{142}$$

or

$$\frac{d}{dX}\left(\frac{D_X}{\rho U_o^2}\right) = \frac{\tau_o}{\rho U_o^2} = \frac{U_*^2}{U_o^2} . \tag{143}$$

Through Eqs. 138 and 143 one may write

$$\frac{U_*^2}{U_o^2} = \frac{d}{dX}\left(\frac{X\ C_f}{2}\right) . \tag{144}$$

Without altering the relationship of Eq. 144, the variable of differentiation may be changed as follows:

$$\frac{U_*^2}{U_o^2} = \frac{1}{2}\frac{d}{d\ R_X}(R_X\ C_f) . \tag{145}$$

Through the use of the previously described relationship between C_f and R_X, Fig. 22, and the approximate differentiation of the product $R_X C_f$ with respect to R_X, the value of U_*^2/U_o^2 can be calculated; that is,

$$\frac{U_*^2}{U_o^2} = \frac{1}{2}\left(\frac{R_{X_2}\ C_{f_2} - R_{X_1}\ C_{f_1}}{R_{X_2} - R_{X_1}}\right). \tag{146}$$

It was found that if the difference between R_{X_2} and R_{X_1} is small, then either value of R_X could be chosen from which to compute U_o. In carrying out this approximate differentiation, X was chosen as 14.0 ft which corresponds to the location of Sta. 6. Therefore, U_* as given by this method is for Sta. 6. The kinematic viscosity was assumed to have a constant value of 2×10^{-4} ft^2/sec. The kinematic viscosity as experienced under actual testing did not vary by more than 4% from this figure.

From the values of U_*^2/U_o^2 obtained through Eq. 146 and U_o, the shear velocity U_* corresponding to each velocity was ascertained. The shear velocity U_* was therefore known in terms of U_o , the ambient velocity as measured by the traverse. Due to the arrangement of the model in the tunnel, U_o as measured by the traverse mechanism (hereafter referred to as U_T) was not the same as U_o measured at the forward tunnel location (hereafter referred to as U_{FT}) , Fig. 23. Using the relationship of Fig. 23, U_* was correlated with U_{FT} instead of U_T .

After the approximate differentiation indicated by Eq. 146 had been carried out over a wide range of R_X , the relationship between U_* and U_{FT} depicted in Fig. 6 was developed. This relationship was used not only in evaluating U_* for the work with the barriers but also U_* for non-barrier work.

In Part I of the Lake Hefner Final Report, the shear velocity was computed by means of the Prandtl-Kármán relationship, Eq. 1. In order to evaluate the shear velocity for the 1952 data on the basis of momentum considerations it was necessary to go through the same steps as followed with the 1953 data to determine if the same relationships, that is Figs. 6, 22, and 23, were still applicable. This work with the 1952 data indicated that the relationship between C_f and R_X arrived at for the 1953 work was representative of the 1952 work. Therefore the relationship depicted in Fig. 6 was used to evaluate U_* for both the 1952 and 1953 data on the basis of momentum principles.

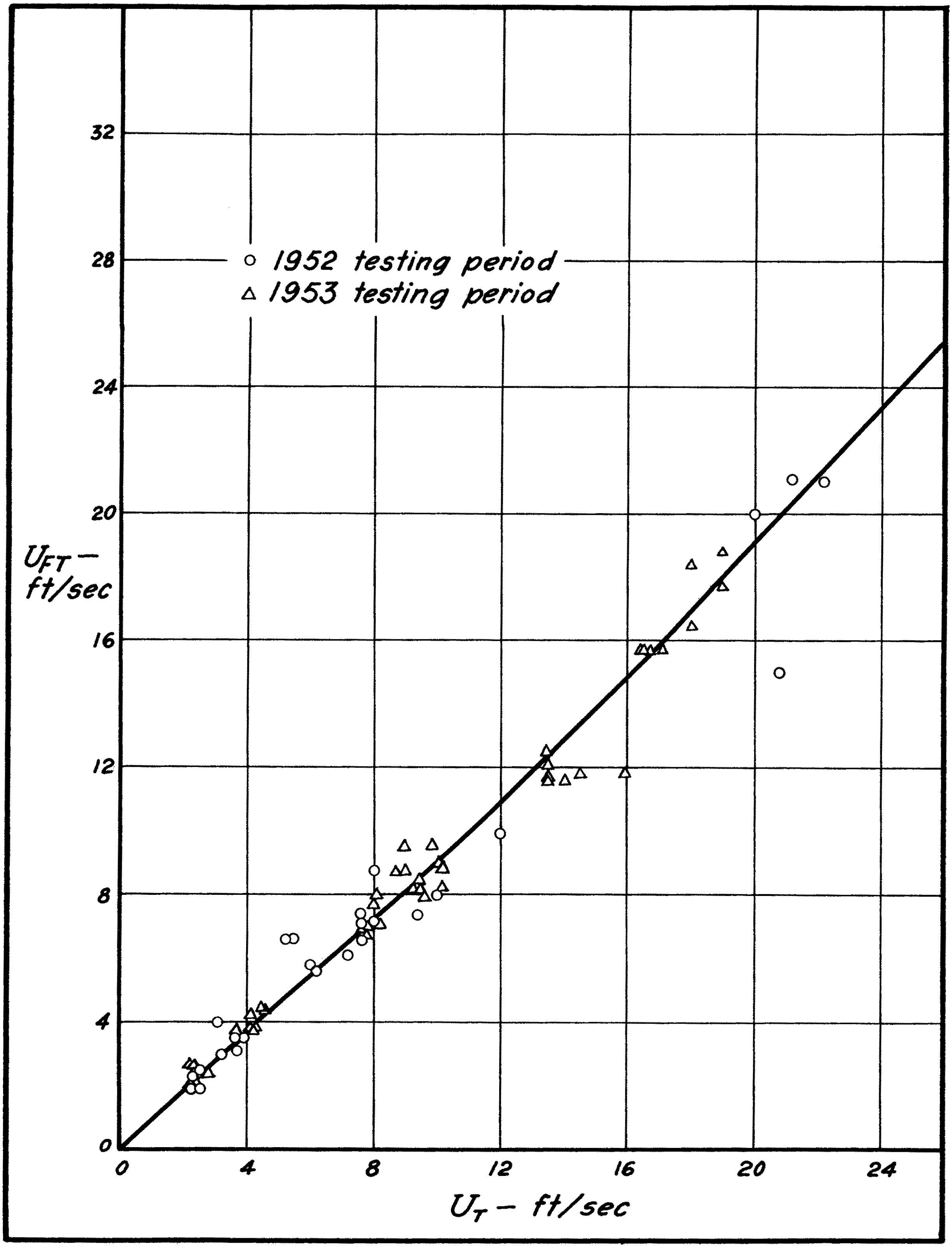

Fig. 23. Variation of U_T with U_{FT} — 1952 and 1953 data.

Appendix D

DETAILED MODEL DATA

In this section of the report the detailed non-barrier model data for 1953 are presented. All pertinent data concerning the barrier model data for 1953 are presented in Table II, Appendix B. The method of identifying the data is similar to that followed in Part I (3).

Part I - Model Tests

Time of day	Height above terrain	Forward tunnel psychrometer T_{AD}-°F	T_{AW}-°F	Traverse psychrometer °F	°F	Traverse wind velocity	Quantity of water evaporated
		Thermo.	Thermo.	Thermo.	Thermo.		
	Inches	#41	#51	#42	#52	ft/sec	cc
		Test No. 1		Date Aug. 10, 1953		Sta. 1	
14:19	0.035	81.2	62.8	75.0			0
14:24	0.040			75.5			40
14:27	0.045	82.3	63.6	75.6			82
14:29	0.050	82.4	63.5	75.8			
14:31	0.060	82.7	63.2	76.3			129
14:33	0.070	82.7	63.3	76.6	65.4		
14:37	0.080	82.6	63.6	77.0	65.4		193
14:40	0.090	83.0	63.7	77.4	65.5		
14:42	0.100	83.1	63.8	77.5	65.5	5.2	
14:43	0.110	83.5	63.6	77.6	65.5	5.3	
14:45	0.135	83.7	64.2	78.6	65.4	5.6	250
14:50	0.160	84.2	63.6	79.2	65.1	5.9	
14:51	0.185	84.0	63.6	79.3	65.1	6.2	340
14:54	0.210	84.2	64.0	79.6	65.5	6.2	
14:56	0.260	84.5	63.7	80.2	65.2	6.5	
14:58	0.310	84.1	63.4	80.1	65.0	6.5	402
15:00	0.360	84.4	63.9	80.7	65.2	6.8	
15:03	0.410	84.5	63.4	80.9	64.9	6.9	
15:06	0.510	84.1	63.1	81.0	64.8	6.9	480
15:08	0.610	84.1	63.1	81.8	64.8	7.0	
15:10	0.710	84.7	63.6	82.3	65.1	7.1	
15:12	0.910	85.1	64.1	82.9	65.3	7.7	500
15:15	1.110	85.1	64.0	83.7	65.6	7.9	
15:16	1.360	85.4	64.0	83.8	65.5	8.3	
15:17	1.610	85.9	64.3	84.4	65.7	8.4	591
15:19	1.860	85.8	64.1	85.0	65.7	8.6	
15:21	2.110	85.9	64.2	85.1	65.8	9.0	
15:24	2.610	85.9	64.3	85.4	65.9	9.0	661
15:26	3.110	85.7	64.1	85.5	66.0	9.0	
15:28	3.610	84.9	63.0	84.9	65.2	9.1	
15:30	4.110	85.4	63.9	85.4	65.7	9.7	
15:32	4.610	86.4	64.0	86.1	65.9	9.6	750
15:34	5.110	86.2	64.1	85.9	65.9	9.6	796
		Test No. 2		Date Aug. 10, 1953		Sta. 6	
15:55	0.020	86.4	64.1	84.6	70.4		0
15:58	0.030	86.9	64.9	84.9	70.7		
16:00	0.040	86.4	64.5	84.7	70.2		53
16:02	0.060	86.7	64.6	85.1	69.5		
16:03	0.080	86.3	64.5	85.3	68.9		
16:05	0.100	86.2	63.9	85.0	67.9	4.9	
16:07	0.120	86.2	64.6	84.9	68.0	4.9	
16:09	0.170	86.2	64.4	85.1	66.0	5.8	156
16:11	0.220	86.2	64.1	85.0	65.4	5.8	
16:15	0.320	86.6	64.7	85.4	66.1	6.0	
16:16	0.420	86.2	64.4	85.2	65.6	6.4	
16:18	0.620	86.2	64.3	85.4	65.5	6.6	250
16:20	0.820	86.3	64.2	85.7	65.4	7.0	
16:21	1.220	86.2	63.9	85.6	65.3	7.5	
16:23	1.720	85.7	63.4	85.2	64.8	7.7	315

Time of day	Height above terrain Inches	Forward tunnel psychrometer TAD-°F Thermo. #41	Forward tunnel psychrometer TAW-°F Thermo. #51	Traverse psychrometer °F Thermo. #42	Traverse psychrometer °F Thermo. #52	Traverse wind velocity ft/sec	Quantity of water evaporated cc
	Test No. 2 (Cont.)						
16:25	2.220	85.4	63.6	85.1	65.0	8.5	
16:28	3.720	85.3	64.0	85.0	64.9	8.8	
16:30	5.220	85.0	64.5	85.0	65.4	9.2	
16:33							418

Time of day	Height above terrain Inches	Forward tunnel psychrometer TAD-°F Thermo. #41	Forward tunnel psychrometer TAW-°F Thermo. #51	Traverse psychrometer °F Thermo. #42	Traverse psychrometer °F Thermo. #52	Traverse wind velocity ft/sec	Quantity of water evaporated cc
		Test No. 3		Date Aug. 12, 1953		Sta. 1	
09:54	0.020	72.7	59.2	66.8			0
09:56	0.025		59.2				
09:57	0.030		58.8				
09:58	0.035	73.6	59.1	67.4			
09:59	0.045		59.6				
10:00	0.055		59.6		60.6		38
10:01	0.065		59.9		60.6		
10:02	0.075	74.1	58.8	69.0	60.2		
10:04	0.085		59.5		60.1		
10:05	0.095		59.6		59.9		
10:06	0.120		60.0		60.0	4.8	75
10:07	0.145	74.6	58.8	69.1	59.0	4.9	
10:08	0.170		59.2		59.8	5.4	
10:09	0.195		59.3		60.0	5.5	
10:09	0.245		59.0		59.6	5.8	
10:10	0.295	73.8	59.5	72.6	59.9	5.9	
10:11	0.345		60.1		60.0	5.9	
10:12	0.395		60.0		60.1	6.0	120
10:15	0.495		60.0		60.2	6.3	
10:15	0.595	74.5	60.6	72.0	60.6	6.7	
10:16	0.695		60.7		60.4	7.0	
10:17	0.895		59.7		59.7	6.9	
10:18	1.095		59.4		59.7	7.0	157
10:20	1.345	75.8	59.6	72.9	59.8	7.3	
10:21	1.595		59.1		59.3	7.3	
10:22	1.845		59.1		59.1	8.0	
10:23	2.095		59.0		59.0	8.0	195
10:25	2.595	75.1	58.9	74.4	58.6	8.4	
10:26	3.095		58.5		58.7	8.7	
10:27	3.595		58.2		58.6	8.6	
10:28	4.095		58.7		59.0	9.0	
10:30	4.595	76.2	57.7	75.2	58.7	9.5	
10:30	5.095		56.9		57.7	9.4	250
10:32	7.095		58.1		58.5	9.4	
10:35	9.095	75.3	58.5	75.2	59.1	9.4	
10:37							318

Time of day	Height above terrain Inches	Forward tunnel psychrometer T_{AD}-°F Thermo. #41	Forward tunnel psychrometer T_{AW}-°F Thermo. #51	Traverse psychrometer °F Thermo. #42	Traverse psychrometer °F Thermo. #52	Traverse wind velocity ft/sec	Quantity of water evaporated cc
		Test No. 4		Date Aug. 12, 1953		Sta. 2	
10:55	0.020	77.1	58.8	70.8	63.4		0
10:57	0.025						
10:58	0.030						
10:58	0.035	77.4	59.5	70.9	62.6		
10:59	0.045						
11:00	0.055						38
11:01	0.065						
11:02	0.075	78.0	59.3	71.6	61.6		
11:03	0.085						
11:03	0.095						
11:04	0.120					4.4	
11:05	0.145	78.7	59.9	72.7	60.8	5.0	
11:06	0.170					5.2	
11:07	0.195					5.4	93
11:08	0.245					5.8	
11:09	0.295	78.3	59.6	73.3	60.2	6.1	
11:10	0.345					6.3	
11:10	0.395					6.3	128
11:13	0.495					6.7	
11:14	0.595	78.8	57.3	74.6	58.9	7.0	
11:15	0.695					7.0	
11:16	0.895					7.2	
11:17	1.095					7.6	
11:18	1.345	79.4	57.8	76.2	58.5	8.0	
11:19	1.595					8.0	207
11:20	1.845					7.9	
11:21	2.095					8.1	
11:22	2.595	80.7	58.1	78.4	58.5	8.5	
11:23	3.095					8.6	250
11:24	3.595					8.7	
11:25	4.095					9.0	
11:26	4.595	78.8	57.7	77.8	58.2	9.0	
11:27	5.095					9.1	289
11:29	7.095					9.4	
11:31	9.095	80.0	57.0	79.0	56.9	9.4	350
		Test No. 5		Date Aug. 13, 1953		Sta. 1	
09:07	0.020	75.0	56.3	67.1	59.0		0
09:08	0.025			67.4	58.7		
09:10	0.030			67.4	58.6		
09:11	0.035	74.7	58.4	67.7	58.6		
09:12	0.045			67.8	58.5		
09:13	0.055			68.6	58.6		
09:14	0.065			68.6	58.6		58
09:15	0.075	75.3	57.2	69.2	58.5		
09:16	0.085			69.0	58.6		
09:17	0.095			69.5	58.7		
09:18	0.120			69.8	58.6	5.8	

Time of day	Height above terrain Inches	Forward tunnel psychrometer T_{AD}-°F Thermo. #41	Forward tunnel psychrometer T_{AW}-°F Thermo. #51	Traverse psychrometer °F Thermo. #42	Traverse psychrometer °F Thermo. #52	Traverse wind velocity ft/sec	Quantity of water evaporated cc
	Test No. 5 (Cont.)						
09:19	0.145	74.8	57.2	69.7	58.6	6.2	
09:20	0.170			70.2	58.3	6.2	
09:21	0.195			70.7	58.2	6.5	120
09:22	0.245			70.7	57.9	7.1	
09:23	0.295	75.7	56.5	71.1	57.7	7.1	
09:24	0.345			71.5	57.2	7.3	
09:25	0.395			71.2	57.2	7.4	
09:29	0.495			72.2	57.4	7.5	
09:30	0.595	76.2	57.2	72.5	57.3	7.1	
09:31	0.695			72.5	57.8	7.8	211
09:32	0.895			73.2	57.8	8.5	
09:33	1.095			74.2	58.4	8.5	
09:34	1.345	76.6	58.0	73.8	58.2	8.6	
09:35	1.595			75.0	58.2	8.6	250
09:36	1.845			75.2	59.0	8.7	
09:37	2.095			75.6	57.2	9.1	
09:38	2.595	77.4	56.7	75.6	57.2	9.9	
09:40	3.095			75.6	57.4	9.9	
09:41	3.595			76.6	57.4	10.0	
09:42	4.095			76.7	57.2	10.1	
09:43	4.595	78.0	55.5	77.0	56.5	10.1	323
09:44	5.095			77.0	56.7	10.1	
09:46	7.095			78.2	57.8	10.1	
09:48	9.095	78.3	58.5	78.1	57.7	10.1	
09:50							406
		Test No. 6		Date Aug. 13, 1953		Sta. 2	
10:09	0.020	78.9	58.6	72.0	60.0		0
10:10	0.025			72.0	60.0		
10:11	0.030			71.6	60.0		
10:12	0.035	80.3	59.0	72.0	59.8		
10:13	0.045			72.2	60.0		
10:13	0.055			72.2	60.0		
10:14	0.065			72.6	60.0		
10:14	0.075	80.7	58.7	72.7	60.4		48
10:15	0.085			72.6	60.6		
10:16	0.095			72.9	60.2		
10:17	0.120			73.1	60.2	5.5	
10:18	0.145	81.0	59.5	73.6	60.4	5.8	
10:19	0.170			73.1	60.4	6.0	
10:20	0.195			74.0	60.0	6.1	87
10:20	0.245			75.0	59.6	6.5	
10:21	0.295	80.6	58.6	74.5	59.3	6.6	
10:22	0.345			75.3	59.0	7.0	
10:23	0.395			75.3	59.5	7.1	128
10:25	0.495			76.2	59.8	7.4	
10:26	0.595	81.1	59.1	76.3	59.6	7.8	
10:28	0.695			77.0	60.5	7.7	

Time of day	Height above terrain	Forward tunnel psychrometer T_{AD}-°F	Forward tunnel psychrometer T_{AW}-°F	Traverse psychrometer °F	Traverse psychrometer °F	Traverse wind velocity	Quantity of water evaporated
	Inches	Thermo. #41	Thermo. #51	Thermo. #42	Thermo. #52	ft/sec	cc
	Test No. 6 (Cont.)						
10:29	0.895			77.6	60.5	7.7	181
10:29	1.095			77.6	60.1	7.8	
10:30	1.345	80.6	59.0	78.3	60.0	8.2	
10:31	1.595			78.3	60.2	8.4	
10:31	1.845			79.1	60.2	8.5	
10:32	2.095			79.3	60.5	9.1	219
10:33	2.595	81.2	60.1	79.7	60.6	9.3	
10:34	3.095			80.6	61.3	9.2	
10:35	3.595			81.2	61.0	9.4	
10:36	4.095			81.7	61.7	9.7	
10:37	4.595	82.4	60.2	81.7	61.1	9.8	
10:38	5.095			81.5	62.0	10.0	250
10:41	7.095			81.5	60.4	10.4	
10:43	9.095	82.3	59.3	82.0	62.2	10.2	
10:44							332
		Test No. 7		Date Aug. 13, 1953		Sta. 3	
11:01	0.020	83.9	61.9	80.3	63.2		0
11:02	0.025			80.5	62.6		
11:03	0.030			80.5	62.7		
11:04	0.035	84.2	61.4	81.0	62.4		
11:05	0.045			80.7	62.3		41
11:06	0.055			81.3	62.3		
11:07	0.065			81.2	62.6		
11:08	0.075	85.6	61.3	81.4	62.6		
11:09	0.085			81.5	61.8		
11:09	0.095			81.9	61.8		79
11:10	0.120			81.9	61.9	6.2	
11:10	0.145	84.6	61.1	81.9	61.4	6.4	
11:11	0.170			81.9	61.3	6.3	
11:12	0.195			82.0	61.5	6.6	
11:12	0.245			83.2	61.6	6.7	
11:13	0.295	85.3	61.3	82.8	61.4	7.1	
11:14	0.345			82.7	61.5	7.0	133
11:15	0.395			82.8	60.7	7.0	
11:16	0.495			83.6	61.0	7.5	
11:20	0.595	85.7	60.2	83.7	60.1	7.8	
11:21	0.695			83.6	60.1	7.8	
11:22	0.895			83.8	60.3	7.9	219
11:23	1.095			84.2	60.3	8.4	
11:23	1.345	86.0	59.6	84.2	60.9	8.5	
11:25	1.595			84.8	60.5	8.6	
11:26	1.845			85.2	60.0	9.2	
11:27	2.095			85.8	59.6	9.4	250
11:28	2.595	86.8	61.3	85.9	60.8	9.3	
11:29	3.095			87.0	60.4	10.0	
11:30	3.595			85.8	60.4	10.0	

Time of day	Height above terrain Inches	Forward tunnel psychrometer T_{AD}-°F Thermo. #41	Forward tunnel psychrometer T_{AW}-°F Thermo. #51	Traverse psychrometer °F Thermo. #42	Traverse psychrometer °F Thermo. #52	Traverse wind velocity ft/sec	Quantity of water evaporated cc
	Test No. 7 (Cont.)						
11:31	4.095			85.8	60.0	10.0	
11:32	4.595	87.2	61.0	87.0	60.9	10.0	353
11:33	5.095			87.7	61.0	10.0	
11:35	7.095			87.3	61.8	10.0	
11:37	9.095	87.8	60.8	87.6	60.7	10.0	
11:39							430
		Test No. 8		Date Aug. 17, 1953		Sta. 1	
9:48	0.020	64.1	58.2	63.1	60.0		0
9:53	0.025	63.1	58.7	62.7	59.9		
9:54	0.030	63.5	58.7	62.9	60.0		
9:55	0.035	63.5	58.4	62.7	60.1		
9:56	0.045	63.2	58.6	63.1	60.1		
9:57	0.055	63.4	58.3	62.8	59.8		
9:58	0.065	63.5	58.9	63.2	60.0		
9:59	0.075	64.0	57.9	63.6	59.9		
10:00	0.085	64.5	58.6	63.2	60.0		33
10:01	0.095	64.4	58.2	63.3	59.7		
10:02	0.120	63.6	58.8	63.2	59.7	4.8	
10:03	0.145	64.0	58.6	63.7	60.2	5.2	
10:04	0.170	64.3	59.1	63.7	60.4	5.2	
10:05	0.195	64.5	59.2	64.0	60.1	5.5	
10:06	0.245	64.6	59.2	64.0	60.3	5.5	
10:07	0.295	64.4	59.0	64.1	60.4	5.7	
10:08	0.345	64.4	58.7	63.6	59.8	5.8	
10:09	0.395	64.9	59.6	64.1	60.3	5.8	
10:10	0.495	64.5	58.4	64.2	60.1	6.4	
10:11	0.595	64.0	59.0	64.0	59.8	6.2	65
10:13	0.695	65.7	60.0	64.6	60.8	6.5	
10:14	0.895	64.9	58.7	64.8	60.4	6.6	
10:15	1.095	64.1	58.7	64.0	60.2	7.1	
10:16	1.345	64.5	59.1	64.5	60.4	7.4	
10:17	1.595	64.4	59.1	64.5	60.4	7.5	
10:18	1.845	64.9	58.7	64.9	60.0	7.8	
10:19	2.095	65.8	59.0	65.8	60.3	8.1	
10:20	2.595	65.5	58.8	65.4	60.4	8.5	
10:21	3.095	65.8	59.0	65.9	60.5	8.8	
10:22	3.595	64.8	59.5	64.8	60.4	8.9	
10:23	4.095	66.2	59.3	65.8	60.7	9.4	108
10:25	4.595	65.1	59.6	65.4	60.4	9.8	
10:28	5.095	65.4	59.5	65.4	60.5	9.8	
10:30	7.095	65.0	58.8	65.0	60.1	9.8	
10:33	9.095	65.7	58.8	65.7	59.9	9.8	145

Time of day	Height above terrain Inches	Forward tunnel psychrometer T_{AD}-°F Thermo. #41	Forward tunnel psychrometer T_{AW}-°F Thermo. #51	Traverse psychrometer °F Thermo. #42	Traverse psychrometer °F Thermo. #52	Traverse wind velocity ft/sec	Quantity of water evaporated cc
		Test No. 9		Date Aug. 17, 1953		Sta. 2	
10:50	0.020	66.2	60.0	65.8	61.5		0
10:51	0.025	66.8	60.2	65.6	61.2		
10:52	0.030	66.9	60.0	65.5	61.3		
10:53	0.035	67.4	60.4	66.2	61.8		
10:54	0.045	67.2	60.2	66.3	61.8		
10:55	0.055	68.0	60.0	66.5	61.7		
10:56	0.065	68.5	60.1	66.6	61.6		
10:57	0.075	67.9	60.7	66.3	62.0		
10:59	0.085	68.5	60.3	66.5	61.8		
11:00	0.095	68.6	60.5	66.7	61.9		
11:01	0.120	68.1	60.1	66.4	61.8	4.4	
11:02	0.145	67.2	60.2	65.8	61.4	4.9	
11:03	0.170	66.9	60.8	65.8	61.7	5.2	
11:04	0.195	66.9	59.4	66.2	61.4	5.4	37
11:05	0.245	67.6	60.1	66.3	61.8	5.5	
11:06	0.295	67.1	59.9	65.8	61.6	5.8	
11:07	0.345	68.1	60.0	66.1	61.6	5.8	
11:08	0.395	67.1	59.8	66.5	61.8	5.9	
11:08	0.495	67.4	60.1	66.2	61.6	6.4	
11:11	0.595	67.2	60.0	66.8	61.6	6.4	
11:12	0.695	68.2	60.4	67.1	61.5	6.4	
11:13	0.895	68.6	60.8	67.7	62.1	7.0	
11:14	1.095	68.4	60.4	67.8	61.8	7.0	
11:19	1.345	69.3	60.5	68.4	61.8	7.1	
11:20	1.595	67.2	59.9	67.2	61.8	7.5	
11:21	1.845	67.5	60.4	67.5	61.3	7.5	94
11:23	2.095	67.4	60.1	67.4	61.4	7.9	
11:24	2.595	67.9	59.8	67.9	61.2	8.2	
11:25	3.095	67.9	59.7	67.9	61.2	8.9	
11:26	3.595	68.4	59.7	68.3	61.2	8.9	
11:27	4.095	68.5	60.0	68.5	61.8	8.9	
11:28	4.595	68.6	60.4	68.6	61.6	8.9	
11:29	5.095	68.4	60.8	68.4	62.4	8.9	122
11:32	7.095	71.5	61.9	72.5	64.0	8.9	
11:35	9.095	70.4	61.3	70.2	62.9	9.0	
11:36							146
		Test No. 10		Date Aug. 17, 1953		Sta. 4	
14:00	0.020	72.1	61.8	72.7	63.9		0
14:01	0.025	72.6	61.9	70.8	63.9		
14:02	0.030	72.0	61.8	70.6	64.0		
14:03	0.035	72.1	61.9	70.5	63.9		
14:04	0.045	71.9	61.6	70.8	64.0		
14:05	0.055	72.0	62.0	70.6	63.8		
14:06	0.065	72.4	61.8	70.8	63.7		
14:08	0.075	72.5	61.8	70.8	63.9		
14:10	0.085	72.1	62.0	70.9	63.9		
14:11	0.095	72.5	62.6	70.6	64.3		45

Time of day	Height above terrain Inches	Forward tunnel psychrometer T_{AD}-°F Thermo. #41	Forward tunnel psychrometer T_{AW}-°F Thermo. #51	Traverse psychrometer °F Thermo. #42	Traverse psychrometer °F Thermo. #52	Traverse wind velocity ft/sec	Quantity of water evaporated cc
	Test No. 10 (Cont.)						
14:12	0.120	72.3	62.7	70.8	64.2	1.1	
14:13	0.145	72.5	62.0	71.1	64.1	1.3	
14:14	0.170	72.2	62.1	71.4	64.0	1.5	
14:15	0.195	71.9	62.2	71.7	63.8	1.9	
14:16	0.245	72.5	62.3	71.8	63.6	3.2	
14:17	0.295	72.4	61.8	71.7	63.7	5.0	
14:17	0.345	72.0	61.9	72.0	63.6	6.0	
14:18	0.395	72.2	62.2	72.1	63.6	6.4	
14:18	0.495	72.1	62.2	72.1	63.6	6.5	82
14:20	0.595	71.7	62.0	71.7	63.3	6.8	
14:21	0.695	71.7	62.0	71.6	63.5	6.6	
14:22	0.895	71.6	62.0	71.6	63.5	7.5	
14:23	1.095	71.5	61.8	71.5	63.5	7.6	
14:23	1.345	71.4	62.0	71.2	63.3	7.6	
14:25	1.595	71.3	62.1	71.3	63.0	8.2	
14:25	1.845	71.3	62.2	71.3	63.1	8.7	
14:26	2.095	71.2	62.0	71.1	63.4	8.6	
14:27	2.595	71.3	61.7	71.3	63.1	8.6	
14:28	3.095	71.4	62.0	71.3	63.5	8.6	135
14:29	3.595	71.6	62.3	71.7	63.3	8.7	
14:30	4.095	72.0	62.5	72.0	63.6	8.7	
14:30	4.595	71.7	62.0	71.4	63.1	8.9	
14:31	5.095	71.7	62.4	71.7	63.2	8.9	
14:33	7.095	72.1	62.3	72.1	62.9	9.1	
14:35	9.095	69.3	62.5	72.0	63.6	9.0	
14:36							189
		Test No. 11		Date Aug. 17, 1953		Sta. 5	
15:13	0.020	73.3	63.6	73.3	65.4		0
15:21	0.025	73.8	63.4	73.4	65.5		
15:22	0.030	73.4	63.2	73.1	65.3		
15:23	0.035	73.1	63.7	73.1	65.5		
15:24	0.045	73.6	63.6	73.5	65.5		
15:25	0.055	73.1	64.0	73.1	65.3		
15:26	0.065	73.3	64.0	73.3	65.3		
15:27	0.075	73.0	63.4	73.0	65.3		
15:28	0.085	72.6	63.7	72.6	65.0		
15:29	0.095	72.7	63.5	72.7	65.0		
15:29	0.120	73.1	63.6	73.1	64.2	3.0	68
15:30	0.145	73.0	64.0	73.1	64.0	3.4	
15:31	0.170	72.7	63.8	72.7	64.1	3.5	
15:32	0.195	73.1	64.0	73.3	64.0	3.9	
15:33	0.245	73.5	64.0	73.5	64.0	4.6	
15:34	0.295	73.9	64.1	73.9	64.0	4.6	
15:35	0.345	73.4	63.8	73.5	63.8	4.8	
15:36	0.395	74.0	64.1	74.0	64.1	5.2	
15:37	0.495	73.6	64.0	73.6	64.1	5.3	
15:38	0.595	73.6	63.3	73.5	63.3	5.6	113

Time of day	Height above terrain Inches	Forward tunnel psychrometer T_{AD}-°F Thermo. #41	Forward tunnel psychrometer T_{AW}-°F Thermo. #51	Traverse psychrometer °F Thermo. #42	Traverse psychrometer °F Thermo. #52	Traverse wind velocity ft/sec	Quantity of water evaporated cc
	Test No. 11 (Cont)						
15:40	0.695	73.8	63.6	73.8	63.6	5.8	
15:41	0.895	74.0	63.3	74.0	63.4	5.9	
15:41	1.095	73.8	63.0	73.8	63.0	6.5	
15:42	1.345	74.1	64.0	74.1	64.0	6.6	
15:43	1.595	73.9	64.0	73.9	64.0	7.0	
15:44	1.845	73.9	64.1	73.9	64.1	7.7	
15:44	2.095	74.0	64.0	74.0	64.0	7.6	
15:45	2.595	73.6	63.9	73.5	63.8	7.8	
15:46	3.095	73.6	64.1	73.6	64.1	8.2	
15:46	3.595	74.2	63.1	74.2	63.2	8.3	167
15:48	4.095	74.9	63.6	74.9	63.6	8.3	
15:49	4.595	74.8	62.7	74.8	62.7	8.7	
15:50	5.095	74.8	63.0	74.8	63.0	8.9	
15:52	7.095	75.9	63.1	75.9	63.0	8.7	
15:54	9.095	76.1	63.6	76.2	63.6	8.7	
15:55							233
		Test No. 12		Date Aug. 18, 1953		Sta. 1	
10:38	0.020	73.1	62.1	65.8			0
10:40	0.030	73.6	62.1	66.0			
10:41	0.040	73.5	62.3	65.4			
10:43	0.060	73.3	62.7	66.8			
10:44	0.080	73.5	62.4	66.0	63.0		
10:46	0.100	74.0	62.8	66.7	62.8		
10:47	0.120	74.1	62.6	67.2	62.9		
10:48	0.170	74.4	62.7	67.7	62.7		
10:50	0.220	74.0	62.4	67.6	62.4	0.30	
10:52	0.320	73.4	62.3	67.7	62.3	0.40	
10:57	0.420	74.5	62.1	68.5	62.1	0.80	
10:58	0.620	74.6	61.7	70.3	61.8	1.2	
11:00	0.820	74.8	61.8	71.0	61.8	1.3	
11:01	1.220	74.7	62.3	71.4	61.6	1.6	
11:03	1.720	74.9	62.0	72.3	61.4	1.8	
11:04	2.220	75.0	61.8	72.6	61.3	2.2	
11:05	3.720	75.6	61.7	74.1	61.7	2.4	
11:06	5.220	75.0	61.8	74.4	61.8	2.3	
11:10	7.220	75.3	61.8	74.5	61.8	2.2	
11:12	9.220	75.1	61.8	74.7	61.8	2.2	
11:13							34
		Test No. 13		Date Aug 18, 1953		Sta. 2	
13:58	0.020	74.2	59.5	72.1	66.0		0
13:59	0.030	74.0	59.6	70.0	66.3		
14:00	0.040	74.6	59.3	69.8	65.8		
14:01	0.060	74.2	59.2	69.4	65.7		
14:02	0.080	73.9	59.0	69.9	64.9		
14:03	0.100	73.8	59.9	70.0	64.0		
14:04	0.120	73.7	59.0	69.7	64.0		

Time of day	Height above terrain	Forward tunnel psychrometer T_{AD}-°F	T_{AW}-°F	Traverse psychrometer °F	°F	Traverse wind velocity	Quantity of water evaporated
	Inches	Thermo. #41	Thermo. #51	Thermo. #42	Thermo. #52	ft/sec	cc
	Test No. 13 (Cont)						
14:06	0.170	73.7	59.0	69.9	63.2	0.31	
14:07	0.220	73.4	59.1	70.4	62.8	0.38	
14:09	0.320	73.2	59.1	69.9	62.7	0.55	
14:11	0.420	73.1	58.9	70.7	62.2	0.93	
14:13	0.620	73.0	58.9	70.8	61.4	1.2	
14:15	0.820	72.6	59.6	71.2	61.3	1.7	
14:17	1.220	72.5	59.8	71.3	61.1	2.2	
14:18	1.720	72.2	59.2	72.2	60.4	2.4	
14:19	2.220	72.6	58.9	72.6	59.6	2.3	
14:22	3.720	72.6	59.6	72.6	59.9	2.4	
14:24	5.220	72.8	59.3	72.8	59.8	2.4	
14:27	7.220	72.8	59.3	72.8	60.0	2.4	
14:29	9.220	72.5	59.1	72.5	59.8	2.4	
14:30							67
		Test No. 14		Date Aug. 18, 1953		Sta. 3	
14:41	0.020	73.5	59.3	71.8	61.8		0
14:43	0.030	75.5	59.7	73.0	60.8		
14:44	0.040	75.9	59.1	73.0	60.9		
14:45	0.060	76.0	60.1	72.1	61.8		
14:46	0.080	76.1	60.7	73.1	61.8		
14:47	0.100	76.2	61.3	72.3	62.6		
14:49	0.120	76.5	62.0	73.4	62.0		
14:50	0.170	76.3	62.4	72.3	62.7	0.30	
14:51	0.220	76.5	61.8	72.6	62.9	0.31	
14:52	0.320	76.3	60.7	73.5	62.0	0.36	
14:53	0.420	76.9	60.9	73.9	61.2	1.0	
14:54	0.620	76.4	60.5	74.0	60.5	1.0	
14:55	0.820	76.6	59.6	74.6	60.4	1.2	
15:00	1.220	77.0	61.0	75.5	61.0	1.6	
15:02	1.720	77.2	61.1	76.2	61.0	2.2	
15:03	2.220	77.2	60.5	75.4	60.5	2.2	
15:06	3.720	76.5	60.4	76.0	60.5	2.3	
15:08	5.220	76.2	60.4	76.2	60.4	2.3	
15:10	7.220	76.6	61.3	76.6	61.3	2.3	
15:12	9.220	76.6	61.4	76.6	61.4	2.3	
15:14							84
		Test No. 15		Date Aug. 18, 1953		Sta. 4	
15:24	0.020	75.3	60.6	71.1	64.9		0
15:25	0.030	75.2	60.7	71.1	64.6		
15:27	0.040	75.2	60.9	71.3	64.4		
15:28	0.060	75.2	60.5	71.6	64.3		
15:28	0.080	75.2	60.4	72.3	63.4		
15:29	0.100	75.2	59.7	72.2	62.8		
15:31	0.120	75.2	59.5	72.1	62.5		

Time of day	Height above terrain Inches	Forward tunnel psychrometer T_{AD}-°F Thermo. #41	Forward tunnel psychrometer T_{AW}-°F Thermo. #51	Traverse psychrometer °F Thermo. #42	Traverse psychrometer °F Thermo. #52	Traverse wind velocity ft/sec	Quantity of water evaporated cc
	Test No. 15 (Cont)						
15:32	0.170	75.4	59.6	72.6	61.3		
15:33	0.220	75.4	60.5	72.6	60.8	0.30	
15:34	0.320	75.4	60.4	73.5	60.4	0.49	
15:35	0.420	74.8	61.2	73.5	61.2	0.82	
15:36	0.620	74.8	61.2	73.6	61.2	1.2	
15:37	0.820	74.6	61.3	73.5	61.3	1.6	
15:38	1.220	74.7	61.3	73.6	61.3	1.7	
15:41	1.720	74.4	61.9	73.0	61.9	2.4	
15:43	2.220	74.6	61.9	73.3	61.9	2.3	
15:45	3.720	73.8	61.8	73.7	61.8	2.4	
15:47	5.220	73.1	62.3	73.1	61.8	2.4	
15:48	7.220	73.3	61.8	73.2	61.8	2.3	
15:49	9.220	73.4	62.6	73.4	62.6	2.3	
15:50							58
		Test No. 16		Date Aug. 18, 1953		Sta. 6	
16:01	0.020	71.8	60.9	72.8			0
16:03	0.030	72.4	60.9	72.8	65.2		
16:04	0.040	72.6	61.4	73.0	65.3		
16:05	0.060	72.4	61.1	72.6	64.9		
16:08	0.080	72.1	61.3	72.9	64.4		
16:09	0.100	72.7	61.5	73.0	63.5		
16:09	0.120	72.5	61.3	72.6	64.5		
16:11	0.170	72.1	61.5	72.2	62.8	0.30	
16:15	0.220	71.6	61.4	72.2	62.3	0.66	
16:16	0.320	72.1	61.6	72.1	61.6	0.82	
16:19	0.420	71.6	61.6	71.6	62.6	0.90	
16:20	0.620	71.5	60.5	71.5	61.6	1.6	
16:22	0.820	72.4	61.6	72.4	61.6	1.4	
16:23	1.220	72.5	61.3	72.5	61.4	2.1	
16:24	1.720	72.6	62.0	72.3	62.0	2.2	
16:25	2.220	72.7	61.9	72.7	61.9	2.2	
16:27	3.720	72.9	60.4	72.9	60.4	2.2	
16:29	5.220	73.1	59.3	73.0	59.3	2.2	
16:30	7.220	73.3	60.0	73.3	60.0	2.2	
16:31	9.220	73.3	60.0	73.3	60.0	2.2	
16:32							77
		Test No. 17		Date Aug. 19, 1953		Sta. 1	
9:53	0.020	67.9	58.2	64.4			0
9:55	0.030	68.0	58.0	64.7			
9:56	0.040	68.0	58.3	64.7			
9:57	0.060	68.0	58.1	65.2			
9:59	0.080	69.0	58.6	65.7	59.6		
10:00	0.100	68.7	58.3	65.2	59.4	1.5	
10:01	0.120	68.7	58.3	65.5	59.3	1.8	

Time of day	Height above terrain Inches	Forward tunnel psychrometer T_{AD}-°F Thermo. #41	Forward tunnel psychrometer T_{AW}-°F Thermo. #51	Traverse psychrometer °F Thermo. #42	Traverse psychrometer °F Thermo. #52	Traverse wind velocity ft/sec	Quantity of water evaporated cc
	Test No. 17 (Cont)						
10:02	0.170	68.6	58.4	65.7	59.2	2.2	
10:03	0.220	68.6	58.2	66.4	59.1	2.3	
10:04	0.320	68.6	58.3	66.3	58.8	2.7	
10:08	0.420	68.7	58.6	66.8	59.2	2.8	
10:09	0.620	69.5	59.2	67.6	59.4	3.0	
10:10	0.820	69.6	59.3	68.1	59.3	3.2	
10:11	1.220	69.2	58.7	67.9	58.7	3.4	
10:12	1.720	69.3	59.0	68.2	59.0	3.6	
10:13	2.220	69.4	58.8	68.2	58.8	3.8	
10:16	3.720	69.4	59.1	69.4	59.0	4.3	56
10:18	5.220	69.5	58.8	69.5	58.9	4.3	
10:20	7.220	69.3	59.2	69.5	59.2	4.5	
10:21	9.220	69.3	59.2	69.3	59.2	4.5	
10:22							89
		Test No. 18		Date Aug. 19, 1953		Sta. 2	
10:33	0.020	69.4	58.9	65.9	59.9		0
10:35	0.030	69.9	59.1	66.1	60.0		
10:36	0.040	69.8	58.7	66.3	60.1		
10:37	0.060	70.1	58.8	66.3	60.2		
10:38	0.080	70.6	59.0	66.4	60.0		
10:39	0.100	70.3	58.7	66.3	60.0	1.3	
10:41	0.120	70.3	58.9	66.3	60.0	1.4	
10:42	0.170	69.8	58.6	67.0	60.3	2.0	
10:43	0.220	70.3	59.2	67.3	60.0	2.4	
10:44	0.320	71.0	59.5	68.0	60.2	2.4	31
10:48	0.420	71.0	59.1	67.6	60.0	2.7	
10:49	0.620	70.7	59.5	68.4	60.1	3.1	
10:51	0.820	71.4	59.7	69.0	60.2	3.2	
10:53	1.220	71.3	60.1	69.4	60.1	3.6	
10:55	1.720	70.8	59.4	70.4	59.8	3.5	
10:56	2.220	70.8	59.5	70.3	59.5	3.7	
10:58	3.720	71.1	60.0	71.1	60.0	4.1	
11:00	5.220	70.8	59.1	70.8	59.3	4.4	
11:02	7.220	71.5	59.2	71.5	60.6	4.4	
11:03	9.220	71.4	59.1	71.4	59.1	4.5	
11:04							104
		Test No. 19		Date Aug. 19, 1953		Sta. 3	
11:14	0.010	72.9	58.6	70.2	60.4		0
11:15	0.020	73.5	59.6	70.8	60.5		
11:16	0.030	72.7	59.9	70.4	60.3		
11:17	0.050	73.4	60.1	70.8	60.7		
11:18	0.070	73.5	59.9	71.4	60.8		
11:19	0.090	73.4	59.5	70.4	60.0		
11:20	0.110	73.0	58.6	70.5	59.8	1.5	

Time of day	Height above terrain Inches	Forward tunnel psychrometer T_{AD}-°F Thermo. #41	Forward tunnel psychrometer T_{AW}-°F Thermo. #51	Traverse psychrometer °F Thermo. #42	Traverse psychrometer °F Thermo. #52	Traverse wind velocity ft/sec	Quantity of water evaporated cc
	Test No. 19 (Cont)						
11:21	0.160	72.9	59.8	70.8	60.1	2.0	
11:22	0.210	73.7	60.1	71.8	60.4	2.1	
11:23	0.310	73.9	60.0	72.2	60.8	2.4	
11:25	0.410	74.6	60.4	72.8	60.6	2.6	
11:26	0.610	74.3	60.1	72.6	60.5	2.7	
11:27	0.810	75.1	60.1	73.8	60.8	3.0	
11:28	1.210	74.3	60.2	73.4	61.4	3.1	
11:29	1.710	75.2	60.3	74.3	61.3	3.2	40
11:30	2.210	73.8	60.1	73.8	61.6	3.5	
11:31	3.710	74.6	59.2	72.4	61.0	4.1	
11:33	5.210	74.5	60.4	73.8	62.6	4.2	
11:35	7.210	75.2	61.0	75.2	63.0	4.1	
11:36	9.210	75.8	61.2	75.8	63.8	4.1	
11:37							80
		Test No. 20		Date Aug. 21, 1953		Sta. 1	
9:27	0.010	64.9	58.6	63.2			0
9:28	0.020	66.2	59.0	64.0			
9:30	0.030	65.0	58.7	63.7			
9:31	0.050	65.3	59.0	63.6			
9:33	0.070	65.9	59.0	64.5			
9:35	0.090	65.7	58.6	63.8			
9:37	0.110	65.1	59.2	64.0		7.5	
9:39	0.160	65.3	58.8	64.4		7.9	
9:41	0.210	65.3	58.7	64.1		8.1	35
9:43	0.310	65.9	59.0	64.6		8.2	
9:44	0.410	66.7	59.2	65.3		8.7	
9:47	0.610	67.3	59.5	66.0		9.3	
9:50	0.810	66.7	59.8	65.3		9.3	
9:52	1.210	67.6	59.5	66.2		10.3	75
9:53	1.710	66.9	59.4	66.2		12.0	
9:54	2.210	66.3	59.2	65.9		12.5	
9:56	3.710	66.8	59.5	66.2		12.8	
9:59	5.210	67.8	60.1	67.6		13.0	
10:02	7.210	68.1	60.7	68.1		13.4	
10:03							131
		Test No. 21		Date Aug. 21, 1953		Sta. 2	
10:18	0.020	68.6	61.3	65.8	61.7		0
10:19	0.030	68.9	60.4	66.0	62.0		
10:20	0.040	67.1	61.0	65.4	61.8		
10:22	0.060	68.2	61.5	66.2	62.3		
10:24	0.080	69.9	61.7	66.6	62.2		
10:25	0.100	68.2	61.2	66.4	61.8	6.8	
10:26	0.120	69.0	61.4	66.6	61.7	7.4	
10:27	0.170	69.5	61.8	66.9	61.8	8.2	

Time of day	Height above terrain Inches	Forward tunnel psychrometer T_{AD}-°F Thermo. #41	Forward tunnel psychrometer T_{AW}-°F Thermo. #51	Traverse psychrometer °F Thermo. #42	Traverse psychrometer °F Thermo. #52	Traverse wind velocity ft/sec	Quantity of water evaporated cc
	Test No. 21 (Cont)						
10:27	0.220	69.0	61.7	67.2	61.7	8.3	
10:28	0.320	69.4	62.2	67.7	62.2	8.9	23
10:31	0.420	69.6	61.7	67.7	62.0	9.3	
10:33	0.620	69.9	61.4	67.2	61.4	9.7	
10:34	0.820	68.5	61.8	68.1	62.0	10.0	
10:36	1.220	69.8	61.5	68.6	61.6	11.2	
10:37	1.720	68.8	61.6	68.8	62.0	11.5	
10:38	2.220	69.4	61.9	69.2	61.8	12.5	
10:40	3.720	70.9	62.5	70.9	62.1	12.8	
10:42	5.220	70.8	62.7	70.7	62.7	13.4	
10:45	7.220	69.9	62.5	69.9	62.5	13.5	
10:46							82
		Test No. 22		Date Aug. 21, 1953		Sta. 3	
10:55	0.020	71.3	62.0	69.5	62.6		0
10:56	0.030	72.5	62.2	70.1	62.4		
10:58	0.040	69.9	62.3	69.8	62.5		
10:59	0.060	71.2	62.6	70.4	62.6		
11:00	0.080	71.3	63.1	70.3	63.1		
11:01	0.100	70.5	63.1	70.2	63.1	7.5	
11:01	0.120	71.0	63.0	70.8	63.0	8.0	
11:02	0.170	72.2	63.0	71.7	63.0	8.7	
11:03	0.220	72.9	62.7	71.0	62.2	8.2	
11:04	0.320	70.7	62.5	70.3	62.7	9.3	
11:06	0.420	71.4	62.8	71.3	62.7	9.5	
11:07	0.620	71.7	62.3	71.6	62.3	10.0	
11:08	0.820	72.1	62.1	70.7	61.9	10.5	
11:09	1.220	70.7	61.9	71.3	62.8	12.0	
11:10	1.720	72.3	63.1	71.8	63.3	12.5	
11:11	2.220	72.2	62.9	72.2	63.1	12.6	54
11:13	3.720	72.7	62.4	72.1	63.5	13.5	
11:15	5.220	72.0	62.2	72.1	62.7	13.5	
11:16	7.220	72.2	62.7	72.2	62.7	13.5	
11:17							84
		Test No. 23		Date Aug 21, 1953		Sta. 4	
11:26	0.020	72.6	62.3	70.4			0
11:27	0.030	72.0	61.7	70.3			
11:28	0.040	72.2	62.2	71.1			
11:29	0.060	72.5	62.0	70.9			
11:30	0.080	72.6	61.7	71.2			
11:31	0.100	72.2	61.7	70.8	62.7	2.3	
11:32	0.120	71.6	61.8	70.3	62.5	2.4	
11:33	0.170	71.8	62.0	70.8	62.2	2.9	
11:34	0.220	72.5	62.7	72.0	63.1	3.3	
11:34	0.320	72.6	62.1	71.4	62.7	7.5	35
11:36	0.420	72.0	62.3	71.2	62.3	10.1	

Time of day	Height above terrain Inches	Forward tunnel psychrometer T_{AD}-°F Thermo. #41	Forward tunnel psychrometer T_{AW}-°F Thermo. #51	Traverse psychrometer °F Thermo. #42	Traverse psychrometer °F Thermo. #52	Traverse wind velocity ft/sec	Quantity of water evaporated cc
	Test No. 23 (Cont)						
11:37	0.620	72.1	61.4	71.4	62.5	10.3	
11:38	0.820	71.6	62.3	71.4	63.0	11.3	
11:39	1.220	72.1	62.3	72.1	62.8	11.5	
11:40	1.720	72.6	61.2	71.7	61.7	12.7	
11:41	2.220	72.2	61.8	71.6	62.1	12.7	
11:43	3.720	72.2	62.2	72.2	62.6	13.0	
11:44	5.220	72.1	61.8	72.0	62.7	13.5	
11:45	7.220	71.7	61.0	71.7	62.6	13.5	
11:46							108
		Test No. 24		Date Aug. 21, 1953		Sta. 6	
11:54	0.020	71.9	61.7	71.9	62.6		0
11:56	0.030	72.2	61.8	71.6	62.5		
11:57	0.040	71.8	61.7	71.5	62.6		
11:57	0.060	71.8	61.9	71.5	62.6		
11:58	0.080	72.1	61.8	71.0	62.3		
11:59	0.100	71.8	61.3	71.6	62.4	7.2	
12:00	0.120	71.6	61.8	71.7	62.7	7.5	
12:01	0.170	72.2	61.8	71.6	62.6	8.6	
12:02	0.220	71.6	61.9	71.6	63.1	8.4	
12:03	0.320	72.2	62.2	71.3	63.0	9.3	33
12:05	0.420	71.7	61.8	71.7	63.1	9.5	
12:06	0.620	71.7	61.8	71.7	62.9	9.4	
12:07	0.820	71.6	62.3	71.2	63.4	10.2	
12:08	1.220	71.3	61.8	71.3	62.7	11.4	
12:09	1.720	71.2	61.3	71.3	62.8	11.6	
12:10	2.220	71.4	61.6	71.4	62.8	12.0	
12:12	3.720	71.7	61.7	71.7	63.0	13.0	
12:14	5.220	71.6	61.4	71.5	63.2	13.5	
12:15	7.220	71.7	62.7	71.7	63.6	13.5	
12:16							114
		Test No. 25		Date Aug. 24, 1953		Sta. 1	
9:25	0.030	73.3	60.4	67.9	59.1		0
9:26	0.040	73.0	59.5	67.7	58.2		
9:27	0.050	73.4	60.5	68.5	59.1		
9:28	0.070	73.0	59.2	68.5	57.8		
9:29	0.090	73.2	60.6	68.8	58.3		48
9:31	0.110	72.7	61.5	68.9	59.0	10.1	
9:33	0.130	73.1	62.7	69.4	58.8	10.1	
9:34	0.180	73.8	62.2	70.3	58.6	11.5	
9:35	0.230	73.0	62.8	69.6	58.7	11.7	
9:36	0.330	73.5	61.3	70.4	59.2	12.0	113
9:38	0.430	73.0	60.9	70.8	60.0	12.3	
9:39	0.630	73.4	61.4	71.6	60.4	12.7	
9:40	0.830	73.5	61.5	71.9	60.9	13.6	

Time of day	Height above terrain	Forward tunnel psychrometer T_{AD}-°F Thermo. #41	Forward tunnel psychrometer T_{AW}-°F Thermo. #51	Traverse psychrometer °F Thermo. #42	Traverse psychrometer °F Thermo. #52	Traverse wind velocity	Quantity of water evaporated
	Inches					ft/sec	cc
	Test No. 25 (Cont)						
9:41	1.230	74.7	61.4	72.6	61.4	14.6	
9:42	1.730	74.6	61.8	73.6	61.8	15.2	181
9:45	2.230	74.0	61.7	72.8	61.4	15.7	
9:47	3.730	73.8	60.9	72.7	62.7	17.8	
9:49	5.230	73.4	60.5	73.4	62.2	18.0	250
9:51	7.230	74.0	60.3	74.0	62.5	18.0	
9:52							279
		Test No. 26	Date Aug. 24, 1953			Sta. 2	
10:07	0.030	75.7	61.3	69.8	60.4		0
10:08	0.040	74.8	61.0	69.8	60.1		
10:09	0.050	75.2	61.5	70.0	60.4		
10:10	0.070	74.9	61.6	70.5	60.5		
10:11	0.090	76.0	61.8	70.3	60.8		
10:12	0.110	75.7	61.8	71.2	60.6	11.6	
10:13	0.130	75.7	61.9	71.3	60.6	11.8	55
10:14	0.180	75.6	61.7	72.3	61.1	12.0	
10:15	0.230	75.6	61.8	71.8	61.1	12.5	
10:16	0.330	75.6	61.8	72.2	61.0	12.8	86
10:19	0.430	76.3	62.4	73.1	61.5	13.5	
10:20	0.630	76.1	62.1	73.8	61.2	13.8	
10:21	0.830	76.7	61.8	74.8	62.0	15.2	
10:22	1.230	76.4	62.4	74.4	61.3	15.8	
10:23	1.730	76.1	62.6	75.5	62.7	16.0	131
10:25	2.230	76.7	63.5	76.3	63.5	17.0	
10:27	3.730	76.6	63.0	76.5	63.2	18.4	
10:29	5.230	76.4	63.2	76.4	64.0	19.5	173
10:30	7.230	77.0	63.5	77.1	64.9	19.0	
10:31							206
		Test No. 27	Date Aug. 24, 1953			Sta. 3	
10:43	0.040	78.8	63.2	76.6	64.8		0
10:45	0.050	78.2	63.6	76.7	64.6		
10:46	0.060	78.5	63.1	76.5	64.7		
10:48	0.080	79.3	63.6	77.4	65.0		
10:49	0.100	78.6	63.6	77.0	64.6	11.7	35
10:50	0.120	78.4	64.1	77.0	65.4	11.9	
10:51	0.140	78.4	64.0	77.0	65.4	11.9	
10:52	0.190	77.5	63.7	77.1	65.4	12.0	
10:53	0.240	78.3	64.4	77.5	65.8	12.8	
10:53	0.340	78.8	64.2	78.1	66.0	13.5	76
10:55	0.440	79.3	65.0	78.8	66.3	13.8	
10:57	0.640	79.7	64.6	78.4	66.9	14.7	
10:58	0.840	78.8	64.2	78.4	66.2	15.5	
10:59	1.240	79.4	65.1	79.3	66.8	16.2	121
11:00	1.740	79.3	64.6	79.3	66.8	17.0	

Time of day	Height above terrain Inches	Forward tunnel psychrometer T_{AD}-°F Thermo. #41	Forward tunnel psychrometer T_{AW}-°F Thermo. #51	Traverse psychrometer °F Thermo. #42	Traverse psychrometer °F Thermo. #52	Traverse wind velocity ft/sec	Quantity of water evaporated cc
	Test No. 27 (Cont)						
11:02	2.240	79.7	64.9	79.7	67.6	12.7	
11:04	3.740	79.7	64.9	79.7	67.2	18.5	
11:05	5.240	80.5	65.0	80.5	67.8	19.0	174
11:07	7.240	79.8	65.4	79.8	67.9	18.8	
11:08							216
		Test No. 28		Date Aug. 29, 1953		Sta. 4	
11:20	0.030	85.4	67.1	77.0			0
11:21	0.040	85.8	66.8	77.6			
11:22	0.050	85.1	66.3	77.9			
11:23	0.070	82.3	66.3	78.1			
11:24	0.090	80.6	66.7	77.5	66.7		
11:25	0.110	82.2	67.3	78.7	67.3	3.2	
11:26	0.130	82.3	67.1	78.4	67.1	3.6	32
11:27	0.180	82.3	67.0	78.8	67.0	4.5	
11:27	0.230	82.4	67.0	80.5	67.0	6.7	
11:28	0.330	82.3	67.2	80.2	67.3	10.8	65
11:31	0.430	82.5	66.3	79.5	66.3	13.0	
11:32	0.630	81.9	66.1	80.6	66.1	13.8	
11:33	0.830	82.3	66.3	80.5	66.2	14.4	
11:34	1.230	82.3	66.0	80.6	66.1	16.0	
11:36	1.730	83.5	67.2	81.6	67.1	16.8	131
11:38	2.230	82.9	67.5	81.7	67.5	16.9	
11:40	3.730	82.8	68.9	82.8	68.9	17.0	
11:42	5.230	82.9	68.2	83.0	69.8	18.0	193
11:44	7.230	83.2	67.7	83.2	70.0	18.0	
11:45							242
		Test No. 29		Date Aug. 27, 1953		Sta. 1	
14:07	0.010	82.3	65.3	74.3			0
14:08	0.020	82.2	65.3	74.4			
14:09	0.030	82.2	65.1	74.3			
14:10	0.050	81.9	64.9	74.4	69.9		
14:11	0.070	82.4	65.1	76.1	69.4		
14:13	0.090	82.3	65.1	75.0	69.0		
14:14	0.110	82.2	65.0	75.3	68.8	0.25	
14:15	0.160	81.9	65.3	76.2	68.5	0.44	
14:16	0.210	81.9	65.5	76.3	68.4	0.55	
14:18	0.310	81.9	65.2	77.5	67.0	0.86	35
14:21	0.410	81.9	65.0	78.8	66.8	1.1	
14:22	0.610	81.9	65.2	79.7	66.2	1.3	
14:23	0.810	81.9	64.9	80.3	65.7	1.9	
14:24	1.210	81.8	65.1	80.6	65.1	2.5	
14:26	1.710	81.9	64.9	81.0	64.9	2.6	
14:27	2.210	81.8	65.2	81.0	65.2	2.8	
14:29	3.710	81.9	65.3	81.1	65.4	2.8	

Time of day	Height above terrain Inches	Forward tunnel psychrometer T_{AD} - °F Thermo. #41	Forward tunnel psychrometer T_{AW} - °F Thermo. #51	Traverse psychrometer °F Thermo. #42	Traverse psychrometer °F Thermo. #52	Traverse wind velocity ft/sec	Quantity of water evaporated cc
	Test No. 29 (Cont)						
14:31	5.210	81.7	65.3	81.1	65.3	2.8	
14:32	6.710	81.4	65.4	81.2	65.4	2.8	70
14:44							107
		Test No. 30		Date Aug. 31, 1953		Sta. 6	
15:32	0.010	91.9	70.8	86.3	72.4		0
15:34	0.020	92.0	69.1	82.7	72.7		
15:35	0.030	91.3	69.5	86.3	71.8		
15:36	0.050	91.4	69.6	86.3	69.6		
15:37	0.070	90.6	69.7	86.5	69.7		
15:39	0.090	91.5	70.0	86.6	68.2		
15:40	0.110	91.8	70.5	87.1	67.7		
15:41	0.160	91.9	70.3	87.0	66.2		
15:43	0.210	91.5	71.3	86.8	65.7	0.26	
15:44	0.310	91.4	71.3	86.8	65.5	0.37	54
15:47	0.410	92.3	72.2	87.5	65.9	0.60	
15:50	0.610	92.3	73.0	88.1	65.6	1.3	
15:52	0.810	91.6	74.9	88.6	65.9	1.5	
15:54	1.210	92.3	79.2	89.4	65.7	1.9	
16:06	1.710	92.8	69.0	89.4	65.7	2.0	
16:08	2.210	92.2	68.6	90.4	65.9	2.1	
16:10	3.710	92.4	68.7	90.7	66.4	2.4	
16:13	5.210	90.4	68.2	90.4	66.4	2.4	
16:15	6.710	90.3	67.9	90.4	67.6	2.4	
16:16							226
16:26							281
		Test No. 31		Date Sept. 21, 1953		Sta. 6	
14:15	0.010	66.0	51.0	65.6	52.5		0
	0.020	65.6	51.4	65.9	52.8		
14:24	0.030	65.1	51.5	66.7	52.7		58
	0.050	65.9	51.3	66.7	52.8		
	0.070	67.0	52.1	66.7	52.7		
	0.090	67.2	51.5	66.5	52.7		
	0.110	67.2	51.3	66.7	52.7	4.1	
14:31	0.160	67.3	51.1	67.1	53.1	4.6	112
	0.210	66.7	50.4	66.5	52.6	4.7	
	0.310	67.5	51.3	67.8	53.1	5.0	
14:41	0.410	66.7	51.4	66.7	52.7	5.3	168
	0.610	66.3	50.8	66.3	52.5	5.8	
	0.810	66.0	50.5	65.9	52.3	6.0	
14:46	1.210	65.9	50.4	65.9	52.5	6.6	207
	1.710	65.8	50.3	65.8	52.7	7.2	
	2.210	65.4	50.2	66.6	52.8	7.3	
14:53	3.710	67.7	51.8	68.1	53.7	7.9	250
	5.210	67.4	50.8	67.1	53.2	8.0	
14:58	6.710	65.9	50.4	65.8	53.7	8.1	276

Time of day	Height above terrain Inches	Forward tunnel psychrometer T_{AD}-°F Thermo. #41	Forward tunnel psychrometer T_{AW}-°F Thermo. #51	Traverse psychrometer °F Thermo. #42	Traverse psychrometer °F Thermo. #52	Traverse wind velocity ft/sec	Quantity of water evaporated cc
		Test No. 32		Date Sept. 22, 1953		Sta. 6	
12:14	0.020	84.1	57.2	80.1	58.2		0
	0.030	84.4	58.1	80.0	58.8		
	0.040	84.7	57.9	80.6	58.7		
12:18	0.060	84.2	58.1	80.7	59.1		42
	0.080	84.1	57.3	80.4	58.2		
	0.100	84.6	58.2	80.7	59.2	3.8	
	0.120	84.5	58.2	81.2	59.3	4.0	
12:22	0.170	84.5	58.2	81.1	59.2	4.3	79
	0.220	85.4	58.7	81.0	59.5	4.7	
	0.320	85.3	58.6	81.2	59.9	4.9	
12:26	0.420	84.6	58.3	81.9	59.9	5.4	120
12:30	0.620	85.2	58.3	81.7		5.4	161
	0.820	85.2	57.6	81.2		5.9	
	1.220	85.5	57.2	82.4		6.2	
12:34	1.720	85.5	57.6	82.5		6.6	200
	2.220	86.6	57.6	84.1		7.0	
12:38	3.720	84.9	58.6	84.2		7.9	240
12:41	5.220	86.2	58.3	84.5		8.0	250
12:42	6.720	85.6	57.9	84.5		8.1	280
12:46							320
		Test No. 33		Date Sept. 22, 1953		Sta. 1	
13:23	0.030	86.6	57.9	78.0	59.8		0
13:25	0.040	85.4	57.8	78.3	59.2		
13:28	0.050	85.0	57.6	78.3	59.2		55
13:30	0.070	84.7	57.6	78.2	59.0		
13:31	0.090	84.8	58.0	78.8	59.4		96
13:34	0.110	86.2	57.8	78.6	59.1	3.9	
13:36	0.130	86.5	58.2	79.5	59.6	4.0	135
13:38	0.180	87.1	58.0	79.9	59.3	4.3	
13:39	0.230	86.8	58.3	80.4	59.5	4.5	
13:41	0.330	86.7	58.1	81.3	59.3	4.6	
13:42	0.430	87.1	58.5	81.3	59.2	5.0	182
13:44	0.630	87.7	58.2	82.3	59.9	5.6	
13:46	0.830	87.6	58.7	83.3	60.0	5.6	
13:48	1.230	87.3	58.4	84.6	59.8	5.9	250
13:49	1.730	87.0	58.5	84.7	60.1	6.3	
13:50	2.230	86.1	58.0	85.7	60.2	6.4	
13:53	3.730	87.3	57.8	85.0	59.7	7.4	304
13:55	5.230	87.2	58.8	87.0	60.4	7.8	336
13:57	6.730	87.6	58.6	87.4	60.6	7.7	
13:58							365
		Test No. 34		Date Sept. 22, 1953		Sta. 2	
14:15	0.020	87.7	58.1	79.3	60.3		0
14:16	0.030	87.7	58.2	79.7	60.2		
14:17	0.040	88.0	58.3	79.5	60.3		

Time of day	Height above terrain Inches	Forward tunnel psychrometer T_{AD}-°F Thermo. #41	Forward tunnel psychrometer T_{AW}-°F Thermo. #51	Traverse psychrometer °F Thermo. #42	Traverse psychrometer °F Thermo. #52	Traverse wind velocity ft/sec	Quantity of water evaporated cc
	Test No. 34 (Cont)						
14:18	0.060	87.5	58.3	79.3	60.7		31
14:19	0.080	88.1	58.6	79.7	60.6		
14:20	0.100	88.0	58.8	80.7	60.3	3.7	
14:21	0.120	88.8	58.6	81.1	60.8	4.1	49
14:22	0.170	87.9	59.0	80.7	60.7	4.6	
14:23	0.220	88.7	59.4	80.8	60.8	4.6	
14:24	0.320	88.6	59.1	81.8	60.4	4.6	76
14:24	0.420	89.2	59.0	82.3	61.2	5.4	
14:27	0.620	88.0	59.0	81.9	60.6	5.1	120
14:29	0.820	88.3	59.2	84.3	60.5	5.8	
14:30	1.220	87.8	59.0	84.7	60.4	5.8	
14:32	1.720	88.4	59.0	86.1	60.8	6.6	175
14:33	2.220	88.1	58.9	86.1	60.6	6.7	
14:35	3.720	88.4	59.6	86.6	61.3	7.5	205
14:37	5.220	88.6	59.4	87.0	61.8	7.5	227
14:38	6.720	89.1	59.4	88.8	61.8	7.7	
14:39							250
		Test No. 35		Date Sept. 23, 1953		Sta. 6	
11:22	0.050	79.7	50.3	77.3			0
11:24	0.060	79.4	49.5	77.1			36
11:26	0.070	79.3	49.5	77.0			65
11:28	0.090	78.8	49.1	76.7			96
	0.110	79.3	49.5	77.4		6.1	
11:30	0.130	79.2	49.7	76.6		6.2	130
	0.150	79.2	49.1	77.1		6.7	
11:32	0.200	79.6	49.7	77.0		7.3	159
11:34	0.250	79.6	49.9	77.0		7.5	192
11:36	0.350	80.3	50.1	77.6		7.7	224
11:38	0.450	79.6	49.5	77.4		8.6	250
11:40	0.650	79.6	49.6	77.9		8.8	286
11:42	0.850	80.2	50.1	77.9		9.2	312
	1.250	79.7	50.5	77.9		10.0	
11:44	1.750	79.7	50.1	78.4		10.1	342
11:46	2.250	79.7	50.2	78.0		11.1	372
11:48	3.750	79.6	50.3	78.3		14.1	403
11:50	5.250	79.5	49.6	79.1		15.0	437
11:52	6.750	79.4	50.4	79.2		14.1	465
11:54							494
		Test No. 36		Date Sept. 23, 1953		Sta. 1	
12:23	0.030	81.0	50.4	75.0			0
12:25	0.040	80.2	50.3	74.3			33
12:27	0.050	80.3	49.6	74.4			66
12:29	0.070	80.6	50.0	74.8			95
12:31	0.090	80.7	50.7	75.7			123
	0.110	80.4	50.7	75.1		6.4	

Time of day	Height above terrain Inches	Forward tunnel psychrometer T_{AD}-°F Thermo. #41	Forward tunnel psychrometer T_{AW}-°F Thermo. #51	Traverse psychrometer °F Thermo. #42	Traverse psychrometer °F Thermo. #52	Traverse wind velocity ft/sec	Quantity of water evaporated cc
	Test No. 36 (Cont)						
12:33	0.130	80.6	50.7	75.4		6.9	150
	0.180	80.6	50.8	75.6		7.2	
12:35	0.230	79.9	50.5	75.8		7.3	179
12:37	0.330	79.8	50.4	76.2		7.9	211
12:39	0.430	80.6	51.3	77.0		8.2	243
12:41	0.630	79.7	51.4	77.9		8.4	250
12:42	0.830	80.3	50.1	78.1		9.0	285
12:44	1.230	80.6	50.2	79.7		9.0	310
12:46	1.730	81.3	50.8	78.4		10.0	338
12:48	2.230	80.6	50.5	79.1		10.0	366
12:50	3.730	80.9	50.9	80.0		14.0	398
12:52	5.230	81.3	50.9	81.0		14.1	427
12:54	6.730	81.6	51.3	81.1		15.1	456
12:56							482
		Test No. 37		Date Sept. 23, 1953		Sta. 2	
13:20	0.040	80.7	50.0	74.8			0
13:22	0.050	81.0	50.4	75.1			35
13:24	0.060	80.7	50.5	74.8			63
13:26	0.080	81.4	50.4	75.7			89
	0.100	81.1	50.5	76.2		6.2	
13:28	0.120	81.0	50.6	75.6		6.7	119
	0.140	81.4	50.4	75.3		7.2	
13:30	0.190	81.3	51.3	76.2		7.5	149
13:32	0.240	81.0	51.1	75.7		8.3	178
13:34	0.340	81.0	50.1	75.4		8.7	206
	0.440	81.2	51.0	77.0		9.0	
13:36	0.640	81.0	51.3	78.1		10.0	233
13:38	0.840	81.0	51.0	78.8		10.0	250
13:40	1.240	81.0	50.6	79.5		10.0	294
13:42	1.740	81.9	50.9	79.7		11.1	322
13:44	2.240	81.1	50.9	79.7		11.1	346
13:46	3.740	80.2	50.7	80.2		14.5	375
13:48	5.240	82.1	50.7	81.9		15.0	412
13:50	6.740	81.5	50.5	81.5		15.9	437
		Test No. 38		Date Sept. 23, 1953		Sta. 6	
14:12	0.020	81.5	51.5	80.6			0
14:14	0.030	82.2	50.8	79.8			
14:16	0.040	81.9	50.7	80.5			
14:17	0.060	80.9	50.9	80.0			
14:18	0.080	81.5	51.1	80.5			62
14:19	0.100	81.8	51.3	80.2		6.3	
14:20	0.120	81.7	51.4	80.5		7.0	
14:21	0.170	81.9	50.7	80.6		7.0	102
14:22	0.220	81.9	50.7	80.5		7.2	
14:23	0.320	80.9	50.7	80.7		7.5	135

Time of day	Height above terrain Inches	Forward tunnel psychrometer T_{AD}-°F Thermo. #41	Forward tunnel psychrometer T_{AW}-°F Thermo. #51	Traverse psychrometer °F Thermo. #42	Traverse psychrometer °F Thermo. #52	Traverse wind velocity ft/sec	Quantity of water evaporated cc
	Test No. 38 (Cont)						
14:24	0.420	80.7	50.8	80.2		7.5	
14:26	0.620	81.3	51.8	80.4		8.2	194
14:28	0.820	80.9	50.6	80.1		9.0	
14:29	1.220	80.6	51.2	79.9		9.3	
14:30	1.720	80.7	50.9	80.0		10.0	248
14:31	2.220	81.1	50.8	80.6		12.0	276
14:33	3.720	81.3	51.3	81.2		13.0	
14:35	5.220	81.1	50.8	81.3		14.0	328
14:37	6.720	81.2	50.6	81.2		14.0	
14:38							355
		Test No. 39		Date Sept. 24, 1953		Sta. 6	
13:20	0.100	79.5	52.0	76.5	55.2	4.8	0
13:24	0.150	78.8	52.8	74.3	55.5	7.8	69
13:27	0.200	78.7	51.9	76.9	55.6	9.1	121
13:29	0.300	78.8	54.7	77.8	55.4	10.0	158
13:31	0.400	78.4	54.8	77.2	54.9	10.7	191
13:33	0.600	78.9	52.1	77.3	54.9	11.4	235
13:35	0.800	78.7	51.6	78.4	55.0	12.2	250
13:37	1.200	78.7	52.0	78.3	55.3	12.8	310
13:39	1.700	78.9	52.3	77.1	55.5	14.0	349
13:41	2.200	79.3	51.4	78.2	54.9	15.0	385
13:43	3.700	78.5	51.9	78.4	56.6	15.5	424
13:45	5.200	77.5	51.9	78.3	55.9	16.5	463
13:47	6.700	77.6	52.2	77.9	58.1	16.5	500
		Test No. 40		Date Sept. 24, 1953		Sta. 1	
14:07	0.100	78.7	51.7	74.8		7.1	0
14:09	0.150	79.0	51.1	73.4		8.5	42
14:11	0.200	79.3	51.7	75.0		9.4	75
14:13	0.300	78.8	51.3	74.8		10.4	115
14:15	0.400	79.2	51.4	75.7		10.8	157
	0.600	78.1	51.4	76.1		11.6	
14:17	0.800	79.9	50.8	77.5		11.9	190
14:19	1.200	78.6	51.4	76.5		13.4	225
14:21	1.700	78.8	50.9	78.2		13.9	250
14:23	2.200	78.8	50.9	77.8		14.3	306
14:25	3.700	78.8	51.8	78.4		15.3	340
14:27	5.200	79.0	51.2	78.6		16.7	378
14:29	6.700	79.3	51.4	78.4		16.7	414
14:31							452
		Test No. 41		Date Sept. 24, 1953		Sta. 2	
14:48	0.050	78.6	51.8	73.9	52.2		0
14:50	0.100	78.8	51.7	73.9	55.0	9.8	30

Time of day	Height above terrain Inches	Forward tunnel psychrometer T_{AD}-°F Thermo. #41	T_{AW}-°F Thermo. #51	Traverse psychrometer °F Thermo. #42	°F Thermo. #52	Traverse wind velocity ft/sec	Quantity of water evaporated cc
	Test No. 41 (Cont)						
14:52	0.150	78.5	51.5	74.0	55.3	9.9	59
14:54	0.250	78.5	51.5	75.0	55.1	11.0	98
14:56	0.350	78.5	50.4	73.9	54.4	11.4	132
	0.550	79.6	51.3	75.5	54.7	12.0	
14:58	0.750	79.2	51.8	76.8	54.6	13.0	174
15:00	1.150	79.7	51.7	77.8	55.7	13.2	200
15:02	1.650	78.3	51.7	78.3	55.9	13.5	245
15:04	2.150	78.4	51.0	78.8	55.1	14.3	288
15:06	3.650	79.7	51.9	79.5	55.9	16.0	326
15:08	5.150	79.4	51.6	79.2	56.8	16.4	361
15:10	6.650	79.2	51.9	79.0	56.8	16.4	389
15:12							429
		Test No. 42		Date Sept. 24, 1953		Sta. 6	
14:30	0.050	79.0	52.1	78.3			0
14:32	0.100	79.0	51.4	78.4		7.9	34
14:34	0.150	77.5	50.9	77.5		9.0	71
14:36	0.250	78.4	50.9	78.3		10.0	107
	0.350	78.7	52.2	78.8		11.1	
14:38	0.550	78.2	52.2	78.2		11.4	147
	0.750	78.2	52.3	77.8		11.9	
14:40	1.150	78.7	51.8	77.9		13.4	183
14:42	1.650	79.5	52.2	78.6		13.8	224
14:44	2.150	79.2	52.2	78.6		14.3	250
14:46	3.650	79.1	52.2	77.4		15.8	291
14:48	5.150	76.6	53.0	76.4		17.1	325
14:50	6.650	75.8	53.0	75.8		17.1	353
		Test No. 43		Date Sept. 25, 1953		Sta. 6	
11:45	0.030	65.8	51.7	63.7	52.0		0
	0.040	64.0	51.3	63.0	51.7		
	0.050	64.3	50.3	63.1	51.7		
	0.070	64.4	51.3	63.2	51.6		
	0.090	65.4	51.0	63.6	51.3	1.3	
	0.110	65.4	51.3	63.1	51.3	1.4	
11:54	0.130	65.4	51.5	63.6	51.3	1.6	26
	0.180	64.3	50.3	63.3	51.7	2.0	
	0.230	63.1	50.1	62.7	51.4	2.2	
	0.330	65.1	50.9	64.0	51.4	2.6	
12:01	0.430	64.9	50.8	63.6	51.3	2.7	50
	0.630	66.2	52.2	65.1	52.3	3.1	
	0.830	66.1	52.0	64.4	52.3	3.1	
	1.230	66.7	52.0	64.1	52.3	3.3	
	1.730	66.4	52.1	65.1	52.7	3.6	
	2.230	66.4	52.1	65.3	52.3	4.0	
12:10	3.730	66.8	52.2	65.5	52.6	4.2	78

Time of day	Height above terrain Inches	Forward tunnel psychrometer T_{AD}-°F Thermo. #41	Forward tunnel psychrometer T_{AW}-°F Thermo. #51	Traverse psychrometer °F Thermo. #42	Traverse psychrometer °F Thermo. #52	Traverse wind velocity ft/sec	Quantity of water evaporated cc
	Test No. 43 (Cont)						
	5.230	68.0	52.2	67.2	52.6	4.2	
12:18	6.730	66.7	52.2	65.8	53.0	4.2	106
		Test No. 44		Date Sept. 25, 1953		Sta. 1	
12:38	0.030	69.4	53.3	63.6	53.9		0
	0.040	70.2	53.3	63.6	54.1		
	0.050	70.3	53.7	63.8	54.2		
	0.070	71.1	53.7	64.6	54.3		
	0.090	72.1	53.2	65.4	54.2		
	0.110	69.4	53.2	64.7	54.0	1.6	
	0.130	69.6	53.6	65.0	54.0	1.6	
	0.180	70.7	54.1	65.9	54.2	2.0	
12:49	0.230	70.7	53.3	65.4	54.0	2.6	32
	0.330	71.3	54.2	66.8	54.2	2.6	
	0.430	71.7	54.0	67.1	54.1	2.7	
	0.630	70.2	53.7	67.8	53.6	3.1	
	0.830	71.4	54.1	68.0	54.1	3.1	
12:57	1.230	69.1	54.1	67.2	54.1	3.6	60
	1.730	71.4	53.8	68.5	54.0	4.1	
	2.230	70.2	54.1	70.3	54.1	4.0	
13:05	3.730	70.8	53.3	69.9	54.2	4.3	90
	5.230	74.3	54.5	73.1	55.9	4.3	
13:11	6.730	73.0	54.8	72.6	56.2	4.3	111
		Test No. 45		Date Sept. 25, 1953		Sta. 2	
13:34	0.010	73.5	54.3	67.3	55.9		0
	0.020	74.0	53.6	67.6	55.0		
	0.030	73.4	53.6	67.5	55.4		
	0.050	75.7	54.1	68.4	55.7		
	0.070	75.7	55.0	68.4	56.3		
	0.090	75.3	54.4	68.0	55.8		
13:42	0.110	75.2	54.1	68.5	55.9	1.6	34
	0.160	76.3	54.5	69.2	55.9	1.9	
	0.210	74.9	54.5	69.6	56.1	2.2	
	0.310	76.5	54.0	70.2	55.4	2.7	
	0.410	76.0	55.0	70.7	56.4	2.6	
	0.610	75.2	54.7	71.2	55.8	2.7	
13:52	0.810	75.7	55.3	72.1	56.2	2.9	75
	1.210	74.4	55.0	72.1	56.0	3.3	
	1.710	74.5	54.8	73.0	56.0	3.6	
	2.210	75.6	55.1	74.2	56.3	3.5	
13:58	3.710	75.6	55.4	75.0	57.1	3.8	100
	5.210	75.8	54.8	75.3	57.2	4.1	
14:06	6.710	76.2	56.3	76.7	58.6	4.1	154

Time of day	Height above terrain Inches	Forward tunnel psychrometer T_{AD}-°F Thermo. #41	T_{AW}-°F Thermo. #51	Traverse psychrometer °F Thermo. #42	°F Thermo. #52	Traverse wind velocity ft/sec	Quantity of water evaporated cc
		Test No. 46		Date Sept. 25, 1953		Sta. 6	
14:24	0.020	77.5	56.9	72.9	57.6		0
	0.030	77.1	57.2	73.5	57.6		
	0.040	77.5	57.1	73.5	57.7		
	0.060	76.6	57.3	73.4	56.4		
	0.080	77.2	56.3	73.3	57.2		
14:33	0.100	78.2	57.2	74.4	57.6	0.34	39
	0.120	78.2	56.9	73.4	57.8	0.32	
	0.170	77.7	57.3	73.9	57.7	0.62	
	0.220	77.5	56.7	73.9	57.7	0.86	
	0.320	77.4	56.8	73.9	57.7	1.1	
	0.420	77.7	56.6	75.3	57.6	1.6	
14:41	0.620	78.1	56.4	74.2	57.8	1.9	75
	0.820	78.8	57.0	76.7	58.2	2.6	
	1.220	79.2	57.0	75.9	58.1	2.7	
	1.720	78.9	57.6	76.1	58.8	3.2	
	2.220	79.0	57.8	77.5	59.0	3.6	
14:49	3.720	78.8	57.8	78.3	59.5	3.6	103
	5.220	78.8	56.4	76.9	58.7	3.6	
14:54	6.720	78.0	56.7	77.9	59.1	3.6	127
		Test No. 47		Date Sept. 30, 1953		Sta. 6	
11:52	0.030	72.5	55.2	67.9	56.3		0
	0.040	71.9	55.0	68.0	56.3		
	0.050	71.9	54.8	68.5	56.3		
	0.070	72.6	55.0	68.1	56.4		
	0.090	73.0	55.5	68.7	56.4		
	0.110	73.1	55.8	68.4	56.7		
	0.130	73.0	56.0	68.4	56.8		
12:04	0.180	73.1	56.0	68.6	56.4	0.10	28
	0.230	73.1	55.9	68.9	56.7	0.19	
	0.330	72.9	55.9	69.4	56.3	0.49	
	0.430	73.0	55.4	69.5	56.3	0.41	
	0.630	73.5	55.4	70.4	56.4	1.20	
	0.830	72.7	55.4	70.9	56.2	1.5	
	1.230	74.1	55.8	71.3	56.3	1.8	
	1.730	74.7	56.0	72.5	56.8	2.2	
12:17	2.230	73.4	55.7	72.1	56.4	2.4	55
	3.730	73.0	55.9	72.3	56.3	2.4	
	5.230	73.0	55.8	71.7	57.2	2.4	
12:26	6.730	75.2	56.9	74.5	58.0	2.2	72
		Test No. 48		Date Sept. 30, 1953		Sta. 1	
12:51	0.040	76.1	57.5	64.9	59.9		0
12:52	0.050	76.4	57.6	65.0	60.1		
12:54	0.060	75.8	57.3	65.4	60.1		
12:55	0.080	76.7	57.4	65.6	60.1		
12:56	0.100	76.7	57.4	65.4	60.1		

Time of day	Height above terrain Inches	Forward tunnel psychrometer T_{AD}-°F Thermo. #41	Forward tunnel psychrometer T_{AW}-°F Thermo. #51	Traverse psychrometer °F Thermo. #42	Traverse psychrometer °F Thermo. #52	Traverse wind velocity ft/sec	Quantity of water evaporated cc
	Test No. 48 (Cont)						
12:57	0.120	76.8	57.4	65.9	60.0		
12:58	0.140	76.9	57.8	66.2	60.0		
12:59	0.190	77.0	57.8	67.3	59.6	0.16	
12:59	0.240	77.1	57.7	68.0	59.3	0.33	26
13:00	0.340	76.9	57.7	68.1	59.1	0.35	
13:03	0.440	76.4	57.0	69.4	58.5	0.62	
13:04	0.640	77.5	57.2	71.9	57.9	1.4	
13:06	0.840	77.3	57.7	73.1	58.0	1.4	
13:07	1.240	77.3	57.9	73.9	57.9	2.2	
13:08	1.740	77.2	57.7	75.0	58.2	2.3	31
13:09	2.240	77.5	57.7	75.9	58.1	2.3	
13:13	3.740	77.9	58.2	76.7	58.8	2.3	
13:16	5.240	78.8	58.2	77.4	59.3	2.3	
13:18.5	6.740	77.9	58.1	77.3	59.5	2.3	51.5
		Test No. 49		Date Sept. 30, 1953		Sta. 2	
13:36	0.020	78.3	58.9	67.9	61.8		0
	0.030	80.6	58.9	68.9	62.0		
	0.040	80.6	59.5	68.6	62.1		
	0.060	80.1	59.5	68.5	62.1		
	0.080	81.2	59.1	69.6	62.0		
	0.100	81.3	59.0	69.4	61.9		
13:47	0.120	80.6	59.5	68.1	62.4		24
	0.170	81.1	59.5	68.1	62.3		
	0.220	81.7	59.5	68.1	62.2	0.11	
	0.320	81.4	59.6	69.0	61.8	0.10	
	0.420	81.9	57.7	70.8	61.0	0.41	
	0.620	81.7	57.7	71.0	61.2	0.41	
	0.820	82.3	57.5	71.6	59.5	0.68	
13:59	1.220	82.8	57.9	72.6	59.8	0.84	48
	1.720	83.2	57.9	75.2	59.3	1.0	
	2.220	82.7	58.3	78.4	59.2	1.5	
14:08	3.720	83.0	57.2	80.9	59.0	2.2	73
	5.220	83.6	57.5	80.5	59.1	2.2	
14:12	6.720	83.0	56.3	82.3	59.1	2.3	85

Part II - Model Runs

Thermocouple Number	Run 1a	Run 1b-2a	Run 2b	Run 3a	Run 3b-4a	Run 4b	Run 5a	Run 5b-6a	Run 6b-7a	Run 7b	Run 8a
1	66.1	67.1	67.5	60.2	60.8	61.2	59.9	59.5	61.3	62.8	60.3
2	64.7	65.3	65.5	59.2	59.4	59.4	58.6	57.8	59.6	61.2	60.3
3	64.4	65.3	65.5	59.1	59.2	59.4	58.3	57.8	59.5	60.7	60.1
4	66.2	65.1	67.9	59.6	60.2	60.7	59.7	59.1	60.8	62.5	60.4
5	65.3	65.9	66.1	59.4	59.7	59.8	59.5	58.6	59.9	61.3	60.4
6	65.3	66.4	66.2	59.4	59.7	60.0	59.6	58.8	59.9	61.3	60.4
7	65.4	66.2	66.2	59.5	60.0	60.0	60.0	59.0	59.7	61.3	60.5
8	65.5	66.4	66.6	59.6	60.0	60.4	60.1	59.1	60.0	61.4	60.5
9	65.6	66.2	66.2	60.0	60.4	60.7	60.5	59.5	60.1	61.3	60.5
10	65.8	66.2	66.6	59.8	60.2	60.5	60.5	59.5	60.0	61.5	60.8
11	67.8	68.8	69.4	61.2	61.9	62.8	61.4	61.0	62.1	64.0	61.4
12	58.7	58.7	62.1	55.9	56.0	56.3	56.6	57.7	58.6	57.8	57.7
13	65.7	66.1	66.2	60.1	60.4	60.8	60.3	59.4	60.1	61.7	60.8
14	66.7	67.6	67.7	60.6	61.1	61.8	60.7	60.3	61.1	62.9	60.8
15	65.9	66.1	66.2	59.8	60.0	60.6	60.4	59.1	59.8	61.4	60.8
16	74.6	76.6	76.9	67.5	69.4	70.7	67.7	69.0	70.4	72.2	64.0
21	68.6	69.8	72.0	61.0	61.2	64.5	61.7	62.2	65.1	67.2	61.3
22	66.7	67.6	68.1	59.5	60.7	61.3	59.5	59.3	61.5	63.2	60.4
23	64.8	66.0	66.6	59.5	60.0	60.1	59.1	58.3	60.3	61.8	60.1
24	65.8	65.8	66.6	59.6	60.4	60.1	59.1	58.3	60.7	61.8	60.8
25	66.7	67.3	68.2	60.0	60.9	61.3	59.4	59.3	61.8	61.2	60.3
26	64.5	65.0	65.8	59.1	59.6	59.6	59.0	58.2	59.8	61.2	60.8
27	64.8	65.0	65.9	59.2	59.8	59.7	59.2	58.5	60.2	61.3	60.0
28	64.4	64.9	65.4	59.2	59.4	59.2	59.0	58.0	59.4	60.4	60.1
41	79.6	85.6	84.0	73.1	78.0	79.8	74.1	78.8	82.7	88.5	63.2
42	73.5	85.1	83.1	68.2	75.0	80.5	67.8	76.3	77.8	86.0	63.5
43	79.7	85.9	83.7	73.0	76.5	80.1	74.0	78.9	83.2	89.3	63.5
44	77.4	81.3	81.6	68.4	71.3	73.9	68.9	72.1	75.3	79.4	63.5
45	75.7	79.0	79.2	68.3	70.7	72.2	68.1	71.9	76.2	77.8	63.2
46	78.7	83.1	84.1	72.5	75.1	77.0	72.1	74.7	77.7	80.5	69.9
51	62.3	64.2	63.2	59.0	60.6	57.7	56.8	57.8	61.4	61.8	58.5
52		68.0	64.5		61.3	59.1		59.3	61.4	62.2	59.5

Thermocouple Number	Run 8b-9a	Run 9b	Run 10a	Run 10b-11a	Run 11b	Run 12a	Run 12b	Run 13a	Run 13b-14a	Run 14b-15a	Run 15b-16a
1	60.8	62.0	64.1	64.2	65.8	61.4	62.7	66.1	66.4	66.9	66.8
2	60.4	61.8	63.7	63.6	65.2	62.2	63.2	65.8	65.5	66.1	66.0
3	60.4	61.3	63.2	63.6	64.5	61.0	62.3	64.8	65.0	65.4	65.3
4	60.8	61.9	64.4	64.6	65.8	61.8	62.7	65.8	65.8	66.0	66.3
5	60.5	61.2	63.5	63.3	64.7	61.0	61.8	65.0	65.2	65.4	65.5
6	60.2	61.2	63.5	63.3	64.5	61.0	61.8	65.0	65.2	65.4	65.5
7	60.4	60.9	63.5	63.4	64.9	60.8	61.4	65.0	65.2	65.4	65.5
8	60.6	61.0	63.5	63.5	64.9	61.4	61.8	65.0	65.2	65.4	65.5
9	60.6	61.1	63.6	63.6	64.9	60.9	61.8	65.0	65.2	65.4	65.5
10	60.6	61.1	63.6	63.6	65.0	60.9	61.7	65.0	65.2	65.4	65.5
11	61.6	62.0	65.2	65.4	66.4	62.0	63.4	66.6	67.0	67.3	67.6
12	57.0	59.0	54.0	61.1	62.0	54.4	55.2	57.8	57.8	58.1	58.0
13	60.5	61.3	64.0	64.0	60.8	60.9	61.8	65.1	65.0	67.3	65.4
14	60.9	61.8	64.7	64.6	65.9	60.9	61.9	65.1	65.3	67.3	65.4
15	64.9	60.8	64.0	63.5	64.9	60.9	61.7	65.1	65.3	65.8	65.4
16	66.8	61.8	70.1	70.8	72.1	65.4	66.3	68.6	69.6	70.4	70.3
21	61.8	63.3	65.8	66.0	67.7	63.7	64.8	69.0	68.2	69.4	69.4
22	60.7	61.9	64.5	64.8	65.8	62.2	63.2	66.2	65.9	66.5	66.4
23	60.3	61.9	63.3	63.4	64.9	61.4	62.0	64.8	64.6	64.6	65.2
24	60.8	62.1	63.6	63.7	64.9	61.8	62.8	65.1	64.6	65.0	65.4
25	61.3	62.2	64.2	64.8	66.8	62.5	64.0	66.8	67.1	67.6	65.5
26	60.5	61.6	64.0	63.8	65.4	62.0	62.8	65.8	65.8	66.3	64.6
27	60.2	61.8	63.6	63.4	64.5	61.0	62.2	64.8	64.8	65.0	65.0
28	60.2	61.2	63.1	63.1	64.5	61.8	62.5	65.3	65.0	65.4	65.0
41	65.8	73.0	72.6	71.7	77.4	72.5	74.8	74.5	73.4	75.9	74.4
42	65.8	69.5	72.9	71.4	77.5	71.0	72.2	73.0	71.6	75.9	73.8
43	66.2	70.8	72.6	71.7	76.6	72.2	74.4	75.1	72.8	75.9	74.0
44	65.0	67.6	71.2	71.0	73.7	66.4	67.8	70.4	70.7	71.6	72.0
45	64.5	66.7	70.8	69.6	72.6	67.1	67.8	70.8	70.7	72.2	69.4
46	71.4	73.4	77.0	77.5	78.3	72.8	74.4	75.6	75.2	76.5	76.3
51	60.5	61.3	62.4	62.2	65.2	61.0	61.1	59.4	58.8	62.5	61.9
52	61.2	62.9	64.4	62.7	65.1	61.0	60.9	62.8	60.4	62.0	64.5

Thermocouple Number	Run 16b	Run 17a	Run 17b-18a	Run 18b-19a	Run 19b	Run 20a	Run 20b-21a	Run 21b-22a	Run 22b-23a	Run 23b-24a	Run 24b
1	66.8	60.5	61.2	61.8	62.4	59.6	60.6	62.0	62.6	63.1	63.5
2	66.2	59.7	60.4	61.1	61.7	59.1	60.4	62.3	63.3	62.9	63.7
3	64.8	59.3	60.0	60.5	60.9	59.1	60.4	61.5	62.2	62.4	62.8
4	66.2	60.1	60.6	61.3	61.8	59.5	60.6	61.8	63.1	63.2	63.6
5	65.6	60.1	60.4	60.8	61.1	59.5	60.1	61.3	61.9	62.1	62.7
6	65.6	60.0	60.4	60.8	61.1	59.5	59.9	61.0	61.7	62.3	62.6
7	65.6	60.0	60.4	60.8	61.1	59.5	60.0	61.0	61.7	62.3	62.6
8	65.6	60.0	60.4	60.8	61.1	59.5	59.9	61.0	61.7	62.3	62.6
9	65.6	60.2	60.4	60.8	61.1	59.6	60.0	61.0	61.8	62.3	62.6
10	65.6	60.1	60.4	60.8	61.1	59.7	59.9	61.0	61.8	62.3	62.6
11	67.9	61.0	61.5	61.9	62.7	60.1	60.8	61.9	62.8	63.6	64.1
12	58.6	58.2	58.2	61.9	57.7	58.8	59.8	61.0	61.9	60.0	62.7
13	65.6	60.0	60.2	60.8	61.0	59.7	60.3	61.2	62.3	60.4	63.1
14	65.6	60.9	60.5	61.6	61.8	60.3	60.6	61.8	62.7	63.5	63.9
15	66.0	60.0	60.4	60.5	61.1	60.0	59.8	60.8	63.7	62.4	62.7
16	70.6	65.1	66.3	67.0	67.6	65.0	66.0	66.6	67.6	68.1	69.0
21	69.4	62.0	62.2	63.4	64.0	60.5	61.4	62.6	63.6	64.5	64.6
22	66.6	60.6	60.8	61.7	62.4	60.4	60.9	62.6	63.0	64.5	64.3
23	64.9	60.0	60.3	60.7	61.4	59.4	60.4	62.0	62.6	62.7	63.3
24	65.1	60.0	60.4	61.1	62.0	59.4	60.4	62.0	62.6	62.7	63.3
25	67.9	61.1	61.4	60.2	63.5	60.5	61.5	62.8	63.6	60.3	65.3
26	66.8	60.4	60.4	61.2	64.0	59.6	60.4	61.5	62.6	62.6	63.2
27	65.0	59.9	60.4	60.0	61.3	59.2	60.3	61.8	62.6	62.2	63.2
28	65.0	59.9	60.0	60.8	60.9	59.2	60.2	61.4	62.1	62.2	62.7
41	73.5	68.3	69.4	71.9	74.9	65.0	65.4	70.9	73.6	72.4	71.7
42	73.0	67.9	69.4	71.5	74.3	64.9	65.4	70.8	72.9	72.4	70.8
43	73.4	68.2	69.4	72.0	74.8	65.1	65.6	70.8	73.5	72.4	70.8
44	71.7	65.4	66.3	68.1	69.4	64.0	65.9	68.0	69.9	70.6	70.3
45	71.7	65.0	66.3	67.6	69.0	63.4	65.4	67.6	69.4	69.7	69.4
46	76.0	70.6	70.3	72.7	73.4	70.0	69.8	73.6	74.9	75.6	76.1
51	59.0	58.3	58.6	59.5	60.4	58.6	60.9	62.1	63.0	61.8	63.4
52	59.4	58.7	59.0	60.8	62.0	64.6	66.9	62.3	63.3	63.1	64.7

Thermocouple Number	Run 25a	Run 25b-26a	Run 26b-27a	Run 27b-28a	Run 28b	Run 29a	Run 29b	Run 30a	Run 30b	Run 31a	Run 31b
1	58.6	59.6	61.4	63.6	65.4	71.3	71.7	73.1	74.1	55.0	56.7
2	59.0	60.1	62.6	65.5	66.8	72.1	72.6	70.7	71.4	55.8	57.2
3	58.1	59.0	61.4	63.3	64.3	68.5	69.5	70.0	70.2	54.8	56.3
4	58.9	59.7	62.0	64.2	65.0	70.6	70.8	73.0	73.1	56.0	57.0
5	58.3	59.0	60.7	62.3	64.1	69.6	72.2	71.2	71.6	53.3	58.6
6	58.3	58.7	60.7	62.1	64.0	69.4	72.2	70.8	71.6	52.3	53.3
7	58.6	58.7	60.2	61.6	63.6	69.4	72.2	70.8	71.6	52.6	53.7
8	58.9	58.7	60.2	61.6	63.9	69.4	72.2	70.8	71.6	52.4	53.7
9	59.1	58.7	60.2	61.6	63.7	69.4	72.2	70.8	71.6	52.8	53.8
10	59.1	59.1	60.2	61.6	63.6	69.4	72.2	70.8	71.6	52.7	53.9
11	59.6	60.1	61.8	63.3	65.4	71.8	72.2	73.0	73.9	52.7	56.1
12	55.3	59.5	61.1	60.0	64.6	69.3	65.8	77.2	69.5	50.9	52.4
13	58.7	59.5	60.4	62.1	64.0	68.6	69.8	69.9	70.8	53.1	54.6
14	59.4	59.8	61.3	62.8	64.9	69.8	70.7	72.5	73.0	54.9	56.0
15	59.1	59.1	60.4	61.7	63.1	69.5	70.2	70.7	71.1	52.6	53.6
16	66.4	6.73	68.4	69.1	70.4	74.3	75.7	77.1	78.4	62.3	63.6
21	59.6	61.1	63.2	66.6	67.0	75.2	76.7	76.5	77.5	58.6	60.0
22	62.7	63.7	65.7	68.6	70.3	75.3	76.2	75.5	76.6	55.9	56.9
23	58.0	59.7	62.0	64.5	65.5	71.2	72.0	72.2	73.0	54.0	55.2
24	57.8	59.1	61.3	63.5	64.1	69.0	69.6	69.6	70.7	54.2	55.2
25	60.9	63.6	65.9	68.2	69.9	74.5	75.3	74.8	76.1	56.3	57.2
26	57.7	58.7	60.8	62.7	63.6	69.4	70.0	70.6	71.0	52.0	53.1
27	58.1	59.2	61.3	63.4	64.4	69.0	69.9	70.3	71.0	54.2	55.0
28	57.6	58.8	60.4	62.3	63.2	68.8	69.4	69.4	70.0	52.3	53.3
41	70.8	74.5	76.7	80.2	85.1	83.8	80.9	91.3	90.1	65.9	65.9
42	68.2	73.7	77.0	79.1	85.0	83.3	79.2	86.3	89.6		
43	70.7	74.3	77.0	79.6	85.0	84.1	80.8	92.0	89.6	65.8	66.2
44	63.4	69.9	72.6	75.3	78.1	78.5	78.3	80.1	82.7	62.8	64.5
45	67.6	70.4	72.6	74.8	77.5	78.5	78.5	82.8	83.6	61.6	62.9
46	69.9	72.9	74.8	76.1	78.3	82.7	83.4	89.0	89.9	71.7	73.2
51	67.1	61.5	64.0	65.6	75.3		65.0	73.0	68.4	50.0	50.7
52	69.0	60.4	65.1	77.2	77.2		65.9	73.0	68.4		

Thermocouple Number	Run 32a	Run 32b	Run 33a	Run 33b-34a	Run 34b	Run 35a	Run 35b-36a	Run 36b-37a	Run 37b-38a	Run 38b	Run 39a
1	61.8	63.6	65.1	66.4	67.7	59.2	60.2	61.4	61.8	62.6	57.5
2	61.2	64.0	65.8	67.2	68.3	64.4	67.5	69.0	70.4	71.8	55.4
3	62.3	63.6	65.9	67.3	67.8	59.6	61.2	61.7	62.1	62.8	54.6
4	61.2	62.7	65.0	66.2	64.9	60.8	62.3	63.2	64.5	66.0	56.8
5	58.2	59.1	59.8	60.5	61.0	55.5	55.5	56.2	56.4	57.2	56.1
6	56.7	58.6	59.2	60.0	61.0	55.5	55.4	56.2	56.4	56.9	55.8
7	56.8	58.6	59.2	60.0	60.8	56.0	55.8	56.3	56.8	56.9	56.1
8	56.7	58.6	59.2	60.0	60.8	56.2	55.9	56.4	56.6	56.9	56.1
9	57.7	58.6	59.2	60.0	60.8	56.6	56.2	56.3	57.1	57.5	56.1
10	57.4	58.3	59.5	60.0	60.8	56.6	56.0	58.8	57.2	57.5	56.6
11	60.4	61.6	63.9	64.9	65.9	59.2	59.7	61.7	61.6	62.3	58.3
12	55.9	57.3	54.0	55.9	61.7	53.8	55.8	62.4	63.6	66.2	51.0
13	58.6	60.4	61.9	63.3	64.5	56.4	56.4	57.7	58.1	58.7	55.8
14	59.1	60.4	61.9	63.0	63.9	58.6	59.6	61.8	63.3	64.7	57.5
15	57.7	58.3	59.5	60.2	60.8	56.4	56.3	56.8	57.3	57.3	56.6
16	64.8	65.9	66.7	67.8	69.0	67.3	67.6	69.0	70.2	70.7	69.3
21	65.9	67.7	71.2	72.1	72.5	65.8	67.2	69.4	69.4	70.5	64.4
22	62.3	64.1	66.9	68.6	69.0	63.2	64.8	67.5	67.8	69.0	56.0
23	60.0	61.3	62.4	63.4	64.5	59.4	59.9	61.3	62.2	63.7	55.1
24	61.0	62.3	63.7	64.4	65.6	60.0	61.0	62.4	62.7	63.1	56.4
25	63.1	65.4	66.9	66.7	69.1	61.0	61.7	64.0	64.6	65.6	58.6
26	57.8	58.7	59.4	60.0	60.8	54.5	54.6	55.5	55.8	55.9	55.3
27	59.5	61.2	61.9	62.9	64.2	57.2	57.8	59.2	59.7	60.5	58.7
28	58.2	59.1	60.5	60.8	61.7	55.5	55.6	56.5	57.6	57.2	59.3
41	80.1	85.8	86.2	86.3	87.7	79.6	81.3	81.2	81.9	81.1	77.5
42											
43	84.9	86.5	86.4	87.7	88.5	79.6	81.0	81.2	80.5	80.6	79.1
44	73.6	75.8	77.2	77.9	79.6	72.9	74.8	76.1	81.8	78.0	73.4
45	71.3	73.1	74.7	77.3	78.2	70.7	72.6	74.1	77.0	75.4	71.2
46	74.4	76.1	77.5	79.2	80.4	73.8	75.3	77.4	75.0	79.9	77.9
51	58.1	58.1	58.7	58.2	58.2	50.1	50.5	50.3	51.0	75.6	52.2
52											

Thermocouple Number	Run 39b-40a	Run 40b-41a	Run 41b-42a	Run 42b	Run 43a	Run 43b-44a	Run 44b-45a	Run 45b-46a	Run 46b	Run 47a	Run 47b-48a
1	58.4	59.3	60.0	59.9	53.2	54.6	56.7	58.6	60.3	58.3	60.1
2	56.9	58.7	60.5	61.8	52.6	53.0	56.3	57.7	58.3	56.3	57.7
3	55.0	56.0	56.4	57.2	52.3	53.4	55.3	57.3	58.3	55.9	57.3
4	55.9	57.7	58.2	58.8	53.1	53.5	56.0	57.8	58.8	56.3	57.7
5	55.7	56.3	56.7	56.8	52.4	53.6	55.0	57.6	58.5	56.8	57.9
6	60.0	55.9	56.4	56.8	52.1	53.3	54.7	56.7	58.2	56.3	57.8
7	55.9	56.0	56.4	56.7	52.3	53.3	54.6	56.4	57.8	56.4	57.8
8	56.4	56.4	56.8	57.2	52.3	53.2	54.8	56.7	57.8	56.3	57.7
9	56.5	56.5	56.8	57.1	52.3	53.6	54.9	57.0	58.2	56.9	57.9
10	56.8	57.1	57.3	57.6							
11	58.7	59.1	59.5	59.9	53.1	54.3	56.5	56.3	59.9	57.9	59.3
12	53.6	53.3	55.4	56.5	46.8	53.2	55.1	51.0	58.2	56.5	57.8
13	56.0	55.9	56.8	56.9	52.3	53.5	55.1	57.0	58.3	56.0	57.2
14	57.7	57.8	58.6	58.7	52.6	54.1	55.9	57.6	58.9	57.0	58.1
15	56.5	56.8	57.2	57.4	52.3	53.3	54.9	56.4	58.2	56.2	57.4
16	56.5	71.8	72.7	73.2	59.8	61.2	63.4	65.5	67.1	62.2	64.0
21	64.2	66.7	66.6	67.4	55.8	56.9	59.1	62.6	63.1	60.0	61.8
22	54.6	56.8	57.9	58.2	53.4	53.6	56.0	58.9	59.1	57.1	58.5
23	54.2	56.3	57.0	57.9	52.8	54.2	56.3	58.5	59.4	56.3	58.2
24	66.4	57.8	58.3	58.7	53.1	54.3	56.3	57.7	59.4	57.0	58.6
25	57.0	60.2	56.0	61.2	53.7	54.6	57.1	60.2	60.9	57.7	59.7
26	55.0	55.9	56.4	56.8	52.2	53.3	55.1	57.2	58.5	56.8	58.2
27	54.0	54.5	54.7	55.5	52.5	53.6	55.3	57.2	58.5	56.8	58.1
28	53.9	55.0	55.3	55.9	52.5	53.2	55.0	57.2	58.2	55.9	57.4
41	79.2	78.3	78.8	75.2	64.1	69.1	74.1	77.4	79.6	72.1	76.2
42										67.7	64.0
43	79.2	78.5	78.8	75.3	64.1	69.1	74.3	77.4	79.6	72.3	76.6
44	74.4	74.8	76.2	74.8	60.1	62.8	65.8	68.8	70.3	64.0	66.3
45	72.0	72.6	73.1	71.6	59.4	62.8	65.5	68.0	70.0	64.1	66.3
46	79.8	80.5	81.8	81.4	68.0	70.4	73.8	76.4	78.4	71.6	73.6
51	51.3	51.8	51.6	43.9	51.3	53.3	53.9	56.3	57.7	55.3	57.0
52											

Thermocouple Number	Run 48b-49a	Run 49b
1	62.0	64.9
2	59.4	60.5
3	59.5	60.5
4	59.2	60.5
5	59.6	61.3
6	59.4	61.3
7	59.1	61.3
8	59.3	61.4
9	59.5	61.4
10		
11	60.9	63.9
12	59.3	61.3
13	59.1	61.4
14	59.6	61.7
15	59.1	61.5
16	65.1	68.5
21	63.7	67.0
22	60.2	61.4
23	59.6	60.8
24	60.2	61.5
25	61.8	63.3
26	60.0	61.5
27	59.6	60.3
28	59.4	60.4
41	79.8	83.6
42	68.0	78.7
43	79.7	84.4
44	68.3	73.1
45	68.8	73.1
46	76.1	79.6
51	57.9	57.3
52		